Synthesis and Biological Activity of Newly designed Cyclic Peptides

By

HISHAM NABIL MAHMOUD FARRAG

Graduate School of Life Science and Systems Engineering

Kyushu Institute of Technology

This dissertation is submitted for the degree of

Doctor of Philosophy

Kyutech
Kyushu Institute of Technology

The members of the Supervisory and Examination Commitee are as follows:

KATO Tamaki, Ph.D
Associate Professor
Graduate School of Life Science and Systems Engineering
Kyushu Institute of Technology, Japan

HARUYAMA Tetsuya, Ph.D
Professor
Graduate School of Life Science and Systems Engineering
Kyushu Institute of Technology, Japan

KITAMURA Mitsuru, Ph.D
Professor
Department of Applied Chemistry
Kyushu Institute of Technology, Japan

PANDEY Shyam, Ph.D
Associate Professor
Graduate School of Life Science and Systems Engineering
Kyushu Institute of Technology, Japan

This is to certify that the dissertation entitled **Synthesis and Biological Activity of Newly designed Cyclic Peptides** by **HISHAM NABIL MAHMOUD FARRAG (Student ID: 17899028)** is fully adequate in scope and quality as a dissertation for the degree of Doctor of Philosophy.

Dedication

To all my family, friends, and colleagues.

Contents

Chapter 1

General Introduction

1. Introduction

Antimicrobial peptides are short peptides containing variable numbers and sequences of amino acid residues. They have become therapies for the treatment of antibiotic-resistant pathogens because they can eradicate them, and also enhance the body's defenses against pathogens [1]. The peptide structure generally includes cationic and hydrophobic residues, which allow the peptide to interact with the bacterial cell membrane *via* electrostatic and hydrophobic forces. That interaction enables penetration of the peptide into the cell membrane, leading to cell death [2]. The unique mechanism of antimicrobial peptides decreases the incidence of microbial resistance to them [3].

The global emergent catastrophe of antibiotic resistance acquired by virulent bacteria has underlined the necessity of investigating substitutes for the presently existing antibiotics [4]. The World Health Organization considers antibiotic-resistant microbes a pending international health tragedy. In the United States, over two million infections related to antibiotic-resistance arise each year, costing more than $20 billion, and the death toll surpasses 23,000 [5]. In developing countries, communicable diseases are the commonest cause of death, now made worse by the evolution of antibiotic-resistant virulent bacteria [6]. The disappointing failure of the strongest antimicrobials to eradicate resistant pathogens highlights the crucial need to investigate alternatives. Infectious diseases such as pneumonia, influenza, and tuberculosis were the principal cause of mortality and morbidity in the human

population before the clinical introduction of antibiotics. In 1935, sulfonamides (sulfa drugs) were introduced into clinic, and penicillin and streptomycin were introduced in 1941 and 1945, respectively. These antibiotics decreased mortality rates caused by infectious diseases [7]. The most important antibiotic classes will be discussed briefly below.

1.1. Important Classes of Antimicrobials

1.1.1. β-Lactams

In 1928, Alexander Fleming discovered the β-lactam penicillin from *Penicillium* fungi. However, its clinical use was delayed because of problems such as instability, low yield, and difficulty with purification. In the 1940s penicillin started to be used as an antimicrobial agent for the treatment of a wide range of infectious diseases, with lower side effects than sulfonamides [8]. In 1945, the large-scale production of penicillin began following the optimization of various production phases. β-Lactam antimicrobials have a bactericidal effect on both Gram-positive and Gram-negative bacteria by interrupting cell wall formation. β-Lactams can bind covalently to critical enzymes and specific penicillin-binding proteins that contribute to the process of peptidoglycan cross-linking [9].

When 6-aminopenicillanic acid was recognized as the functional domain of penicillin, several semisynthetic penicillins began to be developed. The main improvement was the synthesis of penicillinase-resistant penicillins such as oxacillin and methicillin. Furthermore, effective derivatives against Gram-negative pathogens, such as aminopenicillins (amoxicillin, bacampicillin, and ampicillin), ureidopenicillins (azlocillin, mezlocillin, and piperacillin), and carboxypenicillins (ticarcillin and carbenicillin), were produced [10]. Bacterial resistance

is one of the most important drawbacks of penicillin derivatives. Additional improvements to widen the range of activities and to overcome bacterial resistance were the addition of a β-lactamase inhibitor (tazobactam, clavulanic acid, or sulbactam) to a penicillin derivative in a combination.
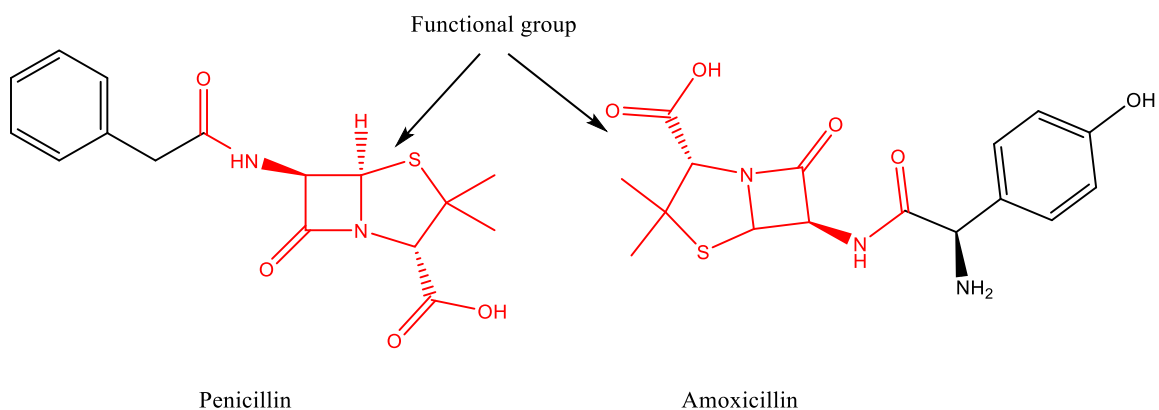
Figure 1.1. Some examples of β-lactam antibiotics.

1.1.2. Aminoglycosides

In 1943, streptomycin was discovered by Albert Schatz by the isolation of two strains of *Streptomyces* that were active against Gram-negative bacteria resistant to penicillin. Aminoglycosides are powerful broad-spectrum antimicrobials that exert their effect by inhibiting the process of protein synthesis [11]. In the following year, clinical trials showed that streptomycin is active against *Mycobacterium tuberculosis* and infectious diseases triggered by Gram-negative bacteria. Despite bacterial resistance and toxic side effects, streptomycin soon became the core drug in the multidrug treatment of tuberculosis. The

introduction of streptomycin into clinical practice significantly reduced mortality rates due to tuberculosis.

In 2007, two cases of tuberculosis with high resistance to all available antibiotics were identified in Italy, resulting in the death of the patients [12]. In the 1980s, aminoglycosides were substituted by more effective antibiotics with lesser side effects, such as fluoroquinolones, carbapenems, and cephalosporins. However, aminoglycoside antibiotics such as gentamycin and kanamycin (Figure 1.2) are still widely used in hospitals for the treatment of severe infections [13].

Gentamycin

Kanamycin
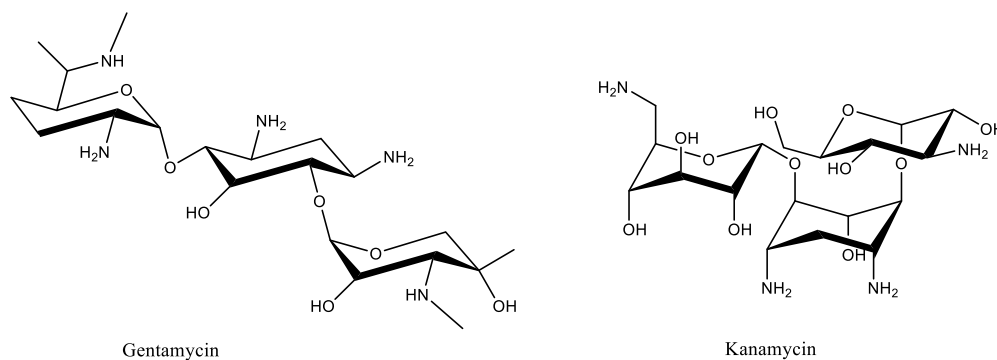
Figure 1.2. Some examples of aminoglycoside antibiotics.

1.1.3. Macrolides

In 1950, pikromycin was discovered and isolated by Brockmann and Henkel from *S. venezuelae*. It was the main precursor to the production of more effective macrolide derivatives [14]. One of the first effective macrolide derivatives was erythromycin (Figure 1.3), which was isolated from *S. erythraeus* [15]. The natural macrolides are mainly characterized by the presence of a 14- to 16-membered macrocyclic lactone ring with at least

one deoxy sugar connected to it. Macrolides are mostly a second-line treatment after β-lactam antibiotics. Like β-lactams, they can affect a wide range of bacteria, but they have lower activity toward Gram-negative bacteria. The observable merit of macrolides over β-lactams is their activity against bacterial pathogens lacking cell walls, such as *Mycoplasma*.

Macrolides have a bacteriostatic effect and act by preventing protein synthesis through the inhibition of the enzyme peptidyltransferase [16]. Many modifications have been carried out on natural macrolides to enhance their pharmacokinetic characteristics, for example, azithromycin (9-dihydro-9-deoxo-9a-methyl-9a-aza-9a-homoerythromycin A) was synthesized by using azalide the scaffold [17]. This has led to the synthesis of new antibiotics with excellent pharmacokinetic characteristics, such as avoidance of drug degradation by cytochrome P450 3A4 [18]. Bacteria can acquire resistance to macrolides by dimethylation of residue A2058 in the 23S rRNA, which protects the ribosome from the antibiotic effect [19].

Macrolides have also shown excellent anti-inflammatory characteristics in the treatment of several noninfectious respiratory diseases. For this reason, macrolides became one of the main therapies for the management of these diseases [20].
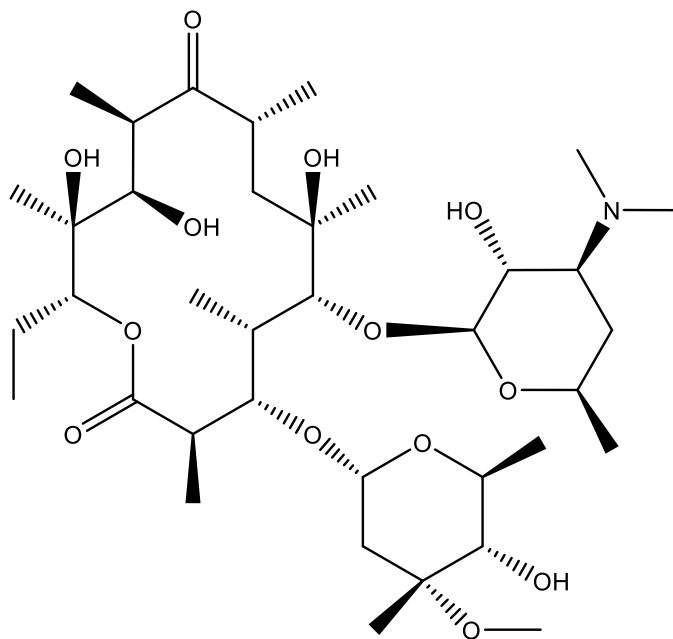
Figure 1.3. Structure of erythromycin, an example of a macrolide.

1.1.3.1. Amphotericin B

Another subclass of macrolides including nystatin and amphotericin B has antifungal properties [21].
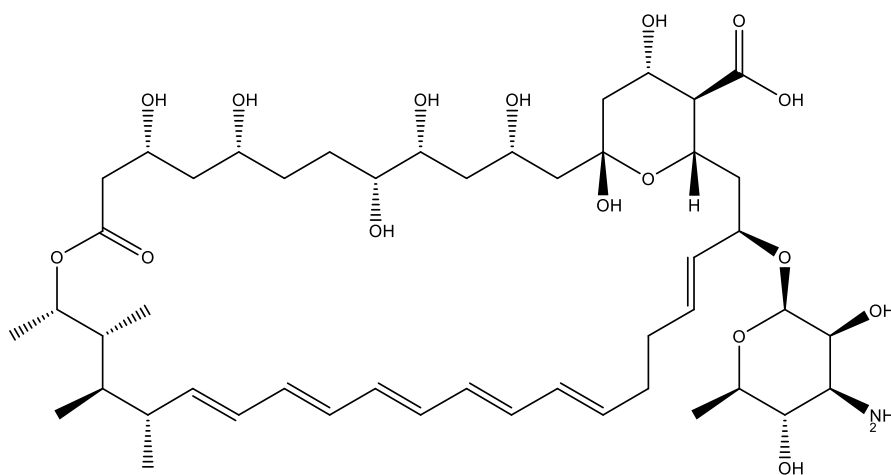
Figure 1.4. Structure of amphotericin B.

Amphotericin B (Figure 1.4) is a potent antifungal usually used as a life-saving medication. It works similarly to antimicrobial peptides by attacking the fungal cell wall. The hydrophobic character of amphotericin B allows it to bind with ergosterol in fungal cell membranes *via* Van der Waals interactions. These hydrophobic interactions help amphotericin B to penetrate fungal cell membranes, leaving pores in the membrane. That loss of membrane uniformity causes fungal cell death [22].

1.2. Antimicrobial Peptides

In 1939, Dubos discovered the first antimicrobial peptide when he extracted an antibiotic from a strain of *Bacillus*. The extract showed high potency in the treatment of pneumococcal infection in mice [23]. In 1940, the antimicrobial agent, gramicidin, was isolated and purified by Hotchkiss and Dubos [24]. Gramicidin is still used for the treatment of ulcers and wounds [25]. In the following year, another antimicrobial peptide was discovered and named tyrocidine; it showed a broad-spectrum effect on Gram-positive and Gram-negative bacteria. In 1941, purothionin was discovered and isolated from *Triticumaestivum* plants and showed high efficacy against many bacteria and fungi [26]. Defensin was extracted from the leukocytes of rabbits in 1956 [27], lactoferrin was isolated from cow's milk, and bombinin was extracted from the epithelia of *Bombina maxima* (the giant fire-bellied toad). Other antimicrobial peptides were also discovered from human leukocytes [28].

1.2.1. Main Classes of Antimicrobial Peptides

1.2.1.1. Antibacterial Peptides

To date, this class is the most investigated among all classes of antimicrobial peptides. Cationic peptides are the major components of this class, and attack the cell membranes of bacteria causing degeneration of the lipid bilayer [29,30]. Most antibacterial peptides have amphipathic character (i.e., they contain both hydrophobic and hydrophilic moieties). These moieties afford them the ability to interact with the negatively-charged cell membrane components (hydrophilic moieties) and the lipid constituents (hydrophobic moieties) [31]. Moreover, investigators have confirmed that some antibacterial peptides can kill bacteria without altering the cell membrane uniformity, especially at relatively low concentrations. These peptides act by hindering essential biological processes in the cell, such as protein biosynthesis or the replication of DNA. Buforin II, drosocin, and pyrrhocoricin are examples of peptides that can diffuse inside bacterial cells and interact with RNA and DNA without affecting the integrity of the cell membrane [32]. Some antibacterial peptides can affect bacteria that resist the effect of standard antibacterial agents. For example, methicillin-resistant *Staphylococcus aureus* (MRSA) strains were sensitive to nisin, while they resisted the effect of vancomycin (a glycopeptide antibiotic) [33].

1.2.1.2. Antiviral Peptides

This class of antimicrobial peptides can affect viruses by interacting with either the host cell membrane (enhancing the immune system) or the viral envelope. Additionally, several antiviral peptides can interact with RNA and DNA inside the protein envelope [34]. Antiviral

peptides can interact with the protein envelope of viruses leading to instability of the membrane, and the viruses then become incapable of infecting host cells [35]. Antiviral peptides are capable of reducing the binding ability of some viruses with host cells, for example, in the effect of defensins on herpes simplex viruses (HSV) [36]. Moreover, some antiviral peptides can inhibit viral receptors, consequently preventing viruses from attacking host cells [37]. HSV needs a negatively-charged molecule called heparan sulfate for attachment to the host cell membrane. Heparan sulfate can bind to some cationic α-helical peptides such as lactoferrin, thus preventing HSV from binding to host cells [38].

Other peptides can cross the host cell membrane into the cytoplasm and induce alterations in gene expression. This can aid the host cell defensive system against certain viruses, or prevent the expression of viral genes. For example, the peptide NP-1 can inhibit viral protein from entering the host cell nucleus, preventing infection by HSV type 2 [39].

1.2.1.3. Antifungal Peptides

Antifungal peptides can affect fungi by interacting with either the cell wall [40] or intracellular constituents [41]. Bacterial cell membranes and the cell wall of fungi are structurally different. The key component of the fungal cell wall is chitin; therefore, the most effective antifungal peptides should be able to bind chitin. [42]. Antifungal peptides, especially those acting on the cell wall, can kill the targeted cells by disturbing the uniformity of the cell membrane [43], by creating holes in the cell membrane [44], or by increasing the permeability of the plasma membranes [45]. Most antifungal peptides possess neutral and polar amino acids in their sequence [46]. Nevertheless, no significant relationship exists

between the structure of the peptides and the nature of the cells that they target. For instance, there are antifungal peptides from different structural groups, for example, β-sheet (defensins [47]), extended (indolicin [48]), and α-helical (P18 [49]) peptides. Theonellamides are novel potent antifungal bicyclic dodecapeptides isolated from marine sponges. They act by attacking fungal cell membranes through hydrophobic interactions with sterols in the lipid bilayer [50].

1.2.1.4. Antiparasitic Peptides

Antiparasitic peptides are a smaller class than the other classes of antimicrobial peptides. Indeed, antiparasitic peptides can kill parasites by targeting their cell membranes, even if the parasites are multicellular organisms [51]. Magainin was the first reported peptide in this group, and can kill *Paramecium caudatum* [52]. A new synthetic antiparasitic peptide was prepared for use in the treatment of diseases caused by *Leishmania* [53]. Cathelicidin is another example of this class, and can eradicate *Caenorhabditis elegans* by making holes in its cell membrane [51].

1.2.2. Mechanism of Action of Antimicrobial Peptides

They can affect microbial cells by disturbing membrane uniformity, initiated through electrostatic interactions with negatively-charged components of the cell membrane [54]. Other mechanisms of action are *via* the inhibition of DNA, RNA, or protein synthesis, or interaction with specific intracellular components. The best-known antimicrobial peptides are cationic [55]. However, negatively-charged (anionic) antimicrobial peptides have been

discovered, such as dermcidin (from human sweat glands) [56], and maximin-H5 (from frog skin) [57].

An antimicrobial peptide generally has selective activity against one group of microorganisms (e.g., viruses, fungi, or bacteria) [58]. However, some have broad-spectrum activity with different modes of action against different classes of microorganisms, such as indolicidin, which can affect human immunodeficiency virus (HIV), fungi, and bacteria [59,60]. It exhibits an anti-HIV effect by interfering with HIV-integrase [61], while it kills *Escherichia coli* by diffusing into cells and preventing the synthesis of DNA [62]. Indolicidin shows its antifungal effect by damaging the fungal cell membrane [63]. Several antimicrobial peptides have similar modes of action against different types of microorganism, such as PMAP-23, which affect parasites and fungi by making holes in their cell membranes [51,64].

Approximately 30% of bacterial proteins are linked with the cell membrane. These proteins are responsible for numerous functions that are essential for the bacterial cell, including respiration, nutrient active transport, and adenosine triphosphate production [65]. The activities of these proteins can be changed by treatment with antimicrobial peptides, even if the cell is not completely lysed. As a result, the rapid killing effect of antimicrobial peptides does not only originate from membrane lysis, but may also arise from the inhibition of essential protein(s).

1.2.2.1. Antimicrobial Peptides Active Against the Microbial Cell Membrane

This category starts the effect by interaction with the cell membrane, even if the ultimate target is an intracellular component [66]. Most of these peptides are amphipathic, which means that they possess hydrophobic and cationic moieties. Their first interaction is with negatively-charged microbial cell membrane components *via* electrostatic forces. This is followed by diffusion inside the cell membrane with the aid of the hydrophobic moieties [2,54]. The electrostatic interactions mainly depend on the cationic face of the peptide, whereas the hydrophobic interactions are influenced by its hydrophobicity.

These peptides are classified, according to their mode of action, into (Figure 1.5):

a- Carpet-like peptides: they act like micelles. First they cover a narrow area of the cell membrane. Then they diffuse through the lipid bilayer, making holes in the membrane [67].

b- Aggregate peptides: they penetrate the cell membrane vertically, creating sphere-like conformations [68].

c- Cell membrane thinning peptides: they create a cavity between lipid components leading to the degeneration of the cell membrane [69].

d- Toroidal-hole peptides: they line up vertically inside the lipid bilayer with their hydrophobic moieties attached to the core of the lipid bilayer while the hydrophilic moieties face the hole [68].

e- Barrel-stave mode peptides: they align horizontally to the membrane, then they start to form a barrel-like shape and penetrate the cell membrane vertically [70].
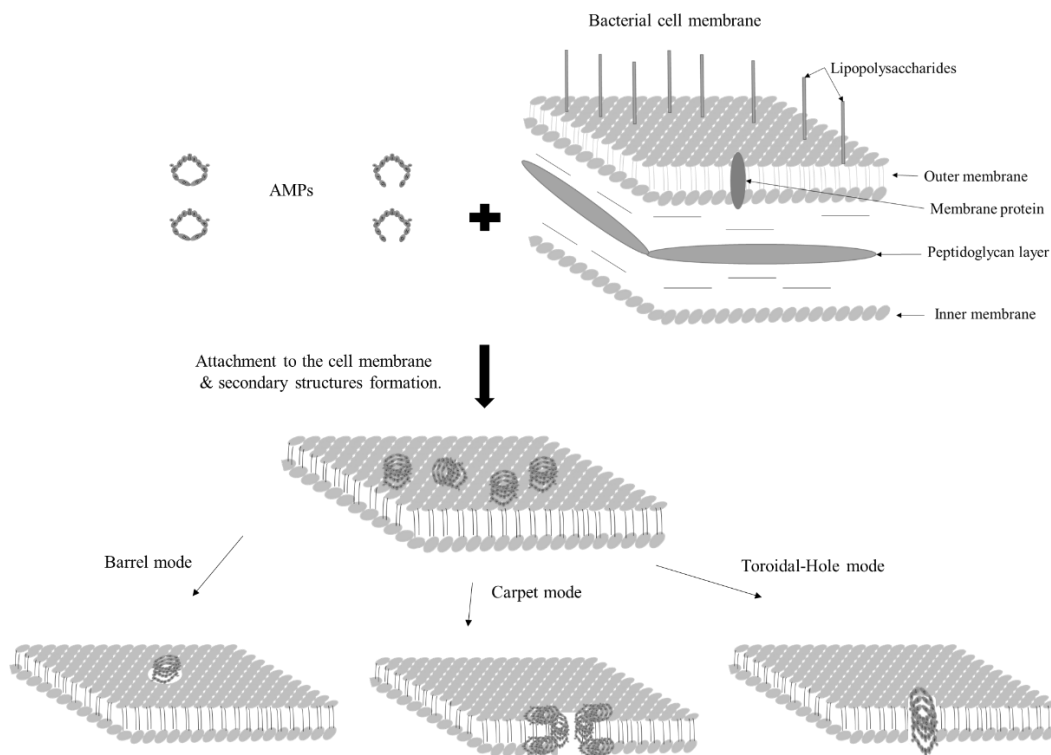
Figure 1.5. Modes of action of antimicrobial peptides that are active against the cell membrane.

1.2.2.2. Antimicrobial Peptides Active Against Intracellular Components

Some antimicrobial peptides can kill microorganisms without affecting their membrane permeability. This discovery highlighted the presence of another mechanism of action—targeting important components within microbial cells. [71]. For example, indolicin can bind to a particular DNA sequence [72]. Many antimicrobial peptides can hinder protein and DNA synthesis [73]. For example, tPMP-1 and aHNP-1, which are derived from the human

immune system, can prevent protein and DNA synthesis within 1 h of entering into bacterial cells [74]. Another example is apidaecin, which inhibits protein synthesis without forming holes in the cell membrane. Apidaecin has a selective effect on Gram-negative bacterial cells. It was proposed that apidaecin is transported inside the cell *via* a carrier protein through an active transport mechanism, and then it inhibits protein synthesis [75]. Histatin 5 can prevent the destruction of periodontal tissues through the inhibition of *Bacteriocides gingivalis* protease [76]. Other peptides, such as eNAP-2, have an inhibitory effect on the serine proteases of some microorganisms [77]. Some peptides can kill microbial cells in particular growth stages, such as diptericin, which interferes with specific metabolic pathways during bacterial growth [78]. Some of the intracellularly-active peptides have several targets, such as seminal plasmin, which inhibits RNA polymerase and can completely inhibit RNA synthesis at lower concentrations than other antibiotics [79]. Alternatively, it can stimulate a protein called autolysin in the target cell, causing autolysis [80].

Antimicrobial peptides can terminate some intracellular processes without disrupting the membrane uniformity, thus, there are other routes for their uptake by the cells. Examples of these routes are endocytosis and direct penetration [2]. Endocytosis includes receptor-mediated endocytosis and micropinocytosis [81]. Micropinocytosis includes folding of the cell membrane internally to create vesicles (macropinosomes) with the aid of special proteins called dynamins. Receptor-mediated endocytosis occurs by covering a membrane fragment with caveolin or clathrin proteins, followed by pit formation, which creates vesicles [82].

1.2.3. Important Structural Characteristics of Antimicrobial Peptides

To date, no information is available about the correlation between the mode of action of an antimicrobial peptide and its structure. Some peptides have similar configurations but they act in significantly different ways [31]. For instance, buforin inhibits RNA and DNA replication, whereas magainin 2 has a similar structure but acts on the cell membrane, leading to microbial cell lysis [83,84]. However, several studies have suggested important features of antimicrobial peptides. The structure is surely vital, while the charge, size, amphipathicity, and hydrophobicity are all critical physiochemical characters for their efficacy and selectivity [85]. Altering these characteristics may aid in modifying the activity and changing the action spectra of these peptides.

1.2.3.1. Charge

The number of ionizable moieties of antimicrobial peptides determines its net charge. The net charge of different peptides differs from positive to negative, and it is the main determinant of preliminary electrostatic interactions with negatively-charged components of cell membranes. By altering the net charge in a peptide sequence, its antimicrobial and hemolytic effects may be changed to increase the selectivity against microbial cells without harming host cells. For example, in the case of V13K, the net charge is +8; changing it to +9 increases its hemolytic effect, whereas reducing it to ≤+4 ends its effect toward *Pseudomonas aeruginosa* [86].

1.2.3.2. Peptide Size

Peptide length is a significant factor because >7 amino acids are required to create amphipathic structures with hydrophilic and hydrophobic faces. The length needed for an antimicrobial peptide to cross the lipid bilayer of the bacterial cell membrane in the barrel mode is ≥8 amino acids for β-sheet peptides and ≥22 amino acids for α-helical peptides [87]. Moreover, the size also influences the secondary structure, mechanism of action, and toxic side-effects. For instance, melittin cytotoxicity toward rat erythrocytes was reduced 300-fold compared with the normal peptide if its length was reduced by 15 amino acids from the *C*-terminus [88]. This illustrates the importance of length when synthesizing new peptides.

1.2.3.3. Hydrophobic Characteristics

The selectivity and activity of an antimicrobial peptide are controlled by its hydrophobic character. Almost all natural antimicrobial peptides contain approximately 50% hydrophobic amino acids in their main sequence [85]. Increasing the hydrophobic properties over the cationic character may, within limits, increase the effect on microbes [89], and lowering the hydrophobic character can diminish the antimicrobial effect [90]. Many researchers have suggested that each peptide should have an optimal hydrophobicity, a large deviation from it will lead to a decline in efficacy [91]. Consequently, when synthesizing a new antimicrobial peptide, one should consider the optimal hydrophobicity. Furthermore, several studies have shown that hydrophobic characteristics can influence the selectivity and the range of activity of an antimicrobial peptide. Increasing the number of hydrophobic moieties in the peptide sequence may alter the range of activity [92,93]. For example, magainin is selectively active

against Gram-negative bacterial cells, but, by increasing the hydrophobicity of some derivatives, they can also affect many Gram-positive bacterial cells [94].

1.2.3.4. Amphipathic Characteristics

The amphipathic character is a very important factor influencing the activity of antimicrobial peptides. It determines the ability of the peptide to interact with microbial cell membranes. Previous studies showed that the amphipathic behavior of peptides is much more important than their hydrophobic characteristics for the interaction with microbial cell membranes [95]. The amphipathicity is needed for the interaction with the cell membrane components. Therefore, the amphipathic characteristics of an antimicrobial peptide should be considered before thinking about other factors during the novel peptide design process.

1.2.4. Effect of Antimicrobial Peptides on Antibiotic-Resistant Microbes

Antimicrobial peptides can target antibiotic-resistant cells such as persister cells (cells showing multidrug tolerance) and biofilms. Highly-resistant pathogens can create biofilms, which are stable bacterial colonies connected to surfaces such as medical implants and human tissues. Biofilms are extremely resistant to antibiotics because of the protective matrix covering the bacterial cells [96].

1.2.4.1. Effect of Antimicrobial Peptides on Persister Cells

Persister cells are usually dormant phenotypic modifications of the normal microbial cell and are extremely resistant to antimicrobials such as *E. coli* HM22 persister cells [97]. However, the integrity of their cell membranes is vital regardless of the cellular metabolic state. Therefore, antimicrobial peptides can affect persister cells by effectively targeting their cell

membranes. For example, (RW)$_4$-NH$_2$, a chemically synthesized peptide, can kill >99% of *E. coli* HM22 persister cells, and, at a concentration of 40 μM, it lowered the number of persister cells in biofilms by approximately 98%. Furthermore, the addition of 5 μg/mL ofloxacin to (RW)$_4$-NH$_2$ had a highly synergistic effect because they completely eradicated living cells (including persister cells) in biofilms of *E. coli* HM22 [98].

1.2.4.2. Effect of Antimicrobial Peptides on Biofilms

The matrix of biofilms is negatively-charged, which is the main reason for the choice of antimicrobial peptides for controlling biofilms, because of the probable electrostatic interactions between them [99]. Many studies have shown inhibitory and killing effects of peptides on bacteria in biofilms. For example, lactoferrin can inhibit the formation of *P. aeruginosa* biofilms at lower concentrations than are needed to kill the planktonic bacteria [100]. Coating the surfaces of medical implants with peptides can inhibit the formation of biofilms without any harm to the eukaryotic cells [101]. The negatively-charged biofilms are usually made by bacterial cells to protect themselves against antibiotics. These biofilms can lower the dispersion of antibiotics toward cells. Antimicrobial peptides should have the ability to diffuse freely through biofilms and kill the bacterial cells inside them.

1.2.5. Bacterial Acquired Resistance Against Antimicrobial Peptides

Bacteria can resist the action of peptides through two main mechanisms: structural resistance and induced resistance. Induced resistance includes modifications of the microbial cell membranes, stimulation of enzymes, expression of efflux pumps to eject peptides out of cells, and alterations to targets inside cells. Structural resistance includes the formation of biofilms

and variations in membrane potential [102]. For example, *S. aureus* can inhibit the activity of peptides by changing the membrane potential. It can produce polymers (adhesins) with positive charge, which adhere to the outer cell membrane. This positively-charged barrier can inhibit the diffusion of cationic peptides by repulsion [103].

Although microbes have several mechanisms for resisting the action of peptides, the structure of the lipid bilayer in the bacterial cell membrane renders it difficult to acquire full resistance to peptides. Furthermore, the resistance acquired by microbes is not like that acquired against other types of antibiotics, and resistance has been reported to only a limited number of peptides.

1.3. Quorum-sensing Peptides

Some bacterial gene expression is regulated depending on the density of the cells, a phenomenon named quorum-sensing (QS). QS includes the formation of signal compounds, termed autoinducers. These autoinducers are ejected from bacterial cells at a specific concentration, leading to the stimulation of certain receptors and regulation of gene expression [104]. The QS genes can activate many biological functions, such as biofilm formation, bioluminescence, and the biosynthesis of antibiotics and virulence factors [105]. Both Gram-positive and Gram-negative bacteria can communicate using QS, and their autoinducers have different structures. Gram-negative bacteria mostly produce *N*-acyl homoserine lactone compounds termed autoinducer-1 (AI-1). Gram-positive bacteria depend on oligopeptide derivatives called autoinducer peptides (AIP) for their communications by

QS [106]. Boron-furan derivative autoinducers (AI-2) are the third type of signal compounds, found in both Gram-positive and Gram-negative bacterial strains [107].

AIPs produced by Gram-positive bacteria include heterogeneous categories of peptides. They are biosynthesized on bacterial ribosomes and modified to the active form during their release from the cell. Generally, the excretion of AIPs from the cell membrane is assisted by an active transport mechanism. When the cell-density surges, the AIP concentration consequently increases in the surroundings. Once the AIPs reach a threshold concentration, they bind to a specific receptor. This receptor starts the stimulation of receptor kinase through phosphorylation of a histidine residue. The stimulated receptor kinase activates the intracellular response regulator by the phosphorylation of an aspartic acid residue [108]. The stimulated response regulator controls specific gene transcription. The QS process differs in the receptors and the genes they control. For example, the QS system of *Bacillus* strains is called Rap-QS, staphylococci use the agr-QS system, and streptococci use the ComX-QS system [108].

AIPs are not only used for communication between bacteria as they possess other biological effects; one example is the antimicrobial nisin, which was isolated from *Lactococcus lactis* [109].

1.4. Research Objectives

The emerging global catastrophe of antibiotic resistance acquired by virulent bacteria has highlighted the need to explore alternatives to the currently available antibiotics. Immediate action is required to reduce the death toll due to antibiotic resistance, otherwise it will exceed

10 million per year by 2050. Antimicrobial peptides are one of the most encouraging candidates to address that problem because they possess high selectivity for prokaryotes, and affect the bacteria *via* a unique mode of action. Standard antibiotics have selective mechanisms of action that can become tolerated by bacteria, whereas peptides induce their effect through electrostatic binding with bacterial cell membranes, followed by cell wall penetration and cell death. This unique mechanism prevents the emergence of complete bacterial resistance.

This study investigated properties of new cationic antimicrobial peptides, such as their continuous activity that was discussed in Chapter 2. That was confirmed by cell viability assays using 30 times the standard bacterial concentration, which showed the ability of these peptides to kill >80% of the bacteria. In Chapter 3, highly potent, fast-acting, novel antibacterial peptides were synthesized having a similar inhibitory effect on various pathogenic bacteria to that of the aminoglycoside antibiotic gentamycin sulfate. This chapter shows that a rigid cyclic form of peptides is not always the most effective form; sometimes linear peptides can assemble into more effective secondary structures than their cyclic counterparts. In Chapter 4, *S. aureus* AIP-III, an example QS peptide, was chemically synthesized by a simple technique. *N*-(3-Dimethylaminopropyl)-*N*-ethylcarbodiimide hydrochloride (EDCI.HCl) and 4-dimethylaminopyridine (DMAP) were used for the thiolactone ring formation. An AIP-III antagonist with a bicyclic structure was also designed and synthesized for the expected competitive inhibition of agr receptors.

Chapter 2

Design and Synthesis of a New Amphipathic Cyclic Decapeptide with Rapid, Stable, and Continuous Antibacterial Effect

2.1. Introduction

Antimicrobial agents can act as double-edged swords, as they can affect the targeted microorganisms but also have harmful effects on the host cells [1–3]. The most effective antimicrobial agents exhibit high selectivity toward a microorganism's cells without affecting the mammalian cells. In addition, microorganisms should show no resistance towards the antimicrobial agent during the treatment. Recently, antimicrobial peptides produced by some types of fungi have been reported to have rapid and strong effects on microorganisms *via* the degeneration of the cell membranes [4]. The degradation end products of such peptides are amino acids, which indicates their potential safety. Thus, many researchers have investigated this type of peptide antibiotic, especially the natural antimicrobial decapeptides, for example, streptocidins and tyrocidins. There are two types of natural peptides, cyclic and linear peptides. Some examples of cyclic peptides include the streptocidins [5], the tyrocidins [6], gramicidin S [7], and the loloatins [110]. Examples of linear peptides include gramicidins A, B, and C [111]. The overall charge of the bacterial cell membrane plays an important role in biological efficacy. It has been shown that most bacterial cell membranes carry negative charges because of the presence of lipoteichoic acid moieties linked to either peptidoglycan or the plasma membrane. The lipoteichoic acid

moieties are negatively charged because of the presence of phosphate ions in their chemical structure [112]. Therefore, bacterial cell walls prefer adhesion to positively charged surfaces rather than negatively charged surfaces. In addition, it has been found that there is no bacterial growth after the adhesion to positively charged surfaces [113].

The hydrophobic residues of peptides are important for the penetration into the bacterial cell wall. These hydrophobic residues can construct a nonlamellar phase *via* a self-assembly process inside the lipid bilayer of the bacterial cell wall [9]. In addition, alanine, valine, and leucine have been investigated for their importance as aliphatic amino acids, to facilitate the formation of secondary structures in the bacterial cell membrane and to increase the solubility of peptides [10].

 Herein, a new anti-bacterial cyclic decapeptide and its linear counterpart were designed (Figure 2.1) and investigated in terms of antibacterial behavior against standard and high concentrations of bacteria. Positively charged moieties incorporated in peptides encourage adherence with the negatively charged bacterial cell wall. For that purpose, four lysine amino acid residues were incorporated into the decapeptides to serve as the source of positive charges. In addition, increasing the hydrophobicity of the whole molecule was achieved by incorporating leucine, valine, tryptophan, tyrosine, and phenylalanine into the decapeptide structure to increase the penetration of the whole peptide inside the bacterial cell membrane. The antibacterial effect was studied against the Gram-positive *Bacillus thuringiensis* and Gram-negative bacterial strain *Escherichia coli*. The minimal inhibitory concentration (MIC) values were determined. Time-kill studies were conducted for both forms of the decapeptides

30

against *E. coli*. Cell viability assays were performed using a high concentration of *E. coli* to study the ability of the antibacterial peptides to overcome and control a source of infection by investigating the maximum killing effect of their secondary structures.
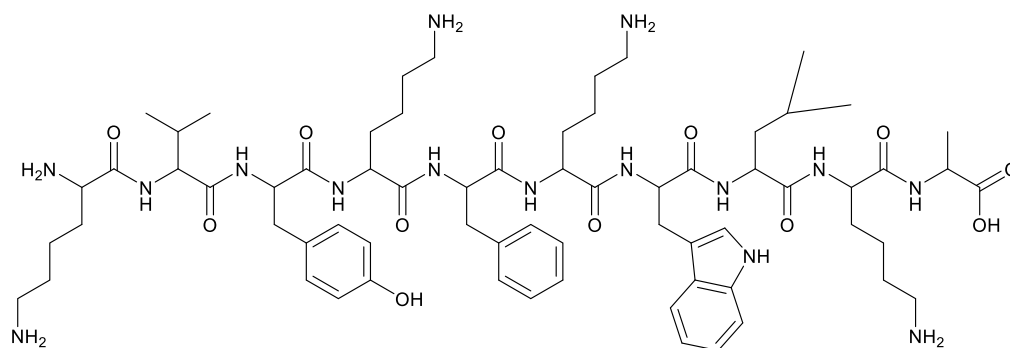
1
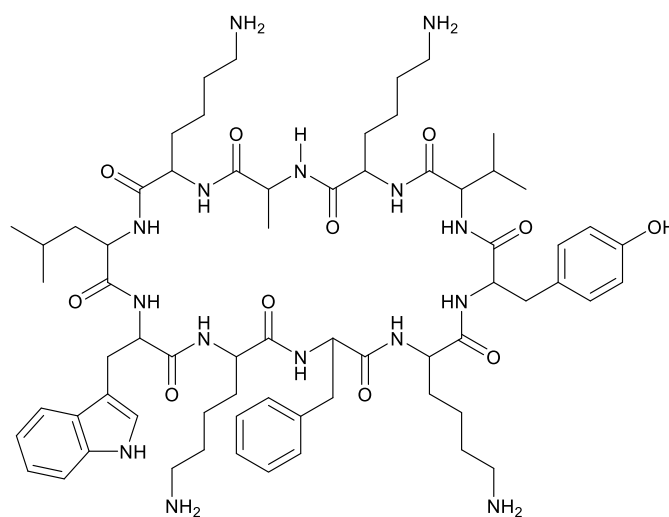
2

Figure 2.1. Design of the linear (**1**) and cyclic (**2**) antimicrobial decapeptides (KVYKFKWLKA).

2.1.1. Previous Studies

The cyclic octapeptide [R4W4] (Figure 2.2) was synthesized and showed a strong antibacterial effect against *Staphylococcus aureus* (methicillin-resistant), and *P. aeruginosa* while, MIC values were 1.95, and 31.3 μM, respectively. [R4W4] was investigated for its synergistic effect with tetracycline, they can together afford high activity against resistant bacteria.
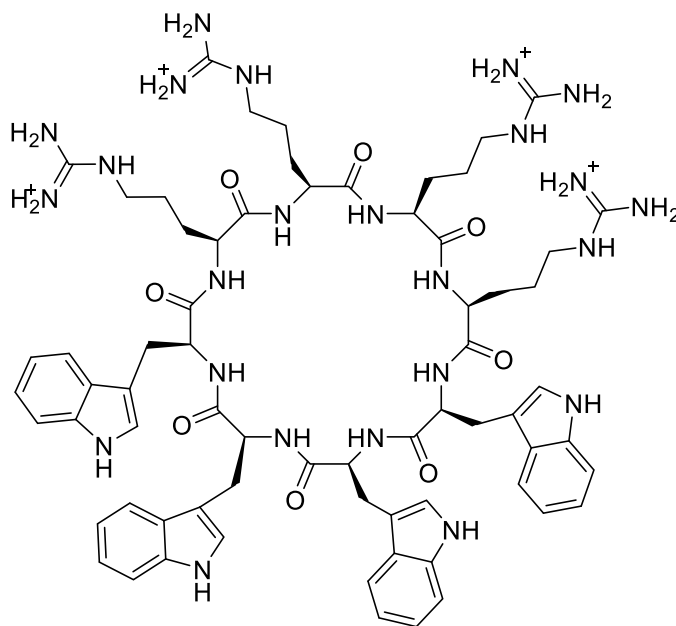

Figure 2.2. Structure of [R4W4].
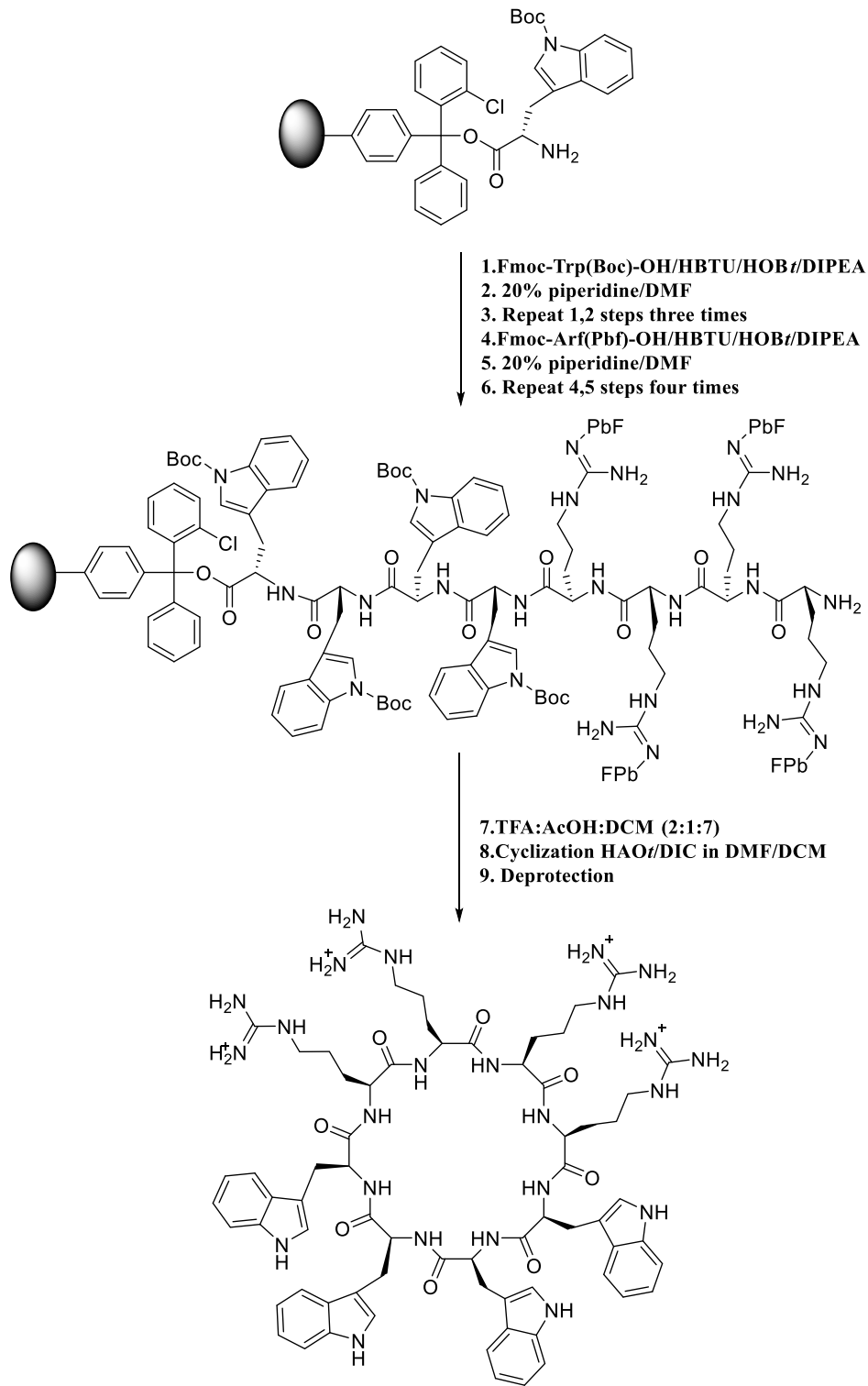
Scheme 2.1. The synthetic protocol of the cyclic octapeptide [R4W4].

As illustrated in scheme 2.1, First, H-Trp(tert-butyloxycarbonyl (Boc))-2-chlorotrityl resin (0.35 mmol) was swollen in dimethylformamide (DMF) for 40 min. Then, 3 successive couplings of Fmoc-Trp(Boc)-OH (1.05 mmol) were carried out using *O*-benzotriazole-*N,N,N',N'*-tetramethyl-uronium-hexafluorophosphate (HBTU 1.05 mmol), 1-hydroxy-benzotriazole hydrate (HOB*t* 1.05 mmol), and *N,N*-diisopropylethylamine (DIPEA 2.1 mmol) in DMF. At every coupling step, the resin and reactants were agitated under N_2 for 60 min. To eliminate the Fmoc group after each coupling, piperidine in DMF [20% (v/v)] was applied. The subsequent Fmoc- Arg (2,2,4,6,7-pentamethyl-dihydro benzofuran-5-sulfonyl (pbf))-OH (1.05 mmol) coupling was carried out four times in a similar procedure. Cleavage of the protected linear peptide from the resin was conducted with trifluoroethanol (TFE)/CH_3COOH/CH_2Cl_2 at a ratio of [2:1:7 (v/v/v)] for 60 min. After evaporation and drying of the filtrate in a vacuum, the cyclization was achieved under diluted conditions. 1-Hydroxy-7-azabenzotriazole (HOA*t* 1.4 mmol) and N,N′-Diisopropylcarbodiimide (DIC 1.54 mmol) were added to a solution of the linear peptide in an anhydrous DMF/DCM mixture [5:3] and this mixture was allowed to stir for 12 h under N_2. Then, to remove sidechain protecting groups, the solvent was evaporated and a reagent mixture of trifluoroacetic acid/thioanisole/ 1,2-ethanedithiol/anisole at a ratio of [90:5:3:2] (R) was applied and stirred for 2 h. The peptide was crystallized and purified by a preparative RP-HPLC system. The structure was confirmed by an AXIMA performance matrix-assisted laser desorption ionization time-of- flight (MALDI-TOF) spectrometer.

One of the drawbacks of this synthesis is the low yields of the products [114].

Other studies were carried out on cyclic hexapeptides and cyclic octapeptides derivatives as described in figure 2.3.
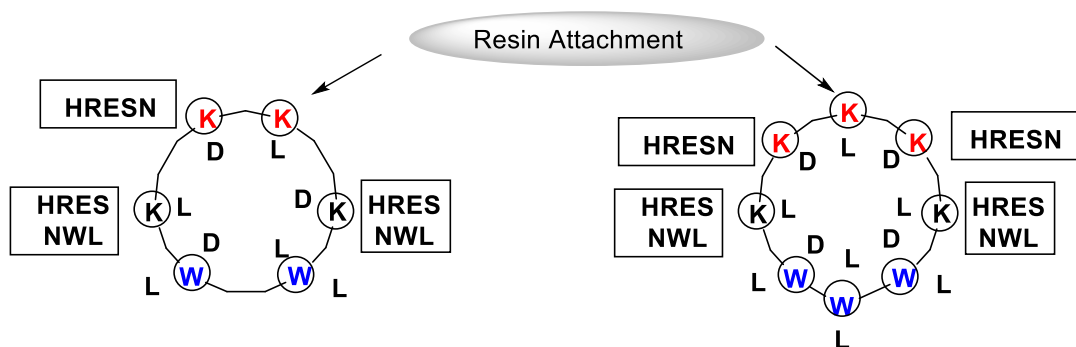
Figure 2.3. Design of synthetic antibacterial cyclic peptides

Using standard Fmoc solid-phase protocols, peptides were prepared on the Fmoc–Lys–O-allyl ester-preloaded 2-chlorotrityl chloride resin. Coupling reactions were conducted over times ranging from 4 to 12 h. These couplings were achieved manually or in an automated peptide synthesizer.

After the complete synthesis of the linear peptide, the peptide-resin was swollen in CH_2Cl_2 for 20 min. Then, 0.5 eq Pd(PPh$_3$)$_4$ in 90% DCM–10% phenyl silane was added to the resin and allowed to be stirred under N$_2$ for 2 h. After the final Fmoc deprotection (using 25% piperidine/DMF), the resin was thoroughly washed with DMF, 10% DIEA-DMF, and 0.8 M LiCl-DMF.

The peptide was cleaved from the resin by washing with DMF and DCM, followed by washing with Methanol. The deprotection was carried out using 95% trifluoroacetic acid, 2.5% H_2O, 2.5% triisopropylsilane for 2 h. Finally, peptides were crystallized with Et$_2$O and

purified by RP-HPLC. In addition, this synthetic process showed low yields of the products [115].

In our study, cyclic peptides were synthesized with high yields (45%, and 75%) compared with other studies. Besides, the hydrophobic and hydrophilic groups were subsequently located within the sequence. Our synthetic goals are to increase the production yield of the cyclic peptides and to reduce the positively charged residues.

2.2. Materials and Methods

2.2.1. Synthetic Protocol

The linear decapeptide H-KVYKFKWLKA-OH (peptide **1**) was designed to contain cationic residues (four lysine residues) to interact with the negatively charged bacterial membrane. Hydrophobic residues were added to the structure (tyrosine, tryptophan, and phenylalanine) to interact with the membrane lipids. In addition, aliphatic residues were incorporated to improve the interaction with the bacterial membrane receptors and to increase the solubility of the peptide. The cyclic decapeptide KVYKFKWLKA (peptide **2**) was synthesized to study the difference in the antibacterial effect of the rigid cyclic structure compared with the linear peptide. Peptide **1** [molecular weight (MW) ~1310] was prepared *via* the standard solid-phase peptide synthesis method using 9-fluorenylmethoxycarbonyl (Fmoc) chemistry (as shown in Scheme 2.1) and 2-chlorotrityl resin as the solid support [11]. All Fmoc-protected amino acids, resin, piperidine, HBTU, HOBt·H$_2$O, DIPEA, and 2,2,2-trifluoroacetic acid (TFA) were purchased from Watanabe Chemical Industries, Ltd, Japan. Other reagents and solvents were purchased from Wako Pure Chemical Industries, Ltd, Japan.

As shown in Scheme 2.2, the synthesis was started by loading an alanine amino acid onto 2-chlorotrityl chloride resin. Fmoc-L-amino acid residues were then coupled to the loaded alanine residue using HBTU, DIEA, and HOBT in *N,N*-dimethylformamide (DMF) as the solvent for the coupling process. The Fmoc protecting groups were removed using 20% (v/v) piperidine in DMF. The cleavage of the side-chain protected linear decapeptide from the resin was performed using a mixture of 2,2,2-trifluoroethanol/acetic acid/dichloromethane at a ratio of 3:1:1 (v/v/v) [12]. Purification was performed using a semi-preparative RP-HPLC Hitachi L-7100 instrument equipped with an XTerra Prep MS C18 OBD 10 μm column (19 × 150 mm; Waters). The mobile phases were acetonitrile containing 0.1% TFA, and H_2O containing 0.1% TFA, and the peak intensity was determined at a wavelength of 220 nm [13].

The removal of the side-chain protecting groups was achieved using a mixture of TFA/tris isopropyl silane (TIS)/H_2O at a ratio of 95:2.5:2.5 (v/v/v). Lyophilization was carried out in a VD-800F freeze dryer (TAITEC) to obtain the linear decapeptide **1**. The cyclization reaction was achieved using a concentration of 0.5 mM of the linear decapeptide **1** to avoid dimer formation. Two equivalents (Equiv.) of HBTU and 5 Equiv. of DIPEA were used for the cyclization process. The removal of the protecting groups of the cyclic decapeptide was carried out using TFA/TIS/H_2O in a ratio of 95:2.5:2.5 (v/v/v). Purification was achieved using semi-preparative RP-HPLC followed by lyophilization to yield the target cyclic decapeptide **2** [116].

2.2.2. Experimental Section

2.2.2.1. Loading of Fmoc-Ala-OH onto Barlos resin

Table 2.1. Calculating the amounts of the loading reaction compounds.

Compound name	MW.	Equiv.	mmol	gm or mL
Barlos resin		1	1.6	1 gm
Fmoc-Ala-OH	311.33	0.3	0.48	0.16 gm
DIEA	129.25	0.5	0.8	0.14 mL
DIEA:DCM 1:1		1	1.6	0.56 mL
Methanol				1 mL

Calculations

- Weight of Fmoc-Ala-OH = Equivalence×resin capacity (mmol/g)/1000 × Molecular weight (MW) = (311.33×0.48)/1000 = 0.16 g.

- Weight of DIEA = Equivalence×Resin capacity×Molecular weight.

- Volume of DIEA = 129.25/[0.742 (density)×1000] = 0.14 mL.

- DIEA:DCM (1:1) = 0.28+0.28 = 0.56 mL.

- Theoretical weight calculations:

- Increase in resin weight (Methanol capping) = 1.6 − 0.48 (Fmoc AA) = 1.12 mmol.

- 1.12×32.04 (MW. of methanol) = 36 mg / 1000 = 0.036 g.

- Decrease in resin weight = 1.6×35.453 (Cl MW.) = 56.7 mg / 1000 = 0.057 g.

- Theoretical weight = 1 gm (resin) + 0.16 gm (Fmoc AA) + 0.036 g (methanol) - 0.057 (Cl) = 1.14 g.

Procedures

In the SPPS reaction vessel (118.710 g):

1 g barlos resin was added, then washed twice with 15 mL DCM until complete swelling. 0.16 g of Fmoc-Ala-OH, 15 mL DCM and 0.14 mL DIEA were added, respectively. the reaction mixture was stirred for 5 min (manually), then 0.56 mL of (DIEA:DCM) at a ratio of (1:1) was added and stirred for 1 h. 1 mL methanol (capping unreacted sites) was added and stirred for 10 min, subsequently, the reaction solvents were removed by a suction pump. The resin was washed using 15 mL DCM (twice), 15 mL DMF (twice), 15 mL isopropanol (twice), 15 mL DMF × 2, 15 mL isopropanol (twice), 15 mL methanol (twice), and 15 mL ethyl ether (twice). Drying under reduced pressure for 1 h was performed. Finally, the resin was weighed and the yield was calculated (119.84 g) i.e. 1.13 g.

% yield = (1.13\1.14)×100 = 99%.

- Loading-rate measurement of Fmoc Alanine-resin:

In three 10 mL volumetric flasks, 1-3 mg of Fmoc-Ala-resin was added with 20% piperidine in DMF until the 10 mL sign was reached. After waiting for 30 min at room temp, two blank samples from 20% piperidine in DMF were prepared. Absorbance values were measured at 290 nm for all samples.

Table 2.2. Measuring of the loading rate.

Sample No.	Resin weight (mg)	A290 nm	Loading-rate (mmol/g resin)
1	1.5	0.33	0.44
2	2.5	0.5	0.4
3	3	0.65	0.44

Loading rate can be calculated from the following equation:

Loading rate = 1000×10×A290 nm/4950 (Fmoc molar absorptivity)×1×weight

=   mmol/g resin.

Mean loading rate/g = 0.43 mmol/g.

Actual Loading rate = 0.43×1.13 = 0.48 mmol.

%Yield = (0.48/0.48) ×100 = 100%.

2.2.2.2. Peptide Chain Elongation.

2.2.2.2.1. Addition of Fmoc-K (Boc)-OH

Table 2.3. Calculating the amounts needed for the addition reactant.

Compound	g/mol	Equiv.	mmol	G or mL
Fmoc-Ala-resin		1	0.5	1.13 g
Fmoc-K (Boc)-OH	468.54	2	1	0.47 g
HBTU	379.45	2	1	0.38 g
HOBt.H$_2$O	153.14	2	1	0.153 g
DIEA	129.25	4	2	0.35 mL

Calculations

Weight of Fmoc- K (Boc)-OH = 469/1000 = 0.47 g.

Weight of HBTU = 1/1000×379.25 = 0.38 g.

Weight of HOBt.H$_2$O = 1/1000×153.14 = 0.153 g.

Volume of DIEA = (2/1000×129.25)/0.742 = 0.35 mL.

Procedures

- Deprotection:

In the SPPS reaction vessel, the Fmoc-protected AA-resin was washed twice by 15 mL DMF until the complete swelling of the resin. 30 mL of 20% piperidine in DMF was added and stirred for 30 min. The reaction mixture was removed and then washed with 15 mL DMF (twice), 15 mL isopropanol (twice), and 15 mL DMF (twice), respectively.

- Coupling:

In the SPPS reaction vessel, the Fmoc-AA-OH was added with 15 mL DMF, HBTU, and HOBt.H$_2$O. Then stirred for 2h, consequently, the reaction mixture was removed and washed with 15 mL DMF (twice), 15 mL isopropanol (twice), 15 mL DMF (twice), and 15 mL DCM (twice), respectively.

A series of coupling reactions were continued until the sidechain protected decapeptide was completely synthesized. Finally, the Fmoc group was removed and the peptide-resin was washed as discussed before, followed by washing with diethyl ether (twice). Consequently, peptide-resin was dried under reduced pressure using a desiccator. The powder was weighed (1.85 g) and the %yield was calculated as follows: %yield = (1.850/1.862) × 100 = 99%.

2.2.2.3. Cleavage from Resin

Trifluoroethanol (TFE) promotes the hydrolysis of ester linkage between the peptide and resin without affecting the sidechain protecting groups, which are cleaved by the addition of trifluoroacetic acid. Therefore, a cleavage cocktail (DCM:TFE:acetic acid) was used at a ratio of 1:3:1 (v/v/v).

Procedures

In the SPPS vessel, the cleavage cocktail was added and rotated using an electric rotator for 2 h at room temperature. The filtrate was collected in a 100 mL round bottom flask (73.589 g) and evaporated under reduced pressure. 2 mL of water was added to the residue to crystallize the protected peptide as white crystals. The crystals were dried under reduced pressure for 1 h, weighed (0.85 g) and the %yield was calculated. The product was checked for its degree of purity by the RP-HPLC as shown in figure (2.4) which showed the relatively high purity of the synthetic process.

% Yield = (0.85/0.862) × 100 = 99%.
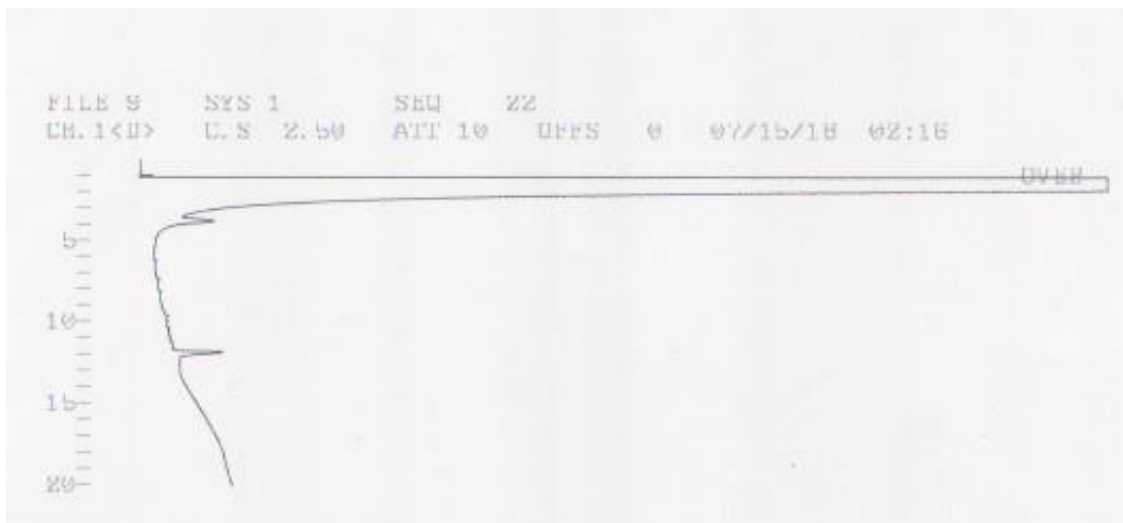
Figure 2.4. HPLC chart of the protected sidechain linear peptide with RT = 11.81 min

2.2.2.4. Cyclization

Cyclization reaction was carried out by using a concentration of less than 0.5 mM of the linear peptide to avoid dimer formation. 2 Equiv. of HBTU and 4 Equiv. of DIEA were used for the cyclization. The reaction was monitored by RP-HPLC as shown in figure (2.5).
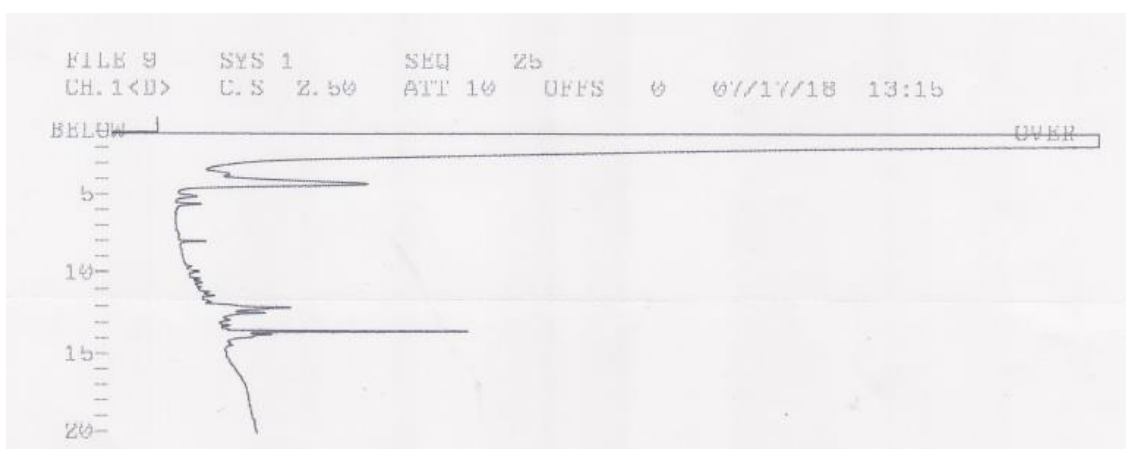
Figure 2.5. HPLC chart during cyclization of the sidechain protected linear peptide.

2.2.2.5. Deprotection of Sidechain Protecting Groups

Removal of the sidechain protecting groups was carried out using TFA:TIS:H_2O at a ratio of 95:2.5:2.5 (v/v/v). The reaction was monitored by RP-HPLC for 2 h, followed by purification by a semi-preparative RP-HPLC [as shown in the figures (2.6), and (2.7)].
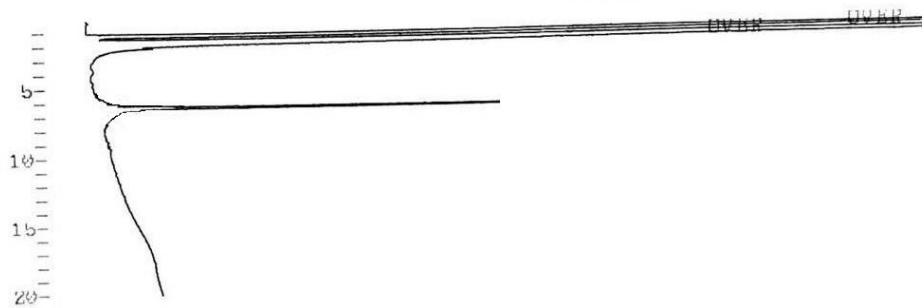
Figure 2.6. RP-HPLC chart of the pure linear peptide with a sharp peak at 6.2 min.
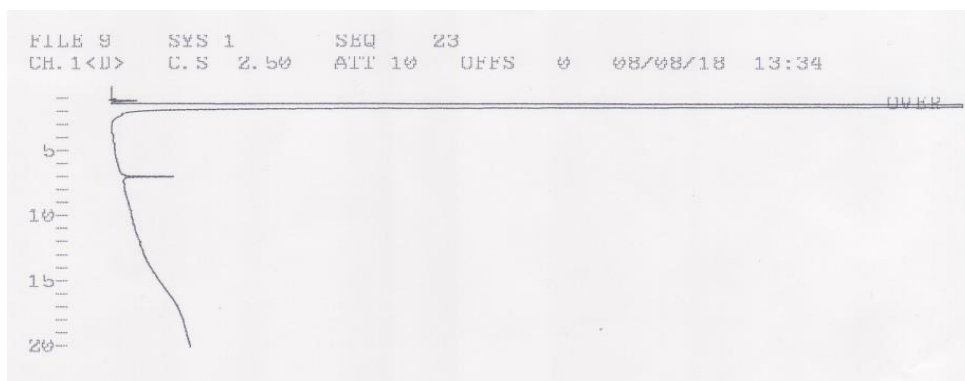
Figure 2.7. RP-HPLC chart of the pure cyclic peptide with RT = 6.89 min
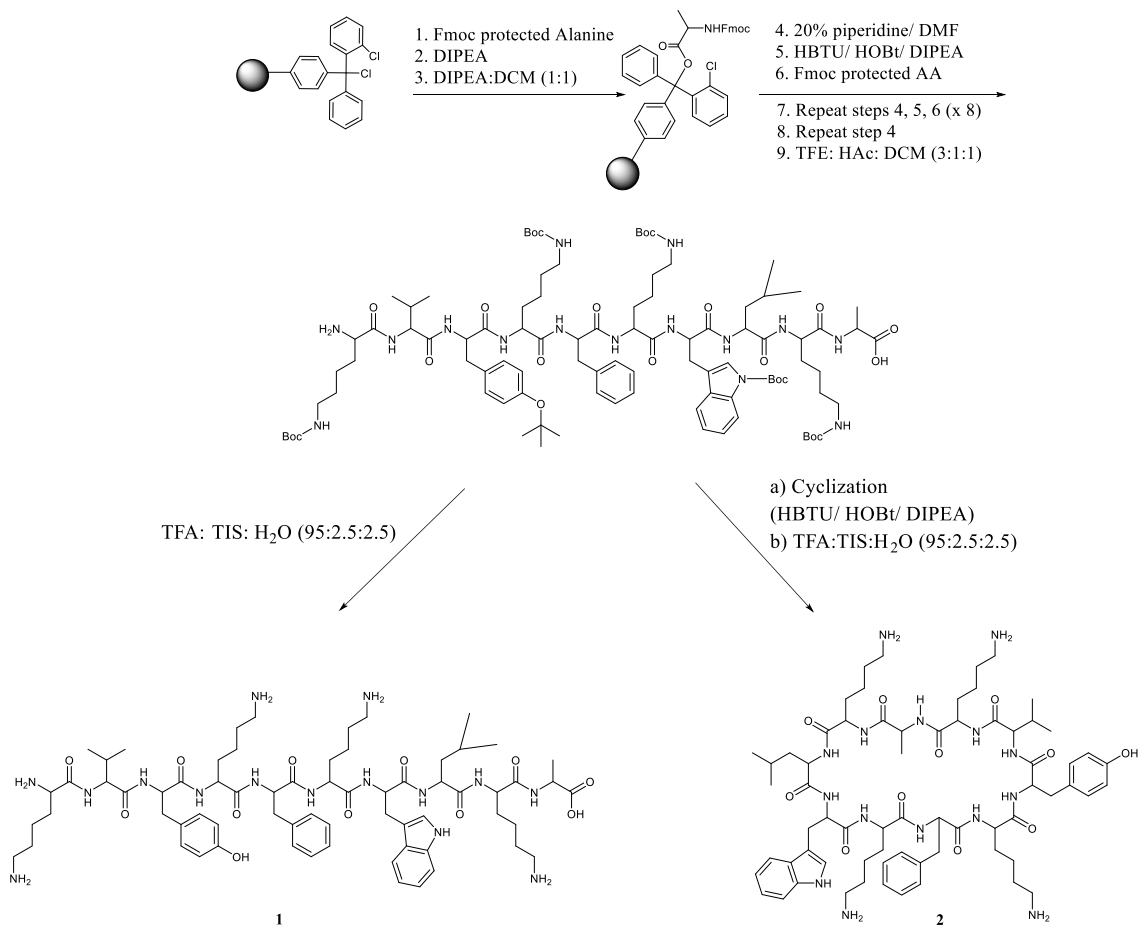
Scheme 2.2. The synthetic protocol of the linear and cyclic decapeptides

(KVYKFKWLKA).

2.2.3. Antibacterial Assay

2.2.3.1 MIC Evaluation

MIC values were determined by the broth microdilution method using 96-well microplates

[117]. *E. coli* and *B. Thuringiensis* bacterial strains were chosen to determine the broad-

spectrum effect of the cyclic decapeptide and the linear counterpart against both Gram-

positive and Gram-negative bacterial strains. The bacterial strains were inoculated in a

freshly prepared Luria Bertani (LB) broth medium at a temperature of 37 °C (for *E.coli*), and in a freshly prepared tryptic soy broth at a temperature of 27 °C (*B. thuringiensis*). Both bacterial strains were shaken at 160 rpm overnight. The cultures were diluted up to 5×10^5 CFU/mL (OD_{600} = 0.05). The cyclic and linear decapeptide solutions were prepared by dissolving each peptide separately in distilled water at a concentration of 1 mg/mL. The stock solutions were diluted across 96-well microplates by 2-fold serial dilution using the growth media to reach a total volume of 200 µL. Negative controls were used to ensure the adequate growth of the bacteria. Kanamycin and ampicillin, 0.25, and 0.5 mg/mL solutions, respectively, were used as positive controls. The bacterial cultures were inoculated with the test and control compounds and incubated for 24 h at the designated temperatures for each bacteria. MIC values were determined as the minimal concentration where no visible bacterial growth was detected. All experiments were carried out in triplicates.

2.2.3.2 Time-Kill Assays

Time-kill assays were performed using *E. coli* and 96-well microplates with clear bottoms (Nunclon™ Surface, Denmark). The bacterial culture was prepared as previously described. The killing effect was measured *via* a colorimetric assay using dimethyl sulfoxide (DMSO), and water-soluble tetrazolium salt (WST-8) reagent (Microbial Viability Assay Kit-WST, Dojindo, Japan). The Kit-WST can detect viable bacterial cells by a colorimetric assay. DMSO acts as an electron carrier, it carries electrons from the viable cells to WST causing a change in color from yellow to orange because of the formation of WST-8 formazan. The color change can be detected by a microplate reader at a wavelength of 460 nm. A blank was made by the media, tested peptide, and the Kit-WST. Peptides **1** and **2** were tested at two

times the MIC values. Runs without the antimicrobial agents were performed to confirm the adequate growth of the bacteria (negative controls). The bacterial culture was added to the tested peptides and incubated in a shaking incubator at 37 °C for 24 h. The absorbance values were measured using a microplate reader (Perkin Elmer, USA) at 460 nm at different time intervals, 1, 6, and 24 h, to determine the surviving bacterial cells. The readings were subtracted from the reagent blank and compared with the negative control to determine the %viability. From the %viability data, the %killing can be determined for the tested peptides. Time-kill assays were conducted in triplicates.

2.2.3.3 Bacterial Cell Viability Assays

Measuring cell viability was achieved by two methods. The first method was carried out by counting colony-forming units (CFU) on freshly prepared agar plates, while the other method used a colorimetric assay in 96-well microplates with clear, flat bottoms (Nunclon™ Surface, Denmark) using Kit-WST reagent. The *E. coli* bacterial strain was used at a high concentration (OD_{600} = 1.6), equal to 32 times the concentration used in the previously described assays (OD_{600} = 0.05). Peptides **1** and **2** were used at the following concentrations: 0.5, 0.25, 0.14, and 0.04 mg/mL. The bacterial cells were cultured in LB broth, then harvested at 4000 r.p.m for 10 min. The precipitated pellets were re-suspended in phosphate-buffered saline (PBS), at a pH of 6.8, and divided into equal volumes, one for each peptide concentration. The treated bacterial solutions were incubated at 37 ◦ C for 12 h, then diluted serially by 2-folds up to three times. Portions (180 µL) of the diluted bacterial suspension were expanded using freshly prepared agar plates incubated for 24 h at 37 ◦ C. Another set of 180-µL portions was added to a 96-well microplate and mixed with 20 µL of Kit-WST

reagent and incubated for 1 h. The absorbance was measured on a microplate reader (Perkin Elmer, USA) at 460 nm. Runs without the antimicrobial agents were carried out for both experiments. All the experiments were performed in triplicates

2.3. Results

2.3.1. Synthetic Protocol

The linear decapeptide **1** was synthesized using a standard Fmoc/ SPPS method as described above. The %yield of the obtained peptide **1** was approximately 97%, which was calculated by dividing the real obtained yield by the theoretical yield (calculated based on the loading rate equation of the first loaded amino acid) multiplied by 100. The structure and the purity were confirmed by mass spectrometry with a sharp peak at 1309.791 m/z (calculated value = 1309.791, chemical Formula: $C_{67}H_{103}N_{15}O_{12}$, 1309.791), as shown in figure 2.8 (a). Peptide **2** was obtained by cyclization of peptide **1** using HBTU and DIPEA as described above and the %yield was approximately 45% after the purification step. The structure and purity were confirmed by mass spectrometry with a sharp peak at 1292 m/z (calculated value= 1292, Chemical Formula: $C_{67}H_{101}N_{15}O_{11}$), as shown in figure 2.8 (b).

(a)
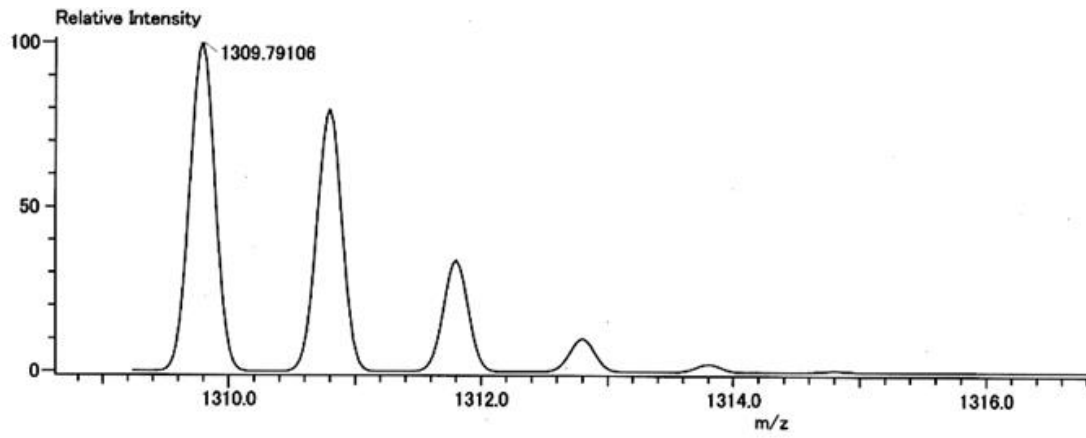
(b)
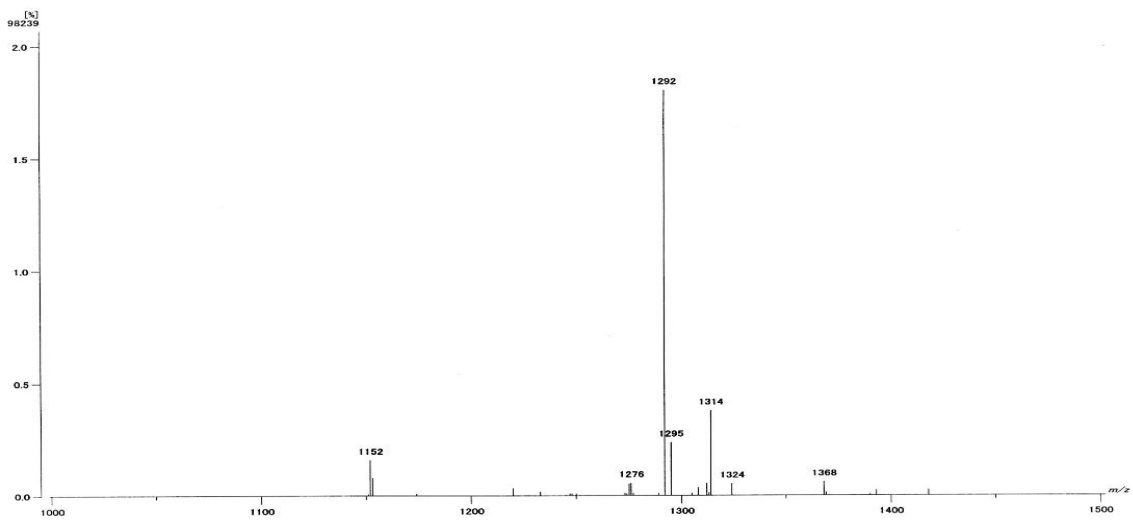
Figure 2.8. Mass spectra of peptide **1** (a) and peptide **2** (b).

2.3.2 Antibacterial Assays

2.3.2.1 MIC Evaluation

The MIC values against *E. coli* and *B. thuringiensis* were evaluated for both peptides as the minimum concentration of the peptides showing no visible growth of the bacteria. Peptide **2** was more effective against the Gram-negative bacteria than the Gram-positive bacteria with MIC values of 0.16 and 0.24 mg/mL, respectively. Peptides **2** and **1** showed similar efficacy against Gram-positive bacteria with a MIC value of 0.24 mg/mL. Peptide **1** was more effective against the Gram-positive bacteria than the Gram-negative bacteria with MIC values of 0.24 and 0.3 mg/mL, respectively. Ampicillin was used as a standard positive control for the Gram-positive bacteria and kanamycin was used as the positive control for the Gram-negative bacteria. MIC value for ampicillin was 0.03mg/mL and the MIC value of kanamycin was 0.015 mg/mL.

The positive controls, kanamycin sulfate, and ampicillin were used in the MIC assay and the MIC values are given above. The antibacterial effects of the positive controls were higher than those of the tested peptides. One of the most important issues with antimicrobial agents is the resistance acquired by bacteria against those antibiotics, which may be solved by the use of antimicrobial peptides. In addition, severe side effects can be caused by kanamycin, for example, kidney toxicity, loss of hearing, and allergic reactions [118]. Side effects observed with ampicillin include hypersensitivity, nausea, vomiting, and other gastrointestinal disorders [119]. Although the use of peptides is still under investigation, they

are considered to be safe as they are short peptides made of unmodified amino acids. Also, bacteria rarely show resistance toward them.

In general, cationic peptides act by attacking the bacterial cell membranes resulting in the degeneration of the lipid bilayer leading to cell death [120]. The amphipathic structures of both the synthesized peptides gave them the ability to penetrate the bacterial cell wall [121]. The cationic residues initiate electrostatic interaction forces toward the negatively charged bacterial cell membrane, while the hydrophobic moieties facilitate the penetration of the peptide [122]. In addition, this amphipathic structure encourages the peptides to act in a micellar fashion by covering small parts of the cell membrane before the diffusion through the lipid bilayer, which leaves holes across the cell membrane [123].

2.3.2.2. Time-kill Assays

E. coli is a major pathogen initiating numerous types of bacterial infections, which has developed multidrug resistance because of the chronic usage of antimicrobial agents. For these reasons, *E. coli* was chosen to perform the time-kill assay. The kit-WST reagent was used in this assay to detect the viable bacterial cells *via* a colorimetric technique using 96-well microplates. The reagent undergoes a reduction to WST-8 formazan by the action of NADPH from the viable bacterial cells. The resulting WST-8 formazan dye (orange color) can be determined by measuring the color intensity using a microplate reader at 460 nm.

The time-kill assay was used to determine the time needed for the peptides to exert the maximum antimicrobial effect against *E. coli* over 24 h (Figure 2.9). The time-kill assay can detect whether the bacteria show any resistance against tested compounds. Peptides **1** and **2**

showed a very rapid maximal bactericidal effect against *E. coli* ($\geq 99\%$) over 1 h of incubation at a concentration of two times the MIC value. *E. coli* exhibited a minimal regrowth after 24 h of approximately 9% for peptide **1**. The obtained data illustrated the rapid effect of both peptides **1** and **2** against the *E. coli* strain, and the highly stable bactericidal activity of peptide **2** over peptide **1**. In addition, the bacterial resistance against peptide **2** (the cyclic form) was negligible, while for peptide **1**, the bacteria showed a low level of resistance.
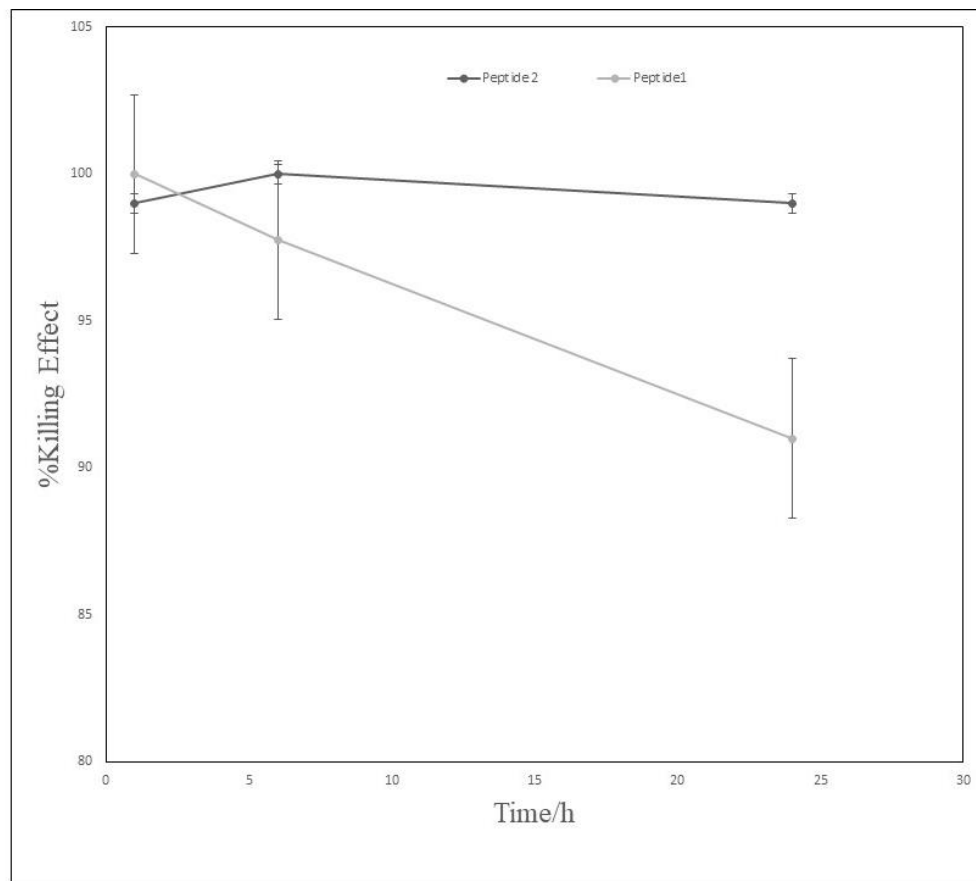
Figure 2.9. Time-kill assay of peptide **1** and peptide **2** using *E-coli*, the killing effect was measured at different time intervals (1, 6, and 24 h), at a peptide concentration of two times the MIC values during incubation at 37 ◦ C for 24 h.

2.3.2.3. Bacterial Cell Viability Assays

The *E .coli* strain was used at a high concentration to detect the efficiency and the continued action of peptides **1** and **2**. As shown in figure 2.10, both assays gave nearly the same results. For the CFU counting method, peptides **1** and **2** at a concentration of 0.5 mg/mL showed a maximum killing effect of 83% and 86%, respectively. While at a concentration of 0.25 mg/mL, the peptides showed the killing effects of 64% and 76%, respectively. At a concentration of 0.14 mg/mL, which is lower than the MIC values of both peptides, the killing effects were 58% and 65%, respectively. The lowest concentration of 0.04 mg/mL killed 21% and 30% of the bacterial cells, respectively.

The colorimetric assay confirmed the results obtained by the CFU counting method showing killing effects for peptide **1** of 71%, 56%, 24%, and 4% at concentrations of 0.5. 0.25, 0.14, and 0.04 mg/mL, respectively. Peptide **2** showed killing effects of 77%, 58%, 35%, and 16%, respectively. These data indicate that both peptides can form highly stable secondary structures at relatively high concentration levels. These structures had a maximum bactericidal effect, killing more than 80% of the total tested bacteria, after 12 h of incubation.
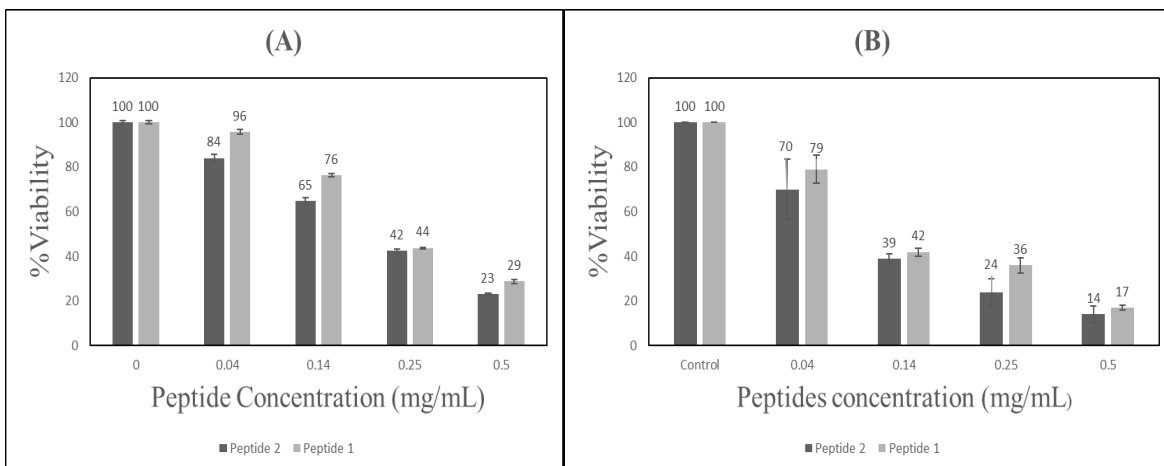
Figure 2.10. (A) Bacterial cell viability assay using Kit-WST reagent and (B) CFU counting method for the antibacterial screening of both cyclic (peptide **2**) and linear (peptide **1**) forms against *E.coli*.

2.4. Discussions

Antimicrobial peptides are oligopeptides having a different number of amino acid residues arranged in varying sequences. They are classified as cationic peptides, cationic amphipathic peptides, cationic host defense peptides, host defense peptides, anionic antimicrobial peptides/proteins, and α-helical antimicrobial peptides [124]. Peptides can attack a wide range of organisms from viruses to parasites. However, peptides have a selective effect on one type of microbes (e.g. antiviral, antibacterial, or antifungal peptides) [125]. Nevertheless, some peptides are exhibiting an effect on a wide range of microbes, for example, indolicidin can kill HIV, bacteria, and fungi [126].

Peptides kill microorganisms *via* numerous mechanisms of action [14,15]. However, antibacterial peptides act mainly by two mechanisms of action. The first method involves interaction with the bacterial cell membrane. Peptides need to possess an amphipathic character to achieve a proper interaction with the cell membrane. To have amphipathic character, the peptides need to include cationic and hydrophobic residues in the main structure of the designed peptide. These residues allow the peptide to interact with the bacterial cell membrane by electrostatic and hydrophobic forces. These interaction forces allow penetration of the peptide into the cell membrane resulting in cell death [122]. The other mechanism of antibacterial peptides is by affecting some essential cell components, such as DNA or other vital intracellular components [21].

Herein, an amphipathic linear decapeptide was synthesized by a standard Fmoc/ SPPS method. The reaction was continued as a one-pot synthesis from the loading of the first amino acid residue until the cleavage of the whole peptide. The purpose of this method was to increase the yield of the reaction and reduce the exposure to atmospheric humidity and oxygen, which have undesirable effects on the synthetic procedures. Both peptides were investigated for preliminary antibacterial action against Gram-positive and Gram-negative bacterial strains.

The MIC values were determined and the obtained results showed that peptides **1** and **2** had similar effects toward Gram-positive bacteria, while peptide **2** showed a higher effect against Gram-negative bacteria than peptide **1**. This is because of the difference in the bacterial cell wall structure between the two strains. As shown in figure 2.11. (A) and (B), the Gram-

negative bacterial cell wall mainly consists of a thin, negatively charged, peptidoglycan layer covered with an outer envelope of lipopolysaccharide. While Gram-positive bacteria (C) have a thicker peptidoglycan layer but lack the outer hydrophobic lipopolysaccharide envelope [112]. Thus, the more hydrophobic peptide **2** could penetrate the outer lipopolysaccharide layer in Gram-negative bacteria better than peptide **1**, while both peptides act in the same manner toward Gram-positive bacteria, which lack the lipopolysaccharide envelope.

A time-kill assay was carried out to determine the time needed for the peptides to initiate their antibacterial effect. This assay showed that both peptides **1** and **2** had a rapid killing effect of approximately ≥ 99% over 1 h against *E. coli*. Bacterial cell viability was measured by the CFU counting method and the results were confirmed with a colorimetric assay. These assays were carried out to determine the effect of peptides **1** and **2** on a high concentration of the tested bacteria of approximately 32 times the concentration used in the earlier experiments. The results showed that a concentration of 0.5 mg/mL of either peptide showed a lethal effect on more than 80% of the total bacterial count over incubation for 12 h. In addition, a concentration of 0.25 mg/mL of either peptide was sufficient to kill more than 50% of the highly concentrated bacterial culture over incubation for 12 h. At a low concentration of 0.04 mg/mL, peptide **1** showed a very low killing effect because of the lack of the rigid structure, and the lower hydrophobicity, compared with peptide **2**. Furthermore, at a low concentration, neither peptide could form the secondary structures that are important for the killing effect. We suggest that both peptides **1** and **2** can exert their action without

being affected, or used by the tested bacterial cells, thus, after bacterial cell lysis, the peptides

can continue to attack more bacterial cells.
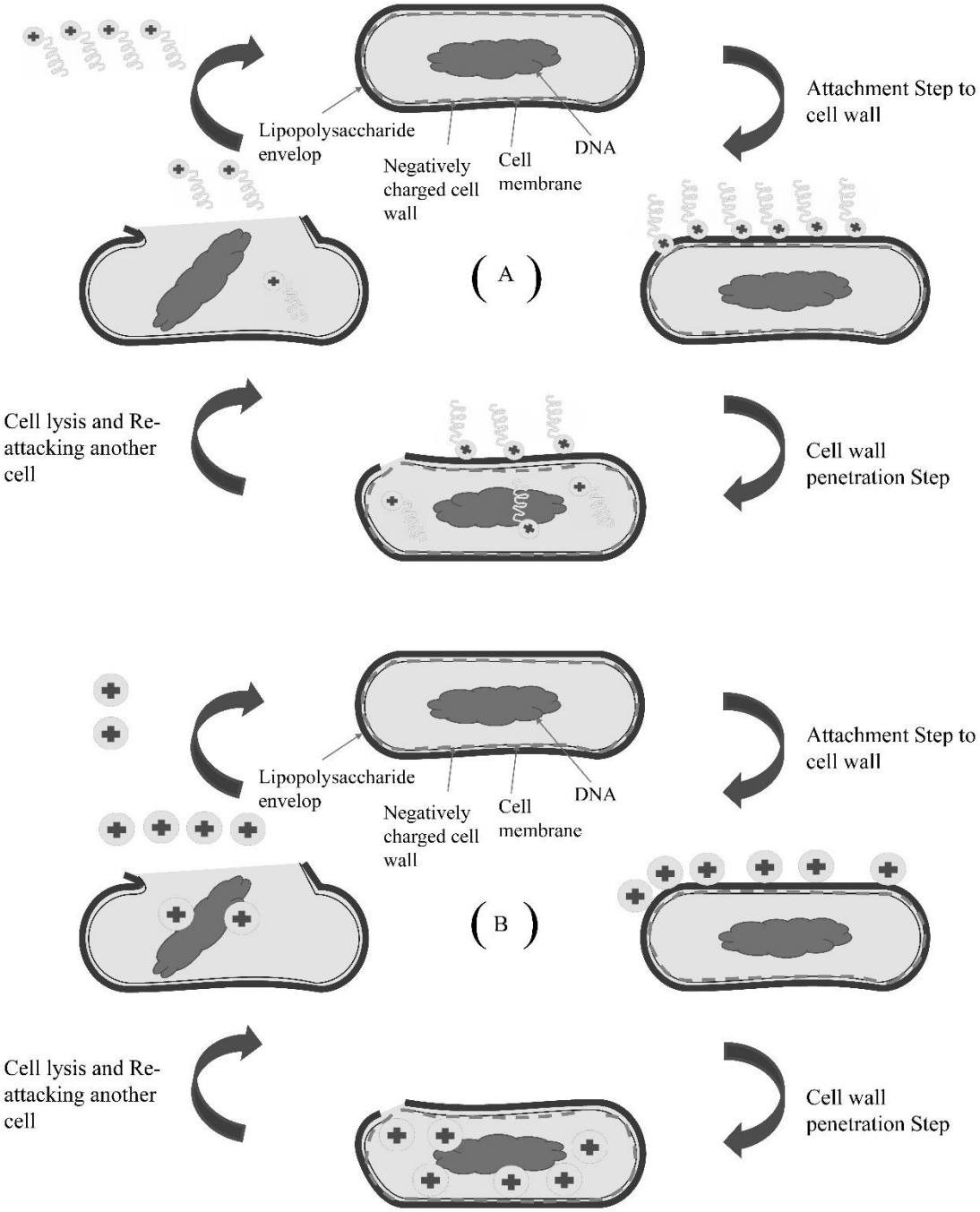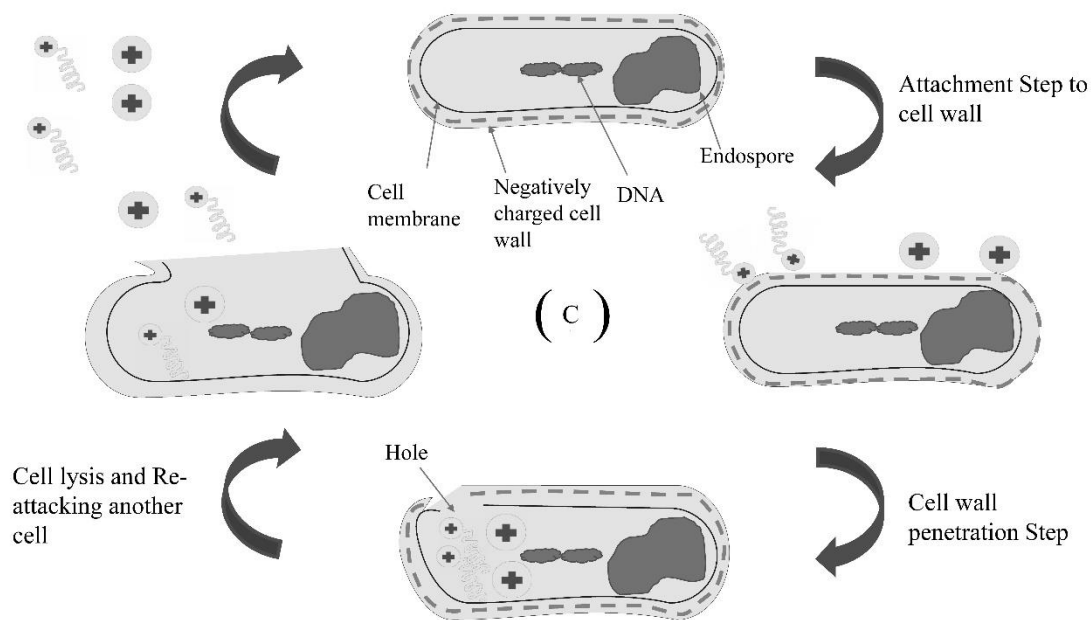
Figure 2.11. Suggested mode of action of peptides **1** and **2** against Gram-negative bacteria [(A) & (B)] and Gram-positive bacteria (C).

2.5. Conclusion

The newly designed cyclic decapeptide (peptide **2)** and its linear counterpart (peptide **1)** were synthesized using a standard Fmoc/SPPS method with yields of 97% and 45%, respectively. Both peptides showed antibacterial activity against the Gram-negative and Gram-positive bacterial strains, *E. coli*, and *B. thuringiensis,* respectively. However, peptide **2** showed a relatively higher potency against Gram-negative bacteria at lower concentration levels because of a superior ability to penetrate the bacterial cell wall compared with the linear counterpart. The MIC value for peptide **2** had a relatively lower value of 0.16 mg/ mL

compared with peptide **1**, which had a MIC value of 0.3 mg/mL, against Gram-negative

bacteria. While both peptide forms showed a similar MIC value of 0.24 mg/mL against Gram-

positive bacteria. A time-kill assay indicated a rapid killing effect of both peptide forms, as

the peptides could kill ≥ 99% of the tested bacterial strain (*E. coli*) after 1 h of incubation.

The bacterial cell viability assay illustrated the maximum efficacy of peptides **1** and **2** causing

the death of more than 80% of cells at a high concentration of the tested bacterial cells.

Chapter 3

Design, Synthesis, and Antibacterial Studies of Novel Cationic Amphipathic Cyclic Undecapeptides and their Linear Counterparts Against Virulent Bacteria

3.1. Introduction

The prevalence of nosocomially-acquired and community-developed diseases due to virulent bacterial species such as *Pseudomonas aeruginosa*, *Staphylococcus aureus*, *Escherichia coli*, and *Bacillus subtilis* has been growing recently [127]. These microorganisms are the commonest causes of urinary tract infections (UTIs), surgical wound infections, nosocomial pneumonia, endocarditis, septicemia, and other fatal diseases [128]. A revolution in the treatment and control of infectious diseases began with the clinical introduction of antibiotics. The antibiotics include β-lactams, tetracyclines, sulphonamides, arsphenamines, macrolides, streptogramins, ansamycins, aminoglycosides, amphenicols, lincosamides, oxazolidinones, and quinolones. These drugs have completely changed the treatment strategies for infections over a long period. Furthermore, they lower mortality and morbidity tolls by controlling bacterial communicable diseases in mankind [113].

The emerging global catastrophe of antibiotic resistance acquired by virulent bacteria has, however, highlighted the need to explore alternatives to the currently available antibiotics [4]. Antimicrobial peptides have emerged as an alternative therapy for the treatment of antibiotic-resistant infections. Cationic peptides uniquely affect microbes by targeting their negatively-

charged membrane lipids [3]. The first natural antimicrobial peptide, gramicidin, was discovered by Dubos and Hotchkiss in 1940 when they fractionated a natural extract from a soil strain of *Bacillus*. This extract was confirmed to shield mice from pneumococcal disease [23]. Gramicidin is still used topically for the treatment of skin ulcers and infections [25]. In the following year, a broad-spectrum peptide, tyrocidine, was discovered and showed activity against both Gram-positive and Gram-negative pathogens [24]. Additionally, antimicrobial peptides have been found in plants, such as the antifungal purothionin, which was isolated from *Triticumaestivum* species [26]. Scientists have discovered many antimicrobial peptides in animals since 1956, when they isolated defensin from rabbit leukocytes [27]. After that, bombinin and lactoferrin were extracted from the skin secretions of *Bombina maxima* (giant fire-bellied toad) and cow milk, respectively [129,130]. Furthermore, antimicrobial peptides were found in the lysosomes of human leukocytes [131]. Generally, in animals, peptides are the first line of the immune shield against all forms of pathogens, which is why they are usually found in organs and tissues exposed to microbes [132].

Antimicrobial peptides are short peptides containing variable numbers and sequences of amino acid residues. They are categorized as cationic amphipathic peptides, cationic peptides, host defense peptides, cationic host defense peptides, and anionic peptides [133]. Peptides can target a large range of organisms from bacteria to parasites. Nevertheless, with a few exceptions, such as indolicidin [59], each peptide is selective in its biological activity [134].

Peptides kill microorganisms by several mechanisms of action [135,136], but there are two main mechanisms. The first is attacking cell membranes. The amphipathic moieties—

hydrophobic and cationic residues incorporated in the peptide sequence—initiate interaction with bacterial cell membranes *via* hydrophobic and electrostatic forces. These forces allow the peptide to penetrate the bacterial cell wall, causing cell death [2]. The other mechanism is *via* targeting vital cell constituents, such as DNA [137].

The charge of the bacterial cell wall is an important factor determining the biological efficacy of antimicrobial peptides. Bacterial cell walls carry negative charges because of the lipoteichoic acid moieties associated with peptidoglycan (in Gram-positive bacteria) or the lipopolysaccharides attached to the cell wall (in Gram-negative bacteria) [138]. Thus, bacterial cell walls attract positively-charged compounds more than negatively-charged compounds. Furthermore, bacteria show no growth when they are linked to positively-charged surfaces, which highlights the importance of the cationic residues incorporated in the peptide [139]. The hydrophobic moieties of the peptide facilitate diffusion inside the bacterial cell wall. Additionally, hydrophobic residues initiate the formation of secondary structures *via* a self-assembly process in the bacterial cell wall [140]. Some peptides are self-assembled into α-helical shapes with the hydrophilic side-chains organized along one side while the hydrophobic side-chains are arranged on the other side. Others are arranged into β-sheet structures. These secondary structures represent the active forms of the peptides, which facilitate the interaction with bacterial cell membranes.

In the work described in this chapter, new cationic amphipathic cyclic undecapeptides and their linear counterparts (Figure 3.1) were studied for their antibacterial behavior against virulent strains of *E. coli*, *P. aeruginosa*, *Bacillus subtilis* and *S. aureus*. These peptides were

designed to have symmetric amino acid sequences with a distinguishing residue in the middle. The first peptide, named [LY], is a linear undecapeptide with amino acid sequence H-QNRNFYFNRNQ-OH (all amino acids are in the L-configuration), while [CY] is its cyclic form. Eight cationic and polar moieties were included to stimulate interaction with the negatively-charged bacterial cell wall and to increase the peptide solubility. The hydrophobicity of the compound depends on the two phenylalanine residues. Tyrosine was incorporated in the middle of the peptide because of its amphipathic behavior. Analogs were designed by replacing the tyrosine with histidine, resulting in peptides [LH] and [CH] to increase the potency of the peptides. MIC values were determined, and time–inhibition studies were carried out against the four bacteria.
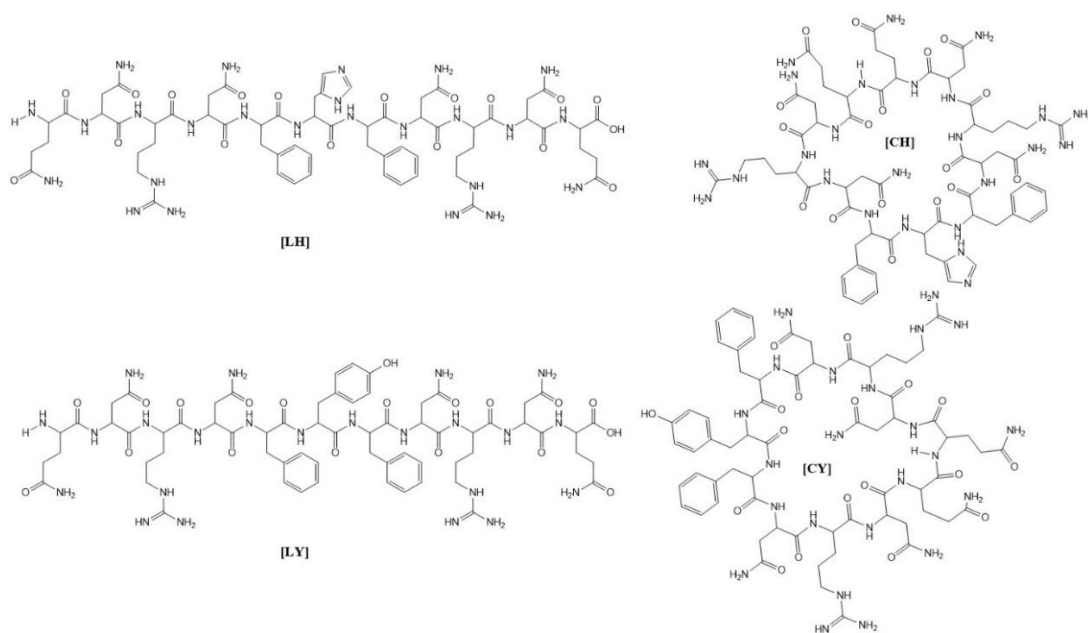

Figure 3.1. Structures of the newly synthesized antimicrobial peptides described in this chapter.

3.2. Materials and Methods

3.2.1. Synthesis Protocol

As shown in Scheme 3.1, peptide [LY] (molecular weight [MW] ~1501) was prepared *via* a standard solid-phase peptide synthesis (SPPS) method using 9-fluorenylmethoxycarbonyl (Fmoc) chemistry and 2-chlorotrityl resin as the solid support [141]. All Fmoc-protected amino acids, resin, piperidine, *O*-benzotriazole-*N*,*N*,*N'*,*N'*-tetramethyl-uronium-hexafluorophosphate (HBTU), 1-hydroxy-benzotriazole hydrate (HOBt·H$_2$O), *N*,*N*-diisopropylethylamine (DIPEA), and 2,2,2-trifluoroacetic acid (TFA) were purchased from Watanabe Chemical Industries, Ltd., Japan. Other reagents and solvents were purchased from Wako Pure Chemical Industries, Ltd., Japan.

The synthesis process was started by loading a glutamine residue onto 2-chlorotrityl chloride resin (Scheme 3.1). Side-chain-protected Fmoc-L-amino acid residues were then coupled to the loaded glutamine residue using 2 equivalents (equiv.) of HBTU, 4 equiv. of DIEA, and 2 equiv. of HOBt in 30 mL of *N*,*N*-dimethylformamide (DMF) as solvent for the coupling process. Piperidine (20% [v/v]) in DMF was used to remove the Fmoc protecting groups. The cleavage of the side-chain-protected linear undecapeptide from the resin was performed by using a mixture of 2,2,2-trifluoroethanol (TFE)/acetic acid/dichloromethane (DCM) (3:1:1 [v/v/v]) [142]. Purification was carried out by using semi-preparative reverse-phase high-performance liquid chromatography (RP-HPLC) Hitachi L-7100 apparatus with an XTerra Prep MS C18 OBD 10 μm column (19 × 150 mm; Waters). The mobile phases were acetonitrile containing 0.1% TFA, and H$_2$O containing 0.1% TFA. The product was detected

by absorbance at 220 nm [143]. The removal of the side-chain-protecting groups was achieved using a mixture of TFA/trisisopropylsilane (TIS)/H_2O (95:2.5:2.5 [v/v/v]). Lyophilization was carried out in a VD-800F freeze dryer (TAITEC). The cyclization reaction (to form [CY]) was achieved by using a low concentration of [LY] (0.5 mM) to avoid dimer formation. Two equivalents of HBTU and 5 equiv. of DIPEA were used for the cyclization process. The removal of the side-chain-protecting groups of [CY] was carried out using TFA/TIS/H_2O (95:2.5:2.5 [v/v/v]). Purification was achieved by semi-preparative RP-HPLC followed by lyophilization to yield the final target cyclic product [144].

[LH] and [CH] were synthesized by the same method; the only difference is in the middle amino acid residue (in [LH] and [CH], the tyrosine residue of [LY] and [CY] is replaced by a histidine residue).
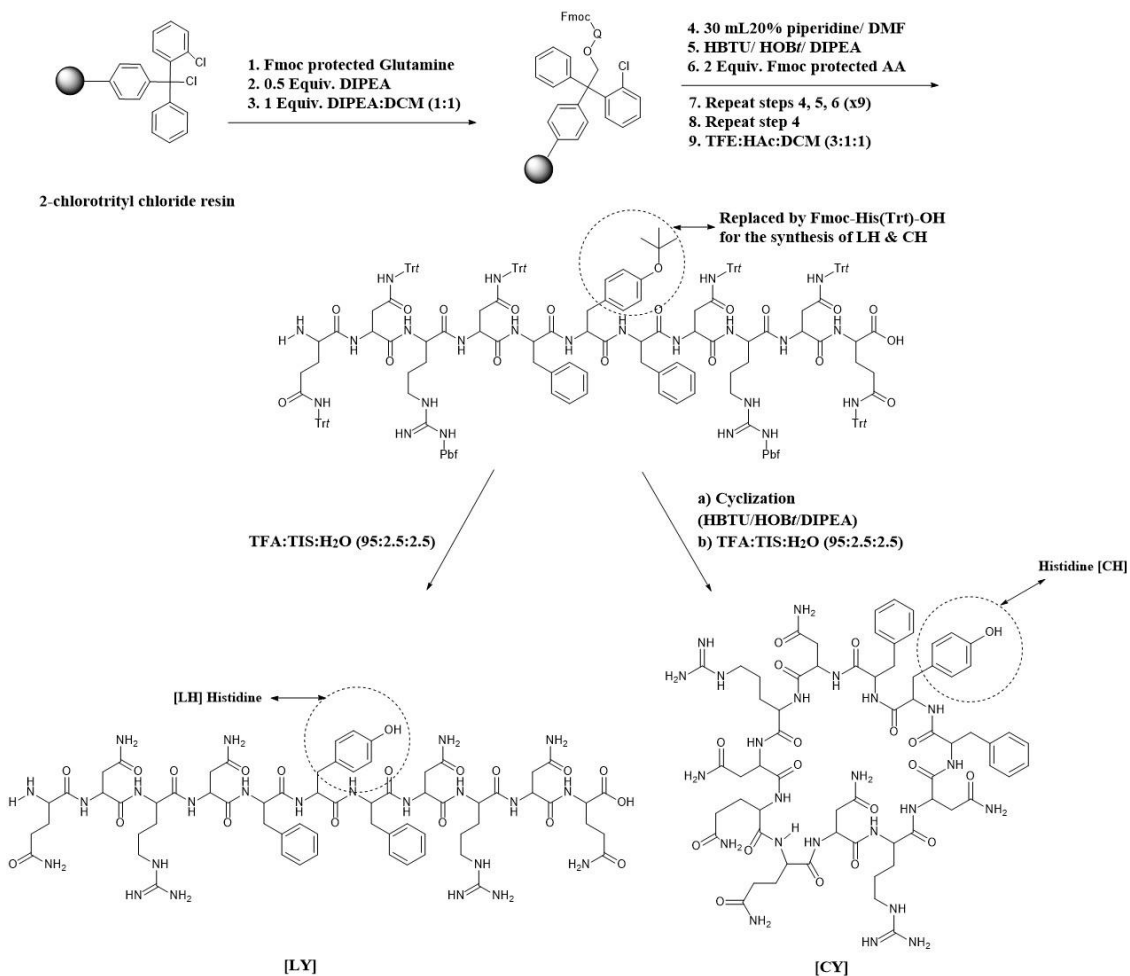
Scheme 3.1. Protocol for synthesis of the novel undecapeptides [LY], [CY], [LH], and [CH] by a standard Fmoc solid-phase peptide synthesis method followed by a cyclization process (for [CY] and [CH]) using a standard liquid-phase system.

3.2.2. Experimental

3.2.2.1. Loading of Fmoc-Gln (Tr*t*)-OH onto Barlos Resin

Table 3.1. Amounts of reactants in the loading reaction.

Compound	MW	Equiv.	mmol	Quantity
Barlos resin		1	1.6	1 g
Fmoc-Gln (Tr*t*)-OH	610.7	0.6	0.96	0.59 g
DIEA	129.25	0.5	0.8	0.14 mL
DIEA:DCM 1:1		1	1.6	0.56 mL
Methanol				1 mL

Calculations

- Weight of Fmoc-Gln (Tr*t*)-OH = Equivalence × Resin capacity (mmol/g)/1000 × MW

    = (610.7 × 0.96)/1000 = 0.59 g.

- Weight of DIEA = Equivalence × Resin capacity × MW.

- Volume of DIEA = 129.25/[0.742 (density) × 1000] = 0.14 mL.

- DIEA:DCM (1:1) = 0.28 + 0.28 = 0.56 mL.

- Theoretical weight calculations:

- Increase in resin weight (methanol capping) = 1.6 – 0.96 (Fmoc-AA) = 0.64 mmol.

- 0.64 × 32.04 (MW of methanol) = 20.5 mg/1000 = 0.021 g.

- Decrease in resin weight = 1.6 × 35.453 (atomic mass of Cl) = 56.7 mg/1000 = 0.057 g.

- Theoretical weight = 1 g (resin) + 0.59 g (Fmoc AA) + 0.021 g (methanol) − 0.057 g (Cl) = 1.55 g.

Procedures

In the SPPS reaction vessel (118.710 g):

Barlos resin (1 g) was added and washed twice with DCM until it was completely swollen; 0.59 g of Fmoc-Gln (Tr*t*)-OH, 15 mL of DCM, and 0.14 mL of DIEA were added, respectively. The reaction mixture was stirred manually for 5 min, then 0.56 mL of DIEA:DCM (1:1 [v/v]) was added and stirred for 1 h. Methanol (1 mL, to cap unreacted sites) was added to the reaction mixture and stirred for 10 min. Subsequently, the reaction solvents were removed using a suction pump. The resin was washed using DCM (twice), DMF (twice), isopropanol (twice), DMF (twice), isopropanol (twice), methanol (twice), and ethyl ether (twice). Drying under reduced pressure was performed for 1 h. Finally, the resin was weighed and the yield was calculated (1.51 g).

% Yield = (1.51/1.55)×100 = 97%.

Loading-rate Measurement of Fmoc-Gln (Tr*t*)-resin

In three 10-mL volumetric flasks, 1–3 mg of Fmoc-Gln (Tr*t*)-resin was added with 20% piperidine in DMF until the 10-mL mark was reached. After waiting for 30 min at room

temperature, two blank samples containing 20% piperidine in DMF were prepared. Absorbance values were measured at 290 nm for all samples.

Table 3.2. Measurement of the loading rate.

Sample no.	Resin weight (mg)	$A_{290 \text{ nm}}$	Loading-rate (mmol/g resin)
1	1	0.55	1
2	2	1.2	1
3	3	1.4	0.94

The loading rate was calculated from the following equation:

Loading rate = 1000 ×10 × $A_{290 \text{ nm}}$/4950 (molar absorptivity of Fmoc) × 1 × weight

= mmol/g resin.

Mean loading rate/g = 0.98 mmol/g.

Actual loading rate = 0.98 × 1.51 = 1.5 mmol.

% Yield = (0.98/0.96)×100 = 102%.

3.2.2.2. Peptide Chain Elongation

3.2.2.2.1. Addition of Fmoc-Asn (T*rt*)-OH

Table 3.3. Calculation of the amounts of reactants needed.

Compound	MW	Equiv.	mmol	Quantity
Fmoc-Gln-resin		1	1.5	1.51 g
Fmoc-Asn (T*rt*)-OH	596.67	2	3	1.8 g
HBTU	379.45	2	3	1.14 g
HOB*t*.H$_2$O	153.14	2	3	0.46 g
DIEA	129.25	4	6	1 mL

Calculations

Weight of Fmoc-Asn (T*rt*)-OH = (596.67 × 3)/1000 = 1.8 g.

Weight of HBTU = 3/1000 × 379.25 = 1.14 g.

Weight of HOB*t*.H$_2$O = 3/1000 × 153.14 = 0.46 g.

Volume of DIEA = (6/1000 × 129.25)/0.742 = 1 mL.

Procedures

- Deprotection:

In the SPPS reaction vessel, the Fmoc-AA-resin was washed twice with DMF until complete swelling of the resin was achieved; 30 mL of 20% piperidine in DMF was added and the mixture was stirred for 30 min. The reaction mixture was removed, and the resin was washed with DMF (twice), isopropanol (twice), and DMF (twice).

- Coupling:

In the SPPS reaction vessel, the Fmoc-Asn (T*rt*)-OH was added with 15 mL of DMF, HBTU, and HOB*t*.H$_2$O. The reaction mixture was rotated for 2 h. The reaction medium and excess reactants were removed, and then the resin was washed with DMF (twice), isopropanol (twice), DMF (twice), and DCM (twice), respectively.

The series of coupling reactions was continued until the side-chain-protected undecapeptide was completely synthesized. Finally, the Fmoc group was removed and the peptide–resin was washed as discussed above (DMF, isopropanol, DMF, then DCM), followed by washing with diethyl ether (twice). The peptide–resin was then dried under reduced pressure using a desiccator.

3.2.2.3. Cleavage from Resin

TFE promotes the hydrolysis of ester linkages between the peptide and resin without affecting the side-chain-protecting groups, which are cleaved by TFA. Therefore, a cleavage cocktail (DCM:TFE:acetic acid, 1:3:1 [v/v/v]) was used.

Procedures

In the SPPS vessel, the cleavage cocktail was added to the peptide–resin and rotated using an electric rotator for 2 h at room temperature. The filtrate was collected in a 100-mL round-bottomed flask (80.7 g) and evaporated under reduced pressure. Water (2 mL) was added to the residue to crystallize the protected peptide as white crystals. The crystals were dried under reduced pressure for 1 h, weighed (3.4 g) and the percentage yield was calculated. The product was checked for its purity by RP-HPLC (Figure 3.2), which showed a high purity.

% Yield = (3.4/3.5)×100 = 97%.

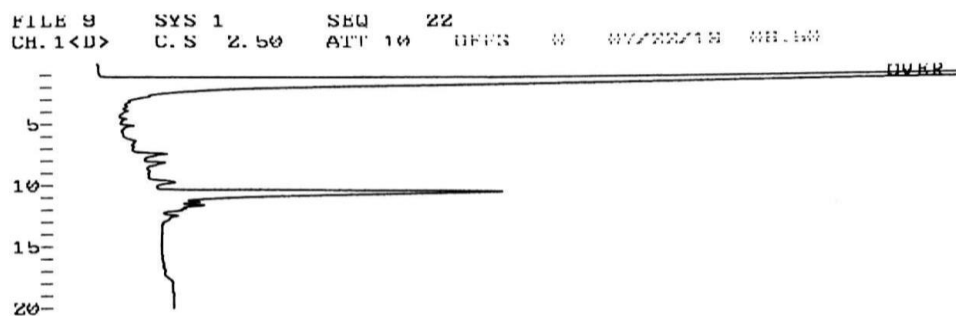**Figure 3.2.** High-performance liquid chromatogram of the side-chain-protected linear tyrosine-containing peptide [LY], retention time (RT) = 10.6 min.

3.2.2.4. Cyclization

Cyclization reaction was carried out by using <0.5 mM of the linear peptide to avoid dimer formation. HBTU (2 equiv.) and DIEA (4 equiv.) were used for the cyclization. The reaction was monitored by RP-HPLC (Figures 3.3 and 3.4).
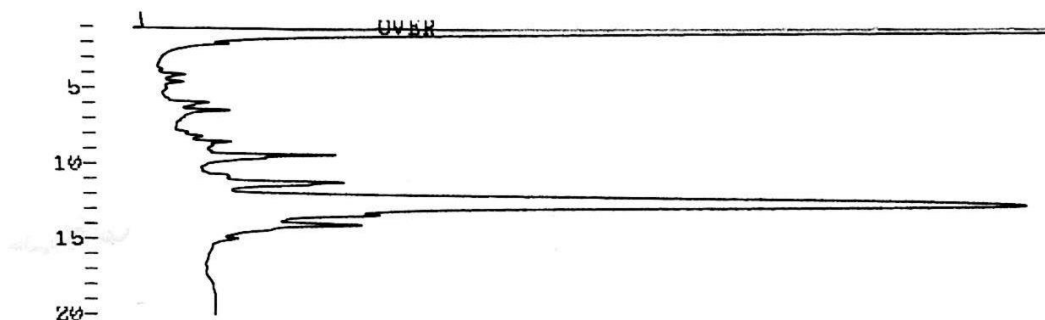
Figure 3.3. High-performance liquid chromatogram of the cyclized side-chain-protected tyrosine-containing peptide [CY] with RT = 12.4 min, prepared by cyclization of [LY].
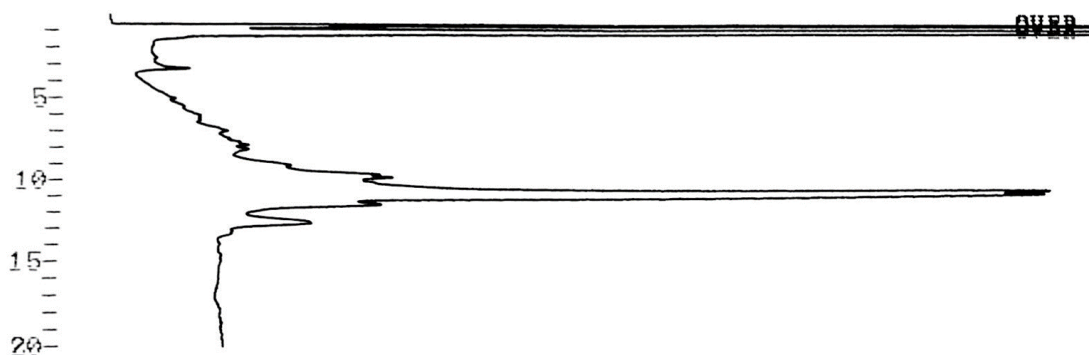
Figure 3.4. High-performance liquid chromatogram of the cyclized side-chain-protected histidine-containing peptide [CH] with RT = 10.6 min, prepared by cyclization of [LH].

3.2.2.5. Deprotection of Side-chain-protecting Groups

Removal of the side-chain-protecting groups was carried out using TFA:TIS:H_2O (95:2.5:2.5 [v/v/v]). The reaction was monitored by RP-HPLC for 2 h, followed by purification by semi-preparative RP-HPLC (Figures 3.5, 3.6, 3.7, 3.8, and 3.9).
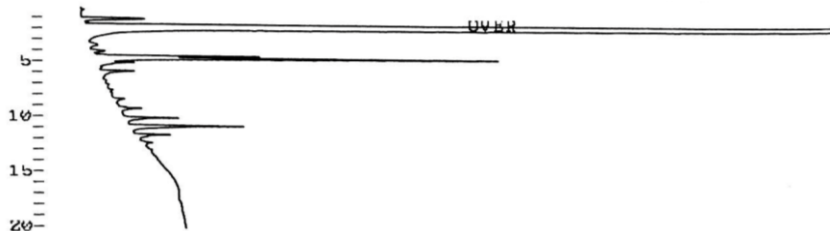
Figure 3.5. Reverse-phase high-performance liquid chromatogram of deprotection of

peptide [LY], RT = 4.5 min.
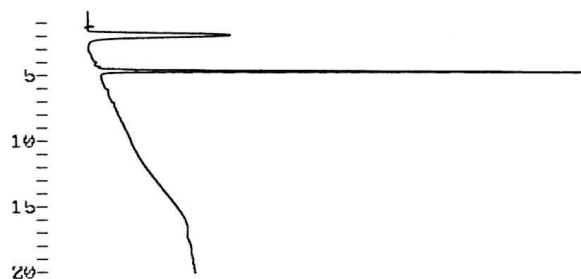
Figure 3.6. High-performance liquid chromatogram of pure peptide [LY] after purification

by semi-preparative reverse-phase high-performance liquid chromatography (RP-HPLC),

RT = 4.48 min.
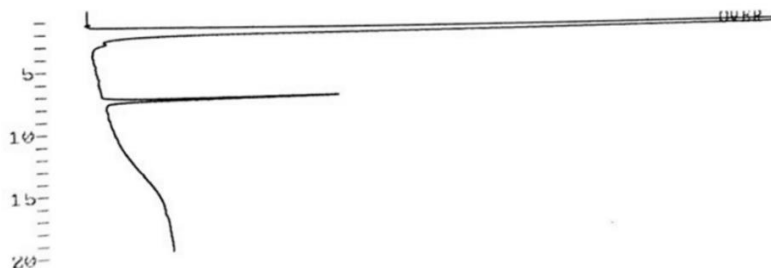
Figure 3.7. High-performance liquid chromatogram of pure peptide [LH] after purification

by semi-preparative RP-HPLC, RT = 7.2 min.
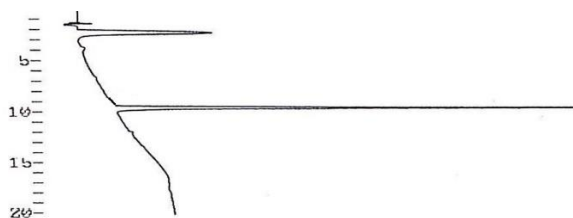
Figure 3.8. High-performance liquid chromatogram of pure peptide [CY] after purification by semi-preparative RP-HPLC, RT = 10.2 min.

Figure 3.9. High-performance liquid chromatogram of pure peptide [CH] after purification by semi-preparative RP-HPLC, RT = 10.9 min.

3.2.3. Evaluation of MIC Values

MIC values were determined by the broth microdilution method using 96-well microplates with clear bottoms (Nunclon™ Surface, Denmark) [145]. *P. aeruginosa* PA14, *E. coli* O157:H7 CR3 (both Gram-negative bacteria), and *S. aureus* 209P and *B. subtilis* ATCC 6633 (both Gram-positive bacteria) were chosen as the model bacterial strains to determine the antibacterial effects of undecapeptides [LY], [CY], [LH], and [CH]. The bacteria were inoculated separately into freshly prepared Luria-Bertani (LB) medium at 37 °C and shaken at 120 rpm overnight. The cultures were diluted to 5×10^5 colony-forming units/mL ($OD_{600} =$

0.05). Peptide solutions were prepared by dissolving each type of peptide separately in dimethyl sulfoxide (DMSO); these solutions were diluted with water to 1 mM. DMSO accounted for ≤5% of the total volume. Peptide solutions (0.1 mL) were added to 0.9 mL of medium to give a concentration of 100 µM. Serial twofold dilutions were applied to reach 0.09 µM, and peptide solutions of varying concentration were distributed across 96-well microplates. Positive controls used an aqueous solution of the broad-spectrum antibiotic gentamycin sulfate, prepared at 50 µM and twofold serially-diluted. Runs without antimicrobials were carried out to ensure the adequate growth of the bacteria. The bacterial cultures were mixed well with the test compounds (1:39 [v/v]). Optical density (OD_{600}) values were determined using a microplate reader (Varioskan Flash dispenser option, Thermo Scientific) before the incubation to be used as a blank (because the tested compounds are partially insoluble in the medium). The 96-well microplates were incubated for 24 h at 37 °C and OD_{600} values were determined. MIC values were defined as the minimum concentration where no visible bacterial growth was detected, confirmed by subtracting the OD_{600} values at 0 h from the OD_{600} values at 24 h. All experiments were carried out in biological duplicates.

3.2.4. Time–inhibition studies

Time–inhibition assays were conducted using *P. aeruginosa* PA14, *S. aureus* 209P, *E. coli* O157:H7 CR3, and *B. subtilis* ATCC 6633 in 96-well microplates with clear bottoms (Nunclon™ Surface). Bacterial cultures were prepared as described in Section 3.2.3. The antibacterial effects of compounds were evaluated by measuring OD_{600} values at different time intervals using a microplate reader (Varioskan Flash dispenser option), which were compared with OD_{600} values determined before adding bacteria (blank values). The peptides

[LH], [CH], [LY], and [CY] were tested at concentrations greater than or equal to their MIC values. Runs without the antimicrobials were performed to confirm adequate growth of the bacteria.

The bacterial cultures were mixed with the tested peptides and incubated at 37 °C for 24 h. OD_{600} values were measured at 0, 4, 8, 18, and 24 h to assess the proportion of surviving bacterial cells. Bacterial growth percentages were calculated according to the equation: [%Growth = (OD_{600} value of bacterial suspension containing the tested antimicrobial /OD_{600} value of the negative control [only bacteria]) × 100]. Inhibition was calculated using the equation: [%inhibition = 100 − %growth]. The inhibitory effects of the tested peptides were calculated before the incubation (at 0 h of incubation) and compared with the negative controls, which consisted of media, solvents, and bacteria. Control OD_{600} values for each bacterium (without antimicrobials) were estimated at 0, 4, 8, 18, and 24 h and compared with the experimental values at the same time. Time–inhibition assays were conducted in duplicate.

3.3. Results

3.3.1. Peptide Synthesis

The standard Fmoc SPPS method was used to synthesize peptides [CH], [LH], [CY], and [LY]. Peptides [LY] and [CY] were designed to possess positively-charged, polar, amphipathic (the tyrosine residue), and hydrophobic moieties. Peptides [CH] and [LH] were designed to have polar, hydrophobic, and more positively-charged (the added histidine residue) moieties to increase the antibacterial potency. The yield of [LY] was approximately 98%, while that of [CY] was around 75%; the yields of [LH] and [CH] were approximately

97% and 75%, respectively. The structure and purity of the cyclic peptides [CY] and [CH] were confirmed by MALDI-TOF mass spectrometry. For [CY], a peak was observed at *m/z* = 1482 (calcd. = 1483, formula: $C_{65}H_{91}N_{23}O_{18}$) (Figure 3.10); for [CH] *m/z* = 1459 (calcd. = 1457, formula: $C_{62}H_{89}N_{25}O_{17}$) (Figure 3.11). After preparative RP-HPLC, the purity of each peptide was >99%.
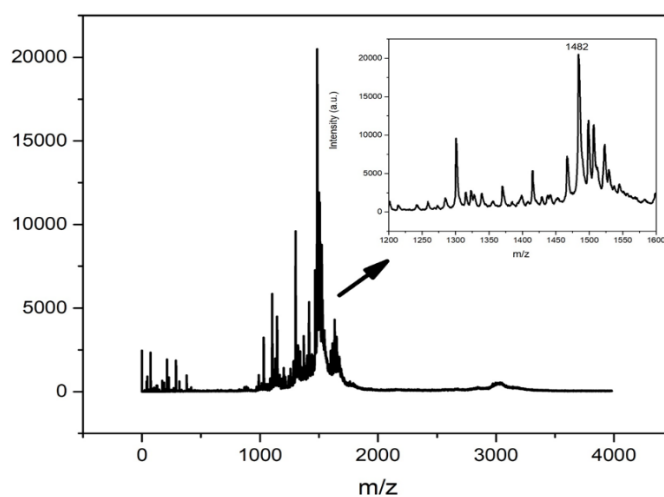
Figure 3.10. MALDI-TOF mass spectra of peptide [CY].
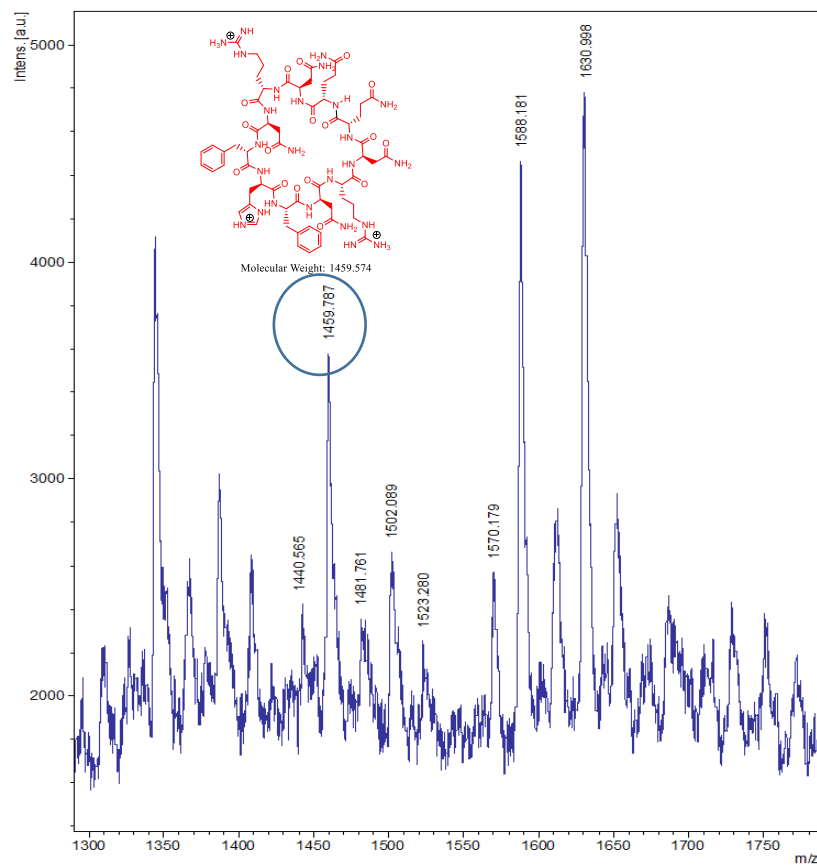
Figure 3.11. MALDI-TOF mass spectrum of peptide [CH].

3.3.2. MIC Evaluation

MIC values were determined for all peptides against *P. aeruginosa* PA14, *S. aureus* 209P, *E. coli* O157:H7 CR3, and *B. subtilis* ATCC 6633 (Table 3.4). *S. aureus* is a Gram-positive bacterium and the commonest cause of nosocomially-acquired infection, for example, pneumonia. *P. aeruginosa* is a Gram-negative bacterium that exhibits multidrug resistance and is one of the commonest reasons for nosocomial UTIs. *E. coli* can cause diarrhea and UTIs, while *B. subtilis* is a major cause of nosocomial septicemia and also causes cardiac diseases [128,146].

Table 3.4. MIC values of the novel undecapeptides against Gram-negative and Gram-positive bacteria.

	MIC value (µM)			
Peptide	*P. aeruginosa*	*E. coli*	*S. aureus*	*B. subtilis*
[LY]	9.3	12.5	12.5	12.5
[CY]	6.25	12.5	12.5	12.5
[LH]	3.1	3.1	3.1	6.25
[CH]	6.25	3.1	6.25	3.1
Gentamycin sulfate	6.25	3.1	6.25	1.6

Generally, all the peptides showed high activities (i.e., low MIC values) against all the bacterial strains. The histidine-containing peptides displayed greater potency against all the bacteria, with MIC values ranging from 3.1 to 6.25 µM, compared with 6.25–12.5 µM for the tyrosine-containing peptides. The linear histidine peptide [LH] was more potent against *P. aeruginosa* and *S. aureus* than the cyclic peptide [CH], whereas [CH] showed greater activity against *B. subtilis*, and they displayed the same effect against *E. coli*.

The broad-spectrum antibiotic gentamycin sulfate was used as the positive control drug for all the bacteria to ensure the validity of the experiment and for comparison with the tested peptides. Peptide [LH] was more effective agent *P. aeruginosa* and *S. aureus* than gentamycin sulfate. [LH], [CH], and gentamycin sulfate had an equal effect against *E. coli*. However, gentamycin sulfate was the most effective antibacterial agent against *B. subtilis*.

3.3.3. Time–inhibition Studies

Figure 3.12 shows the antibacterial behavior of the novel peptides against *S. aureus* at five different time intervals. All the tested peptides had good and stable effects against *S. aureus*, which did not show any significant resistance to them. After 24 h of incubation, [LH] was the most effective peptide; it could reach >99.99% inhibition. [CY] and [LY] also showed high efficacies during the test period. Peptide [CH] had a lower effect than its linear counterpart and the two tyrosine-containing peptides.
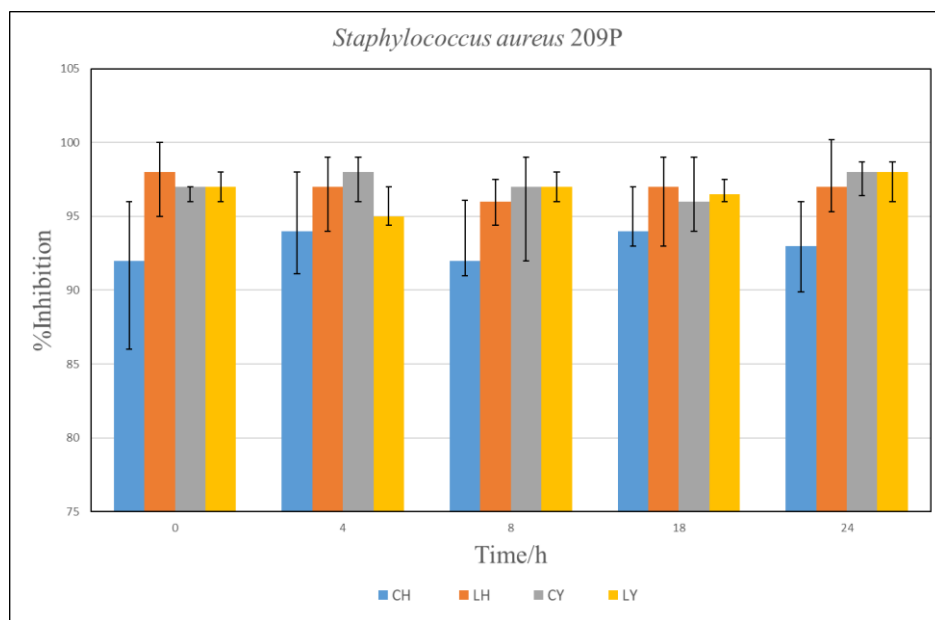
Figure 3.12. Time–inhibition assays of the newly-synthesized peptides against

Staphylococcus aureus strain 209P.

P. aeruginosa causes severe and long-lasting diseases in several hosts; the infectivity of this species varies with the particular strain. Strain PA14 is one of the most virulent [147]. Among the novel peptides tested in this work, [CY] showed the greatest antibacterial effect against

P. aeruginosa PA14 when used at a concentration equal to or higher than the MIC value, as shown in Figure (3.13). Its antibacterial activity was unwavering over 24-h incubation, and it affected >99.99% of the bacteria from time zero of incubation. [LY] came next to [CY] in efficacy, and affected >97% of the bacteria from the start of the incubation. [CH] and [LH] exhibited lower efficacies than the tyrosine-containing peptides; in early measurements (0 and 4 h), they inhibited >95% and >92% of the bacterial growth, respectively, while their maximum antibacterial effect was observed after 24 h of incubation.
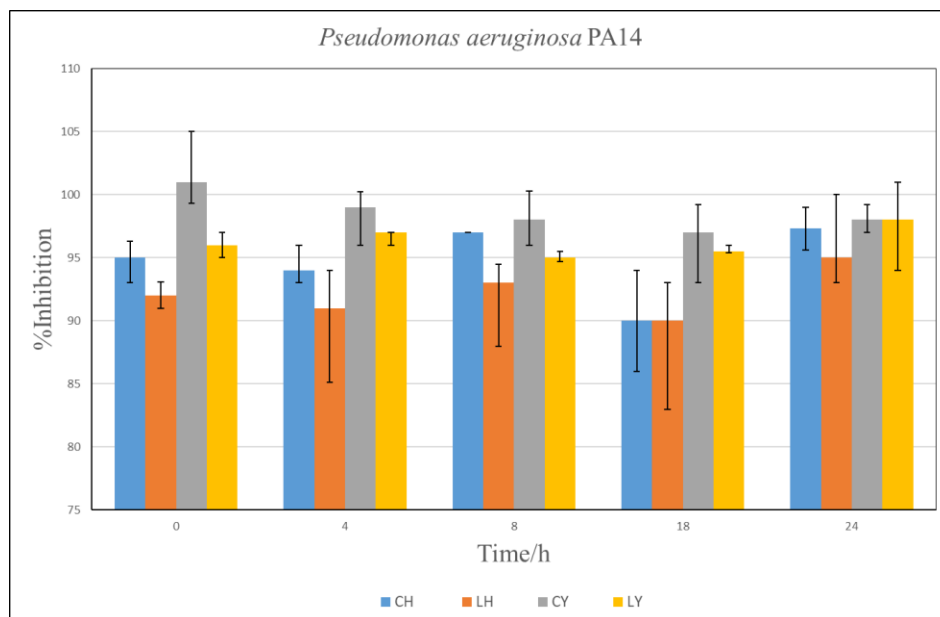
Figure 3.13. Time–inhibition assays of the newly-synthesized peptides against *Pseudomonas aeruginosa* strain PA14.

E. coli O157:H7 CR3 can induce diseases including kidney failure and hemorrhagic diarrhea [148]. As illustrated in Figure 3.14, among the peptides designed and tested in this work, [CY] and [LY] were initially the most active against *E. coli*. They could affect >97% of the

bacteria at 0 h of incubation. [CY] was the most effective of the peptides against *E. coli* at later time points (≥8 h). [LH] and [CH] had a greater effect on *E. coli* after 24 h than at earlier timepoints.
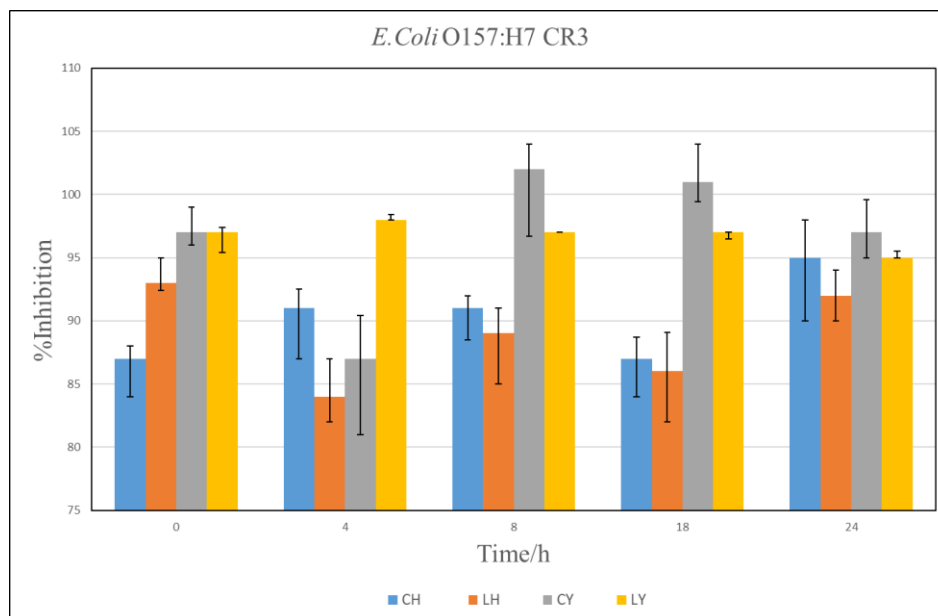
Figure 3.14. Time–inhibition assays of the newly-synthesized peptides against *Escherichia coli* strain O157:H7 CR3.

One of the reasons for the choice of *B. subtilis* for assessment in this work is its ability to form endospores that enable this species to withstand harsh conditions. Antimicrobial peptides are likely to act on persister cells such as endospores [55]. As shown in Figure 3.15, [CY] was the most potent of the peptides against *B. subtilis*, with a stable antibacterial effect over the examination time, except after 4 h. The bacteria were susceptible to this peptide at 0 h, started to show some resistance to it (observed at 4 h), but, after 8 h, the peptide could overcome the bacterial resistance and inhibited >99.99% of the bacterial growth. [LY] was

the next most efficacious of the peptides, and reached its maximum inhibition at 4 h of incubation (the bacteria showed some resistance to this peptide at 0 h). *B. subtilis* could resist the antibacterial effect of [CH] and [LH] from 4 to 18 h, but, after that, these peptides could inhibit >95% and >99.99% of the bacteria, respectively.
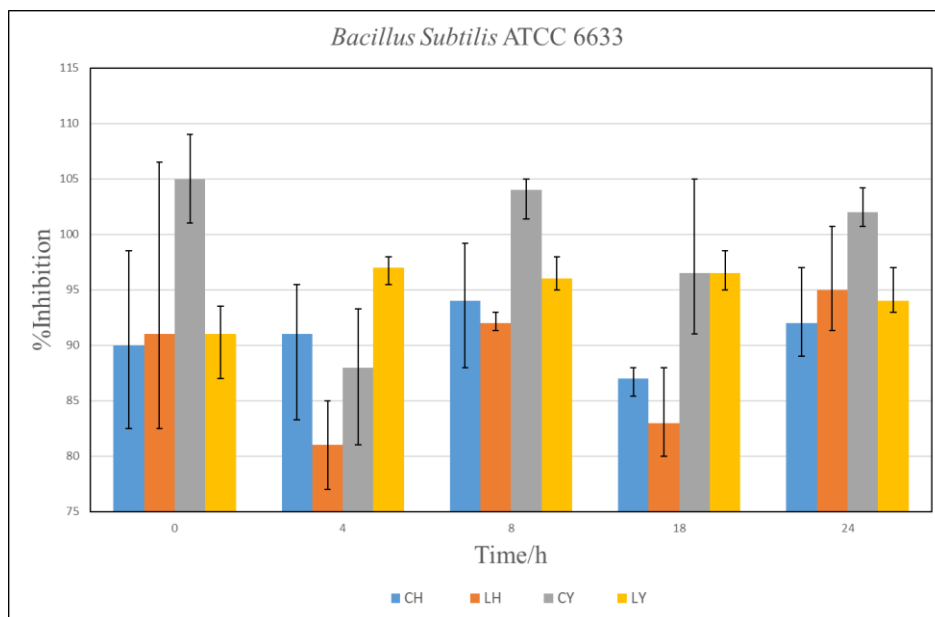
Figure 3.15. Time-inhibition assays of the newly-synthesized peptides against *Bacillus subtilis* strain ATCC 6633.

Figure 3.16 shows the percentage of viable bacteria present in the test samples at the start of incubation (i.e., immediately after mixing the bacteria and the antimicrobial peptides [15 min]). [CY] showed the highest activity (except toward *S. aureus*); it could inhibit the growth of *P. aeruginosa* and *B. subtilis* completely, whereas the percentage growth of the other bacteria was approximately 3%. Peptide [LY] showed the second highest activity, except toward *S. aureus*, against which it showed the same efficacy as [CY]. [LH] was the most

active peptide against *S. aureus* (bacterial growth ~2%). [CH] showed the lowest antibacterial activity, except against *P. aeruginosa*, when it was more active than [LH].
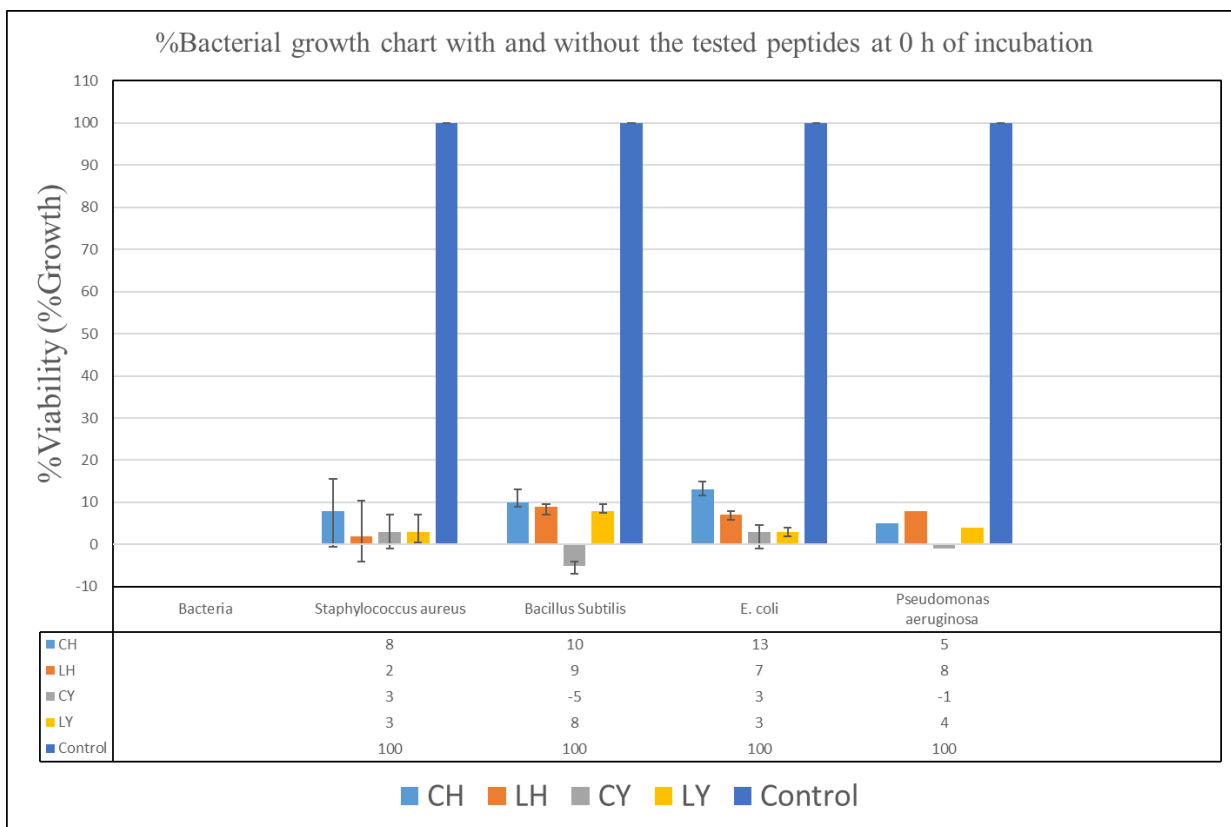
Figure 3.16. %growth of bacteria in the presence of the newly-synthesized peptides compared with negative controls (only bacteria) at 0 h of incubation (before incubation).

3.4. Discussion

Cationic amphipathic peptides are positively-charged, short peptides with amphiphilic characteristics. They have been isolated from mammals, fish, birds, amphibians, plants, insects, and even prokaryotes. They can undergo self-assembly into a large variety of

secondary structures. The most common secondary structure elements are α-helices, β-strands, loops, and other extended assemblies [149].

The most investigated classes of cationic peptides are those with antibacterial effects. Cationic peptides interact with the cell membranes of bacteria *via* electrostatic forces between the positively-charged peptides and the negatively-charged lipids in the bacterial cell membrane. Hydrophobic interactions are responsible for insertion of the peptides inside the bacterial cell. The flexibility of a peptide is very important for its penetration into bacterial cell membranes by the formation of secondary structure [150]. Some peptides show their secondary structures only when they interact with bacterial cell membranes. Peptide activity can be altered by changing the secondary structure; for example, the activity of indolicidin against Gram-negative bacteria was increased by changing its flexible secondary structure [151]. This mode of action makes antibacterial peptides drugs of choice for nosocomial infections.

Herein, newly-designed cationic amphipathic cyclic undecapeptides and their linear counterparts were synthesized in quantitative yields of the linear peptides (~97%) and good yields of the cyclic peptides (~75%). The tyrosine-containing peptides [LY] and [CY] showed remarkable antibacterial activities against all the tested bacteria. It is posited that the presence of a tyrosine residue between two phenylalanine residues created a highly penetrating nucleus of the peptide (Phe–Tyr–Phe) that can penetrate the bacterial cell membrane due to hydrophobic forces. The amphipathic character of tyrosine augmented these interactions, and improved penetration of the peptide into the bacterial cell membranes.

The polar symmetric wings of the peptides were ideal for interaction with the negatively-charged components of the bacterial cell membranes.

The cyclic tyrosine-containing peptide [CY] showed an improved antibacterial effect against *P. aeruginosa* compared with that of the linear peptide [LY]. However, both [LY] and [CY] showed the same antibacterial activity against the other three tested species of bacteria. The higher activity of [CY] toward *P. aeruginosa* may depend on its more rigid structure and the higher hydrophobicity of the cyclic conformation.

Replacing the tyrosine residue with a histidine improved the overall antibacterial effect of the resulting peptides ([LH] and [CH]) compared with that of peptides [LY] and [CY]. Moreover, the linear peptide [LH] was more active against the tested bacteria than the cyclic [CH], except toward *B. subtilis* (Table 3.4). The increase in the antibacterial effect relative to the tyrosine-containing peptides might be due to the positively-charged histidine residue located between the two phenylalanine residues that created a nucleus with more penetrating ability into the bacterial cell membrane than the tyrosine-containing nucleus. Secondary structure formed by the linear histidine-containing peptide can penetrate bacterial cell membranes more effectively than its cyclic form. The cell-penetrating abilities of [LH] and [CH] were augmented by the electrostatic interaction of the positively-charged histidine residue with the negatively-charged bacterial membranes. It is suggested that this interaction happens during the penetration of the hydrophobic side-chain groups surrounding the histidine moiety into the membrane. These double interaction forces increase the overall penetration of the peptide, resulting in greater inhibition of bacterial cell growth.

Figure 3.17 shows the suggested mechanism of action of the novel antimicrobial undecapeptides. First, they attach to the lipopolysaccharide layer in Gram-negative bacteria or the lipoteichoic acid moieties in the peptidoglycan layer of Gram-positive bacteria. Cationic residues initiate electrostatic interactions with the negatively-charged bacterial cell membrane components. The amphipathic structure of the novel peptides gives them the ability to create secondary structures inside the bacterial cell wall [2]. The hydrophobic moieties facilitate the penetration of the peptides into the bacterial cells by diffusion through the lipid bilayers, leaving holes in cell membranes, ultimately causing the degeneration and death of the bacterial cells [133].
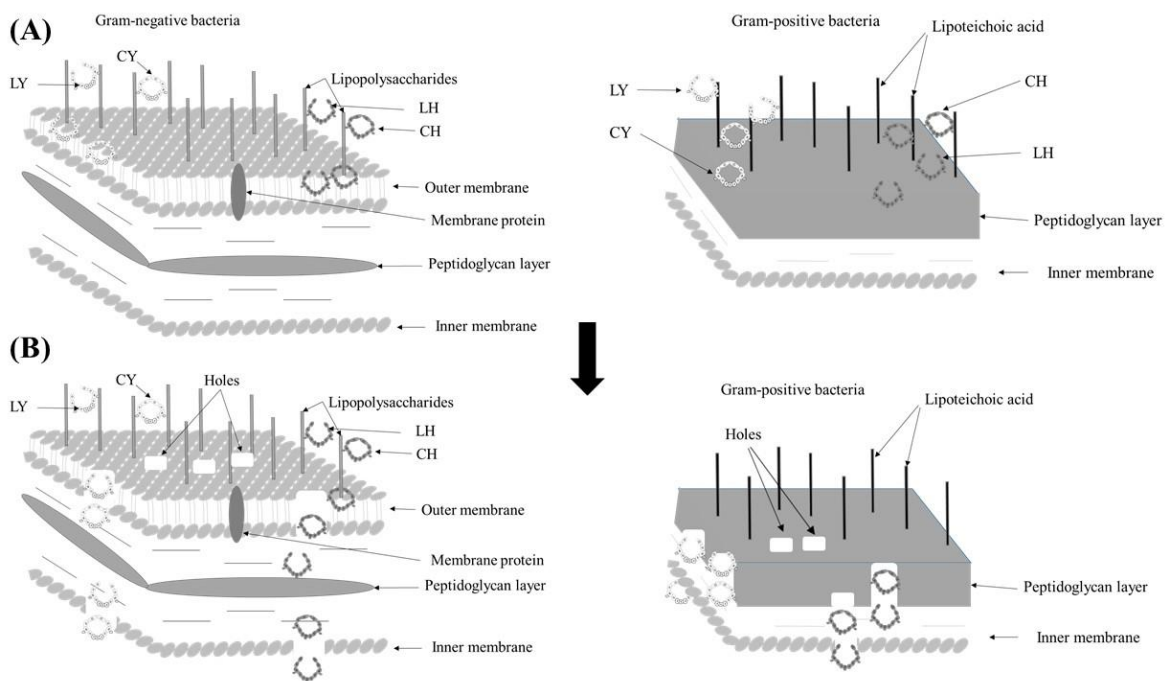

Figure 3.17. Suggested mechanism of action of the novel peptides described in this chapter. (A) Electrostatic interactions between the peptides and negatively-charged bacterial cell walls. (B) Penetration of the peptides into the bacterial cell walls, creating holes.

Time–inhibition assays of the peptides against *S. aureus*, *P. aeruginosa*, *B. subtilis*, and *E. coli* were carried out at peptide concentrations of double the MIC values. The peptides with the Phe–Tyr–Phe nucleus had a fast, broad-spectrum antibacterial effect and the tested bacteria did not develop any resistance to them. The peptides with the Phe–His–Phe nucleus needed more time to exert their maximum antibacterial effect, and the bacteria showed a little resistance to them. The peptides with the Phe–His–Phe nucleus possibly form secondary structures at lower concentrations than those having the Phe–Tyr–Phe nucleus. These secondary structures can penetrate the bacterial cell membrane, which would explain the lower MIC values of [CH] and [LH] compared with [LY] and [CY]. However, the penetration ability of the Phe–Tyr–Phe nucleus through the bacterial cell membrane is higher than that of the Phe–His–Phe nucleus after the formation of secondary structures. Thus, the peptides [LY] and [CY] have better antibacterial activities than [CH] and [LH] at higher concentrations.

3.5. Conclusions

Newly-designed cyclic cationic amphipathic undecapeptides and their linear counterparts were synthesized with high yields (75% and 97%, respectively) using a standard Fmoc SPPS method. Tyrosine-containing peptides were synthesized first and tested for their antibacterial activity. Histidine analogs were then synthesized to study the effect of changing the middle amino acid residue from Tyr to His on the antibacterial effect. All the peptides showed excellent activities against Gram-negative (*P. aeruginosa* and *E. coli*) and Gram-positive (*S. aureus* and *B. subtilis*) bacteria. The histidine-containing peptides showed higher potencies against all the bacteria at lower concentration. This is suggested to be because they have

greater capability for secondary structure formation at lower concentration (assisted by the histidine residue) than their tyrosine-containing counterparts. These secondary structures are responsible for penetration of the bacterial cell membrane. This would explain the lower MIC values of the histidine-containing peptides, ranging from 3.1 to 6.25 μM, compared with 6.25–12.5 μM for the tyrosine-containing peptides. However, time–inhibition assays demonstrated the rapid antibacterial effects of both [CY] and [LY], which could affect ≥97% of the bacteria at 0 h of incubation. Furthermore, bacterial resistance to these peptides was negligible after incubation for 24 h. Peptides [CH] and [LH] showed their maximum antibacterial effects after 24 h of incubation. It is suggested that, at concentration of greater than or equal to the MIC value, the secondary structures of the tyrosine-containing peptides can better penetrate the bacterial cell membrane than those of the histidine-containing peptides.

Chapter 4

New Technique for the Total Synthesis of *Staphylococcus aureus* Autoinducer Peptide-III and an Analog

4.1. Introduction

The emergence of bacterial resistance to almost all antibiotics has prompted scientists to change their strategies for fighting bacteria. Almost a century after the first discovery of antimicrobials, the fight against infectious diseases caused by resistant bacteria is still ongoing. Recently, medicines that weaken bacterial virulence rather than growth have garnered much attention. Analogies to combat are frequently used to describe the war between bacteria and host cells: here, the battle is a fourth-generation type—let your enemy destroy itself, or help it to remain weak throughout the war. For bacteria, this could be possible by understanding the communication pathways (QS) used by pathogens to coordinate their degree of virulence [152].

Normal antibiotics either kill or inhibit the growth of bacteria by targeting vital biological pathways related to the cell membrane, nucleic acids, or protein synthesis. This selectivity leads to the emergence of antimicrobial resistance. No novel antimicrobial groups with a new mechanism of action have reached clinical trials in recent times [152]. Accordingly, there is a critical need to develop alternate strategies expected to guide the development of therapeutically valuable antibiotics. The need for different therapeutic tactics to cure or inhibit bacterial infections induced by resistant strains has encouraged investigation toward the detection and improvement of antivirulence medicines. *In vitro* antibacterial studies may

differ from what happens *in vivo*. Bacteria may adapt to grow in host tissues with a diverse set of environmental conditions. Bacteria have multiple virulence factors and can create biofilms that induce host cell damage and chronic infectious diseases, which in turn are adjusted by complicated regulatory pathways. Therefore, antibiotics that can prevent colonization, affect metabolism, weaken virulence, or affect gene expression without disturbing *in vitro* bacterial growth offer significant advantages. These may include widening the range of drug activity, and reducing the development of resistance [153].

Most pathogens begin attacking human tissues through adhesin production. Pathogens invade host cells and form biofilms to guard the bacterial growth against the host defenses. This is followed by the efflux of enzymes and exotoxins, which assist in tissue degradation and nutrient release [154].

QS is a route of communication between bacterial cells that enables them to coordinately modify gene expression according to their cell density. QS includes the production and secretion of signal compounds into the outer environment. The signal compound concentration increases gradually with bacterial growth until it reaches a threshold, at which it stimulates a receptor. The QS receptor initiates a biological response in all cells of the bacterial population by regulating gene expression. Thus, QS allows a bacterial community to alter its behavior and virulence like a multicellular organism [155].

QS affects many biological processes, including competence, bioluminescence, motility, antibiotic biosynthesis, biofilm formation, and virulence factor expression, in human, animal, and plant pathogens [155]. Mutagenesis may disrupt QS systems in several pathogens,

leading to a remarkable reduction in virulence. Correspondingly, QS can affect antimicrobial susceptibility, either by enhancing tolerance to antimicrobials in biofilms [156], or by controlling antimicrobial resistance genes directly. For example, MecA regulates methicillin resistance in *S. aureus* [157], or by regulating the antimicrobial resistance genes acquisition as detected in *Streptococcus pneumoniae* [158]. Therefore, hindering QS may decrease bacterial virulence and/or restore conventional antimicrobial susceptibility.

QS is an encouraging target for the development of new antivirulence drugs. Antivirulence protocols that are concerned with the disruption of QS systems are usually called quorum quenching (QQ). An effective QQ protocol needs a comprehensive awareness of the molecular aspects and structural design of the targeted QS protocol [159]. In QS systems, the signal compound holds information that is sent by a "donor" cell to an "acceptor" cell. This system offers several targets for the action of compounds or enzymes interfering with QS-systems, specifically: (i) the synthesis of the signal compounds by the donor cell; (ii) the availability and functionality of the signal compound; and (iii) the decoding of the message of the signal compound by the acceptor cell (Figure 4.1).
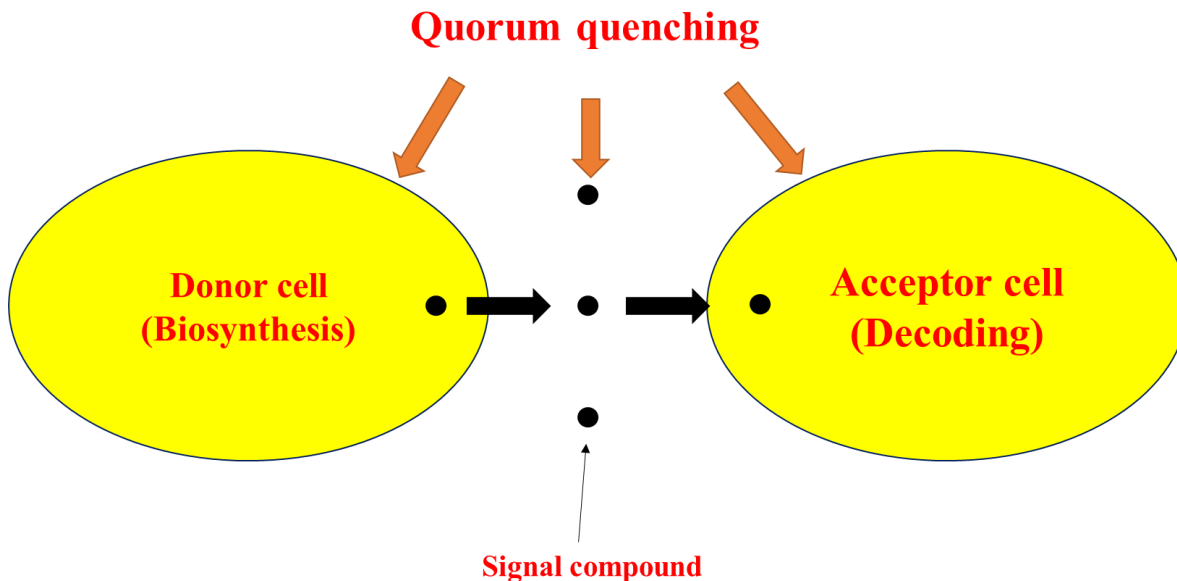
Figure 4.1. Quorum quenching systems may work by targeting the signal compound biosynthesis, its availability in the surrounding environment, or by preventing the decoding of the signal compound by the acceptor cell.

Staphylococcus aureus strains are divided into four classes according to the AIP that they produce. Every AIP selectively stimulates its specific AgrC receptor, and hinders other AgrC receptors through competitive antagonism [160]. A previous study showed that the administration of AIP-II to agr class-I *S. aureus*-infected mice hindered agr stimulation enough to prevent the formation of abscesses [160,161]. Many studies have shown that the macrocycle (thiolactone ring) included in the AIP3 structure is essential for its effect, while changing the thiolactone group to a lactam or lactone moiety effectively abolishes the receptor stimulation.

In this chapter, a simple new technique was used for the total synthesis of *S. aureus* AIP-III. AIP-III was chemically synthesized *via* an SPPS method using 2-chlorotrityl chloride resin as a solid support. The thiolactone ring cyclization was carried out using a water-soluble carbodiimide, EDCI.HCl, and DMAP. Purifications during the synthesis were carried out by washing with water. The final purification was performed using semi-preparative RP-HPLC. The yield was up to 86%, with purity of approximately 99%. A second intramolecular cyclization was carried out to yield an analog of AIP-III, called "HAK" (Figure 4.2).
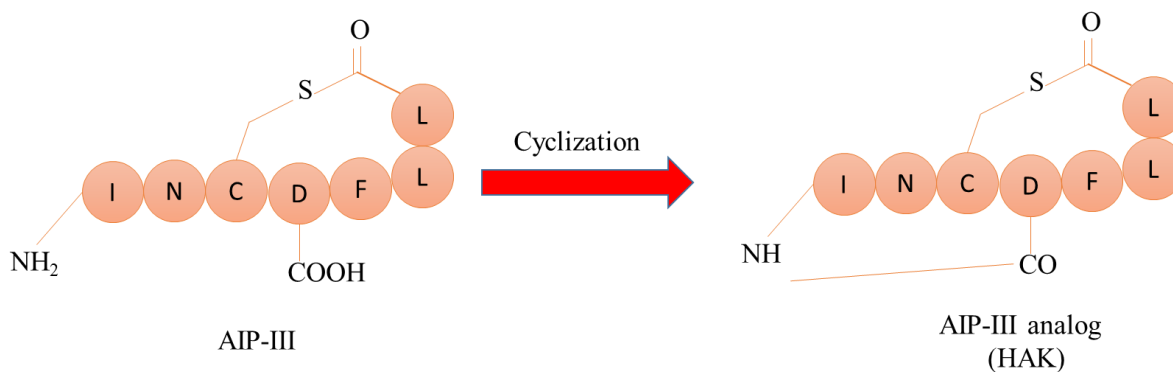
Figure 4.2. QSynthesis of AIP-III analog (HAK) by ring-tail cyclization.

4.1.1. Previous Studies

A previous study used a standard Fmoc/tertiary butyl (*t*Bu) SPPS protocol to synthesize linear peptides on 4-hydroxymethyl-phenylacetamido-methyl polystyrene resin (Scheme 4.1). Ethanethiol and dimethyl aluminum chloride were used to initiate the macrocycle formation. Intramolecular thiol–thioester exchange of the linear peptides was performed by dissolving the purified peptide thioester in 6 M guanidinium chloride in 0.1 M phosphate buffer and

acetonitrile (3:2 v/v) at an adjusted pH of 6.9. The peptide was then agitated using a multipurpose rotator at 50 °C for 2 h to yield a macrocyclic product (yield 25%−50%) [162].
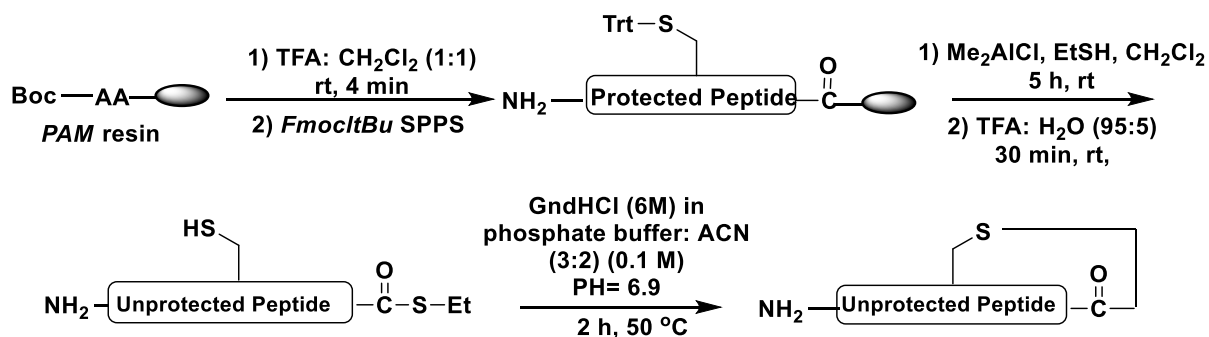
Scheme 4.1. Solid-phase synthesis of autoinducer peptides (AIPs) and their analogs.

Another study illustrated the formation of AIPs using on-resin cyclization, as shown in Scheme 4.2.

Purities 56-87%
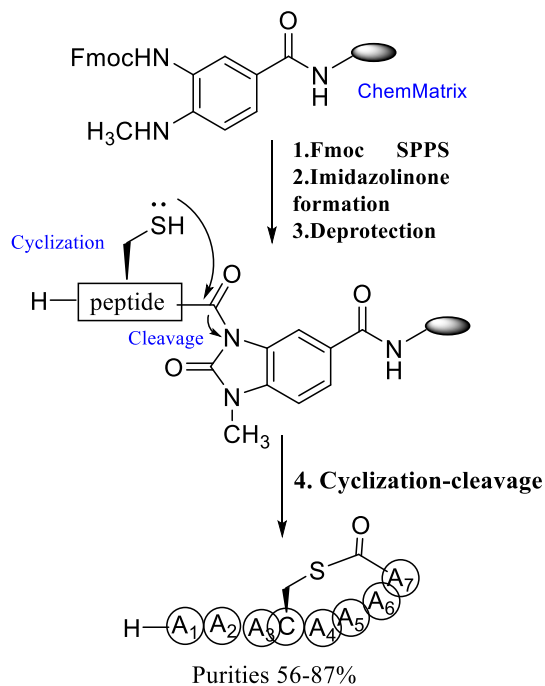
Scheme 4.2. On-resin cyclization−cleavage strategy for preparation of AIPs.

N-acyl-benzimidazolinone (Nbz)-Gly-ChemMatrix resin was used as the solid support. Cyclization was carried out after cleavage from the resin by adding 0.2 M phosphate buffer (pH 6.8) and acetonitrile [1:1 (v/v)] to the resin, then the suspension was stirred for 2 h at 50 °C. Purification was carried out by preparative RP-HPLC. Fractions containing pure peptides were lyophilized to give the desired product (14% yield) [163].

The main disadvantages of these approaches were the low yield and the use of high temperatures for 2 h. The approach described in this chapter can provide high yields at room temperature.

4.2.   Materials and Methods

4.2.1. Synthesis Protocol

AIP-III was prepared *via* an SPPS method using Fmoc and 2-chlorotrityl resin as the solid support [141]. As shown in Scheme 4.3, the synthesis process was started by loading a leucine residue onto 2-chlorotrityl chloride resin. Side-chain-protected Fmoc-amino acid residues were then coupled to the loaded amino acid residue using 2 equiv. of HBTU, 4 equiv. of DIEA, and 2 equiv. of HOB*t* in 30 mL of DMF. Piperidine 20% (v/v) in DMF was used to remove the Fmoc protecting groups. A trityl side-chain group protecting cysteine was selectively removed by washing with a 0.4 M I_2 solution in DMF for 30 min. The disulfide side-product was reduced to the free-thiol form by washing the peptide–resin with 0.4 M dithiothreitol (DTT) in DMF for 1 h. Cleavage of the side-chain-protected linear peptide from the resin was performed using a mixture of TFE/acetic acid/DCM (3:1:1 [v/v/v]) [142]. Macrocycle formation was achieved by using 0.9 mM of the linear peptide (to avoid dimer

side-products), 2 equiv. of EDCI.HCl, and 4 equiv. of DMAP in DMF. The removal of the side-chain-protecting groups was carried out using TFA/TIS/H_2O (95:2.5:2.5 [v/v/v]). The final deprotection of the Fmoc group was carried out using 20% piperidine in DMF. Purification was carried out by semi-preparative RP-HPLC (Hitachi L-7100 apparatus, XTerra Prep MS C18 OBD 10 μm column [19 × 150 mm; Waters]). The mobile phases were acetonitrile containing 0.1% TFA, and H_2O containing 0.1% TFA. Products were detected by absorbance at 220 nm [143]. Lyophilization was carried out in a VD-800F freeze dryer (TAITEC) to yield the pure cyclic target product [144].
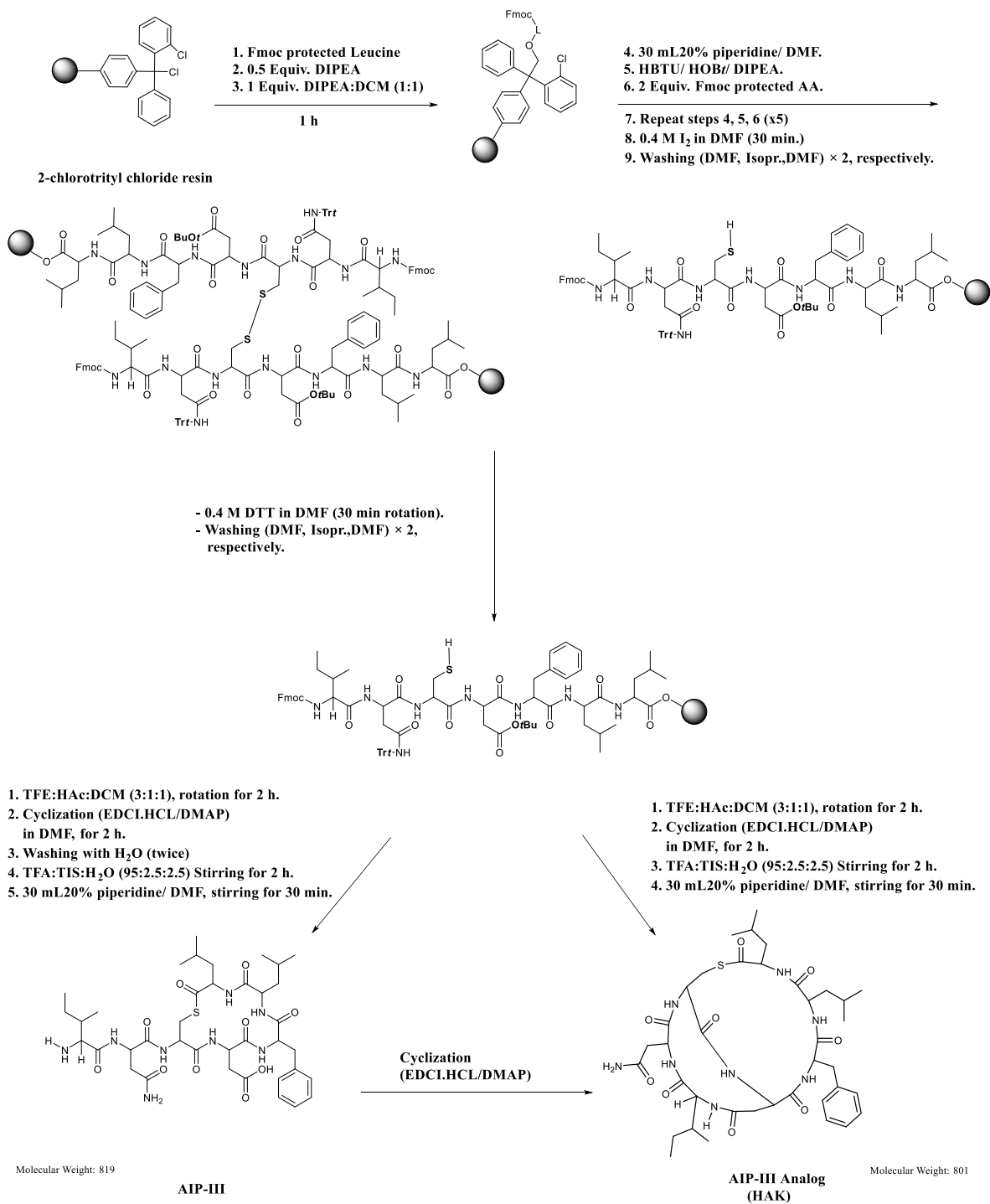
Scheme 4.3. The total synthesis of AIP-III and its analog HAK using an I$_2$/ *N*-(3-dimethylaminopropyl)-*N*-ethylcarbodiimide hydrochloride (EDCI.HCl) method

4.2.2. Experimental

4.2.2.1. Loading of Fmoc-Leu-OH onto Barlos Resin

Table 4.1. Amounts of components in the loading reaction.

Compound	MW	Equiv.	mmol	Amount
Barlos resin		1	1.6	1 g
Fmoc-Leu-OH	353.4	0.6	0.96	0.34 g
DIEA	129.25	0.5	0.8	0.14 mL
DIEA:DCM 1:1		1	1.6	0.56 mL
Methanol				1 mL

Calculations

- Weight of Fmoc-Leu-OH = Equivalence × Resin capacity (mmol/g)/1000 × MW = (610.7 × 0.96)/1000 = 0.34 g.

- Weight of DIEA = Equivalence × Resin molarity × MW.

- Volume of DIEA = 129.25/[0.742 (density) × 1000] = 0.14 mL.

- DIEA:DCM (1:1) = 0.28 + 0.28 = 0.56 mL.

- Theoretical weight calculations:

- Increase in resin weight (by methanol capping) = 1.6 – 0.96 (Fmoc-AA) = 0.64 mmol.

- 0.64 × 32.04 (the MW of methanol) = 20.5 mg/1000 = 0.021 g.

- Decrease in resin weight = 1.6 × 35.453 (the atomic weight of Cl) = 56.7 mg/1000 = 0.057 g.

- Theoretical weight = 1 g (resin) + 0.34 g (Fmoc AA) + 0.021 g (methanol) − 0.057 g (Cl) = 1.3 g.

Procedures

In the SPPS reaction vessel (118.710 g):

Barlos resin (1 g) was added and washed twice with DCM until complete swelling of the resin occurred. Fmoc-Leu-OH (0.34 g), 15 mL of DCM, and 0.14 mL of DIEA were added, respectively. The reaction mixture was stirred manually for 5 min, then 0.56 mL of DIEA:DCM (1:1 [v/v]) was added and stirred for 1 h. Methanol (1 mL, for capping unreacted sites) was added to the reaction mixture and stirred for 10 min. Subsequently, the reaction solvents were removed using a suction pump. The resin was washed using DCM (twice), DMF (twice), isopropanol (twice), DMF (twice), isopropanol (twice), methanol (twice), and ethyl ether (twice). Then, drying under reduced pressure was performed for 1 h. Finally, the resin was weighed, and the yield was calculated (1.26 g).

% Yield = (1.26/1.3)×100 = 97%.

- Loading-rate measurement of Fmoc-Leu-resin:

In three 10-mL volumetric flasks, 1–3 mg of Fmoc-Leu-resin was added with 20% piperidine in DMF until the 10 mL mark was reached. After waiting for 30 min at room temperature,

two blank samples containing 20% piperidine in DMF were prepared. Absorbance values were measured at 290 nm for all samples.

Table 4.2. Measurement of the loading rate.

Sample no.	Resin weight (mg)	$A_{290\ nm}$	Loading-rate (mmol/g resin)
1	1	0.45	0.91
2	2	0.9	0.91
3	3	1.3	0.88

Loading rate = 1000 ×10 × $A_{290\ nm}$/4950 (Fmoc molar absorptivity) × 1 × weight

= mmol/g resin.

Mean loading rate/g = 0.9 mmol/g.

Actual loading rate = 0.9 × 1.26 = 1.13 mmol.

% Yield = (0.9/0.96)×100 = 94%.

4.2.2.2. Peptide Chain Elongation

4.2.2.2.1. Addition of Fmoc-Leu-OH

Table 4.3. Calculation of the amounts of reactants needed.

Compound	MW	Equiv.	mmol	Amount
Fmoc-L-resin		1	1	1.26 g
Fmoc-Leu-OH	353.4	2	2	0.71 g
HBTU	379.45	2	2	0.76 g
HOBt.H$_2$O	153.14	2	2	0.31 g
DIEA	129.25	4	4	0.7 mL

Calculations

Weight of Fmoc-Leu-OH = (596.67 × 3)/1000 = 0.71 g.

Weight of HBTU = 2/1000 × 379.25 = 0.76 g.

Weight of HOBt.H$_2$O = 2/1000 × 153.14 = 0.31 g.

Volume of DIEA = (4/1000 × 129.25)/0.742 = 0.7 mL.

Procedures

- Deprotection:

In the SPPS reaction vessel, the Fmoc-AA-resin was washed twice with DMF until it was completely swollen; 30 mL of 20% piperidine in DMF was added and stirred for 30 min. The

reaction mixture was removed, and the resin was washed with DMF (twice), isopropanol (twice), and DMF (twice).

-   Coupling:

In the SPPS reaction vessel, the Fmoc-Leu-OH was added with DMF (15 mL), HBTU, and HOBt.H$_2$O. The reaction mixture was rotated for 2 h. The reaction medium and excess reactants were removed, then the resin was washed with DMF (twice), isopropanol (twice), DMF (twice), and DCM (twice).

The series of coupling reactions was continued until the side-chain-protected linear peptide was completely synthesized. The Fmoc protecting group was kept bonded to the linear peptide–resin complex to prevent head-to-tail cyclization during the thioester cyclization.

4.2.2.3. Selective Deprotection of the Thiol Group

The S-trityl protecting group of cysteine is susceptible to oxidation by iodine, whereas the N-trityl protecting groups of other amino acids are stable with respect to iodine [164]. Therefore, the resin–peptide complex was rotated with 30 mL of 0.4 M iodine in DMF for 30 min. The reaction mixture was removed and the resin was washed with DMF (twice), isopropanol (twice), and DMF (twice). Deprotection of the S-trityl group may form a peptide with a free thiol group or a disulfide-bonded dimer; dimer was subsequently reduced to the free-thiol form by reduction with 0.4 M DTT solution in DMF and rotation for 30 min. The reaction mixture was removed and the resin was washed with DMF (twice), isopropanol (twice), and DMF (twice).

4.2.2.4. Cleavage from the Resin

TFE promotes the hydrolysis of ester linkages between the peptide and the resin without affecting the side-chain-protecting groups, which are cleaved by TFA. Therefore, a cleavage cocktail (DCM:TFE:acetic acid, 1:3:1 [v/v/v]) was used.

Procedures

In the SPPS vessel, the cleavage cocktail was added to the peptide–resin and rotated using an electric rotator for 2 h at room temperature. The filtrate was collected in a 100-mL round-bottomed flask (80.7 g) and evaporated under reduced pressure. Water (2 mL) was added to the residue to crystallize the protected peptide as white crystals. The crystals were dried under reduced pressure for 1 h, weighed (1.29 g), and the percentage yield was calculated. The product was checked for its purity by RP-HPLC (Figure 4.3).

% Yield = (1290/1377)×100 = 94%.
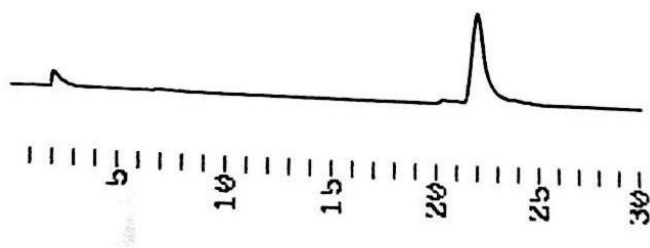
Figure 4.3. High-performance liquid chromatogram of protected-side-chain linear AIP-III with a free thiol group, RT = 21.9 min.

4.2.2.5. Macrocycle Formation (Thioester Formation)

Cyclization was carried out using 0.5 mM of the linear peptide to avoid dimer formation. Two equivalents of EDCI.HCl and 4 equiv. of DMAP were used for the cyclization. The reaction was monitored by RP-HPLC (Figure 4.4). The protected peptide is insoluble in water, which allowed the removal of the excess reactants and side-products by washing with water (Figure 4.5).
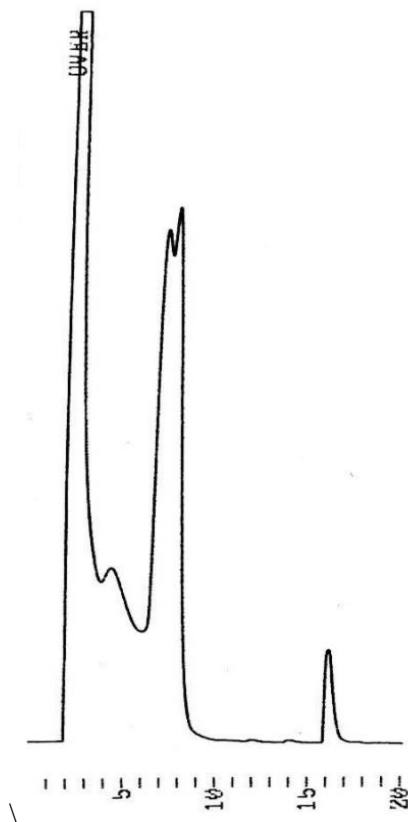
Figure 4.4. High-performance liquid chromatogram of the protected AIP-III after macrocyclization, RT = 15.98 min.
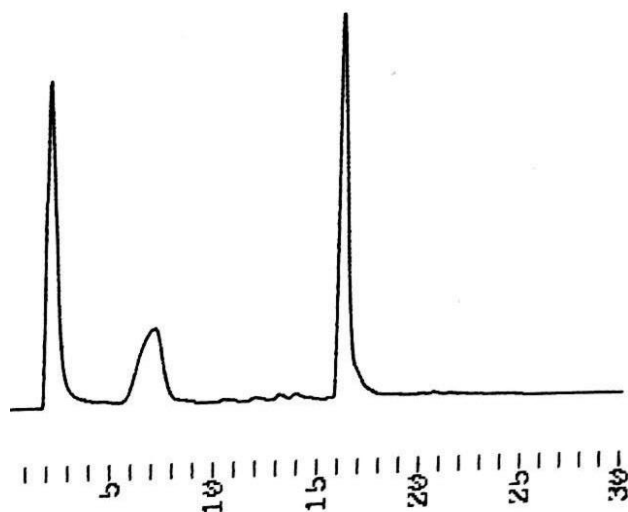
Figure 4.5. High-performance liquid chromatogram of the cyclic protected AIP-III after washing with distilled water, RT = 15.98 min.

4.2.2.6. Deprotection of Side-chain Protecting Groups

Removal of the side-chain-protecting groups was carried out using TFA:TIS:H_2O (95:2.5:2.5 [v/v/v]). The reaction was monitored by RP-HPLC for 2 h (Figure 4.6), followed by deprotection of the Fmoc group using 20% piperidine in DMF. The peptide was purified by semi-preparative RP-HPLC to yield the final product AIP-III after crystallization by water (Figure 4.7).

% Yield = (350/407)×100 = 86%.
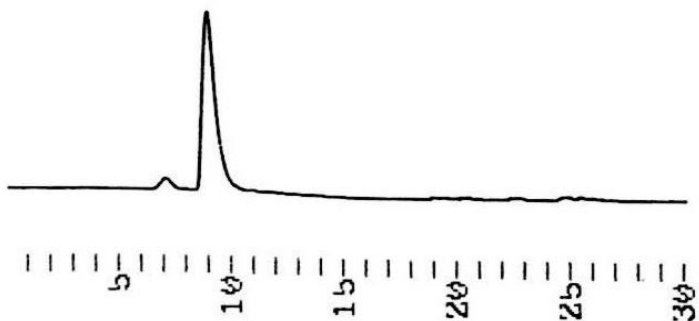
Figure 4.6. High-performance liquid chromatogram of Fmoc AIP-III, RT = 8.85 min.
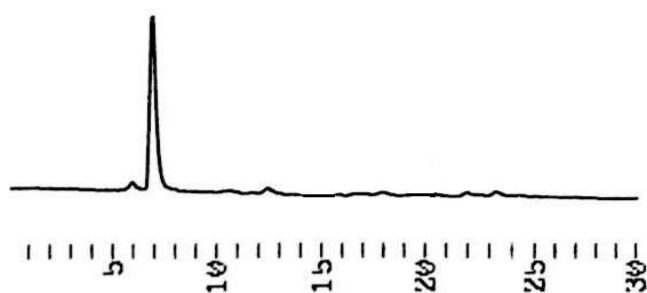
Figure 4.7. High-performance liquid chromatogram of pure AIP-III, RT = 6.75 min.

4.2.2.7. Intramolecular Second Cyclization

As shown in Scheme 4.3, EDCI.HCl and DMAP were used for the second cyclization, to form HAK from AIP-III, after removal of the Fmoc protecting group. The reaction was monitored by HPLC and confirmed by mass spectroscopy.

4.3.   Results and Discussion

4.3.1. Synthesis Protocol

S. aureus AIP-III and its analog HAK were synthesized using a standard Fmoc/SPPS method as described in Section 4.2.1. The yields of the obtained AIP-III and HAK were approximately 86% and 80%, respectively. The yield was calculated by dividing the real obtained yield by the theoretical yield (calculated based on the loading rate equation of the first loaded amino acid) multiplied by 100. The structure of the peptide HAK and its purity were confirmed by mass spectrometry (*m/z* 801, calcd. 801, formula: $C_{38}H_{56}N_8O_9S$) (Figure 4.8).
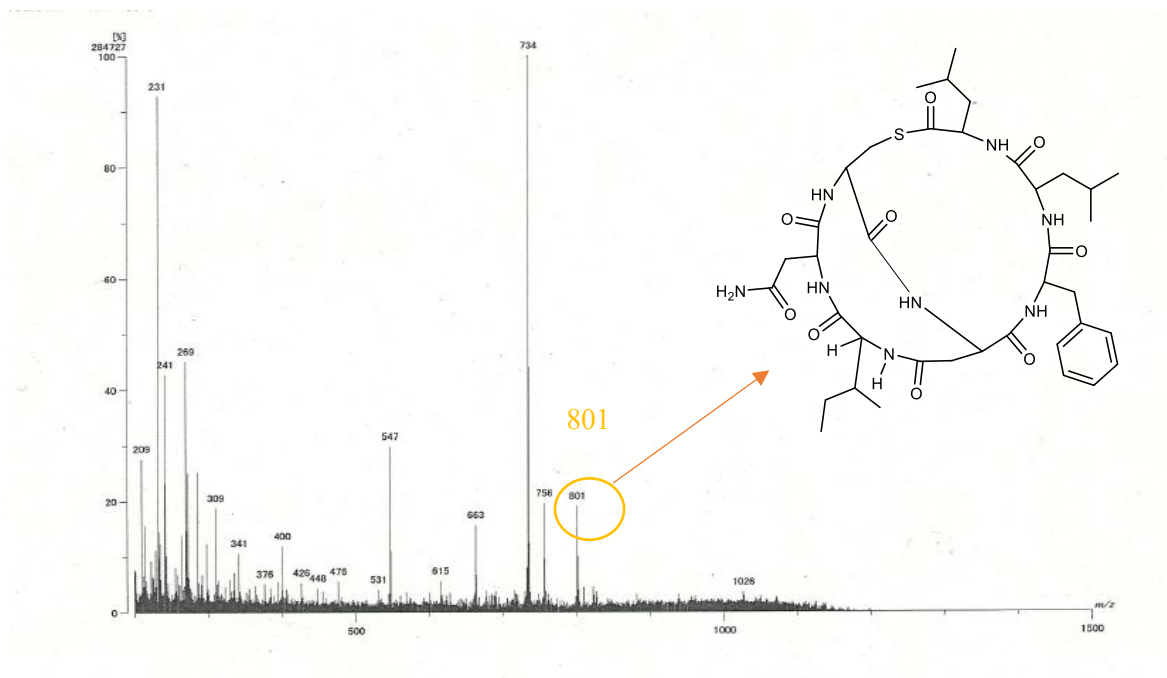
Figure 4.8. Mass spectrum and structure of the AIP-III analog HAK.

4.3.2. Selective Deprotection of Thiol Group

The reaction of short peptides including Cys(Trt) amino acids with I$_2$ results in the immediate elimination of the trityl group. The resultant peptides may be converted to a symmetrical dimer, or mixtures of monomers and dimers, according to the solvent and peptide concentration. The reaction rate depends on the solvent; in polar solvents such as methanol, Cys(Trt) reacts fast, but in nonpolar solvents, such as CHCl$_3$, the reaction becomes very slow [165].
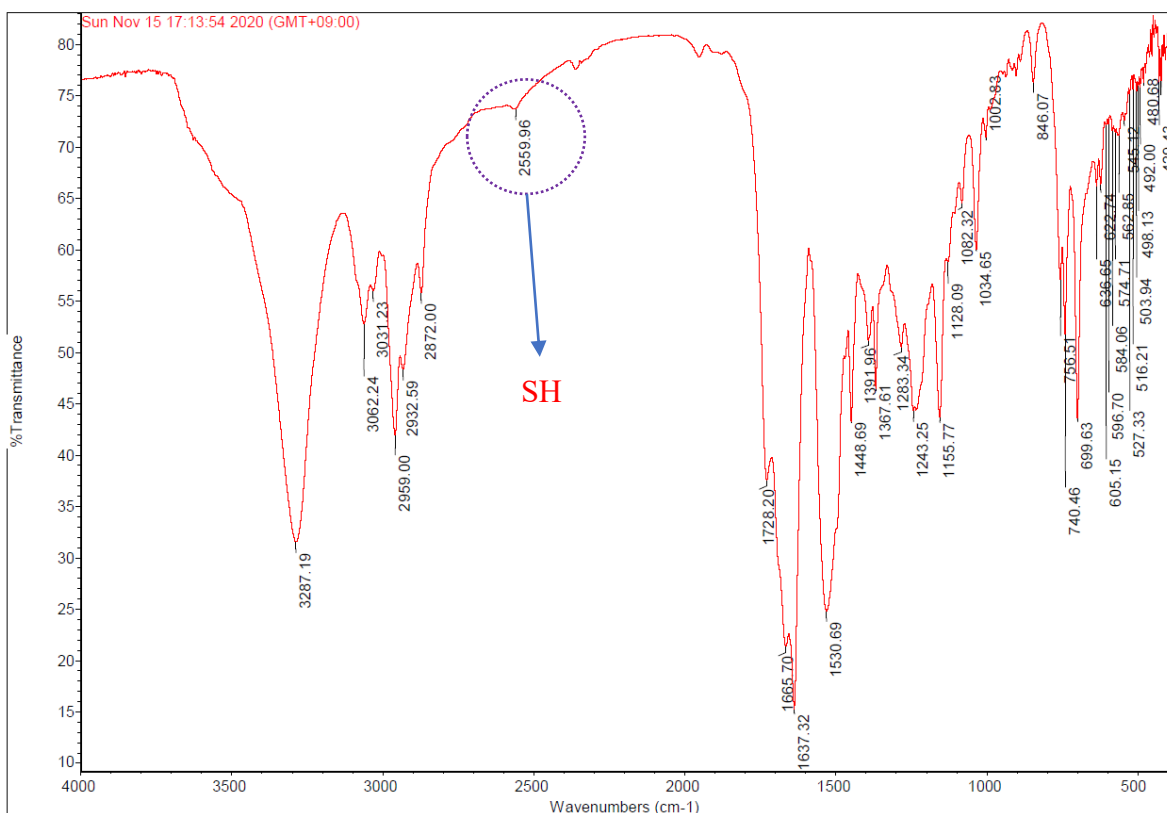
Figure 4.9. Fourier-transform infrared spectrum of protected linear AIP-III with a free thiol group.

Figure 4.9 shows the efficient removal of the trityl group from cysteine residue by oxidation with iodine, followed by reduction with DTT to produce free thiol groups. Thiol groups appear in FTIR spectra as a weak band at 2600 to 2550 cm^{-1} [166], which was detected in this case at 2559.9 cm^{-1}.

4.3.3. Macrocycle Formation (Thioester Formation)

A dicyclohexylcarbodiimide (DCC)/DMAP coupling system has been used by some researchers for the formation of thioester linkages in organic synthesis. DMAP can accelerate the DCC-induced carboxylic acid esterification with thiols. DMAP offers the advantage of preventing the formation of side-products, and improves the yields of the thioester compound at room temperature [167]. However, dicyclohexylurea is an insoluble side-product of DCC that can interfere with target product purification. Therefore, here, the EDCI.HCl/DMAP system was used for the intramolecular cyclization as its side-product is water-soluble urea. Washing with distilled water only can thus remove all excess reactants and side-products, leaving the water-insoluble AIP-III as crystals.

The macrocyclization reaction was confirmed by the disappearance of the thiol group peak from the FTIR spectrum, as shown in Figure 4.10.

4.3.4. Intramolecular Second Cyclization

The second intramolecular cyclization, required to form HAK, was achieved successfully using the EDCI.HCl/DMAP system after removal of the *N*-terminal Fmoc group. The AIP analog HAK consists of two unsymmetric rings (16- and 12-membered rings, respectively). The two rings are separated by an amide bond and they represent a new double-cyclic

structure that is different from catenane, which consists of two interlocked cyclic compounds.

HAK was confirmed by mass spectroscopy (Figure 4.8).
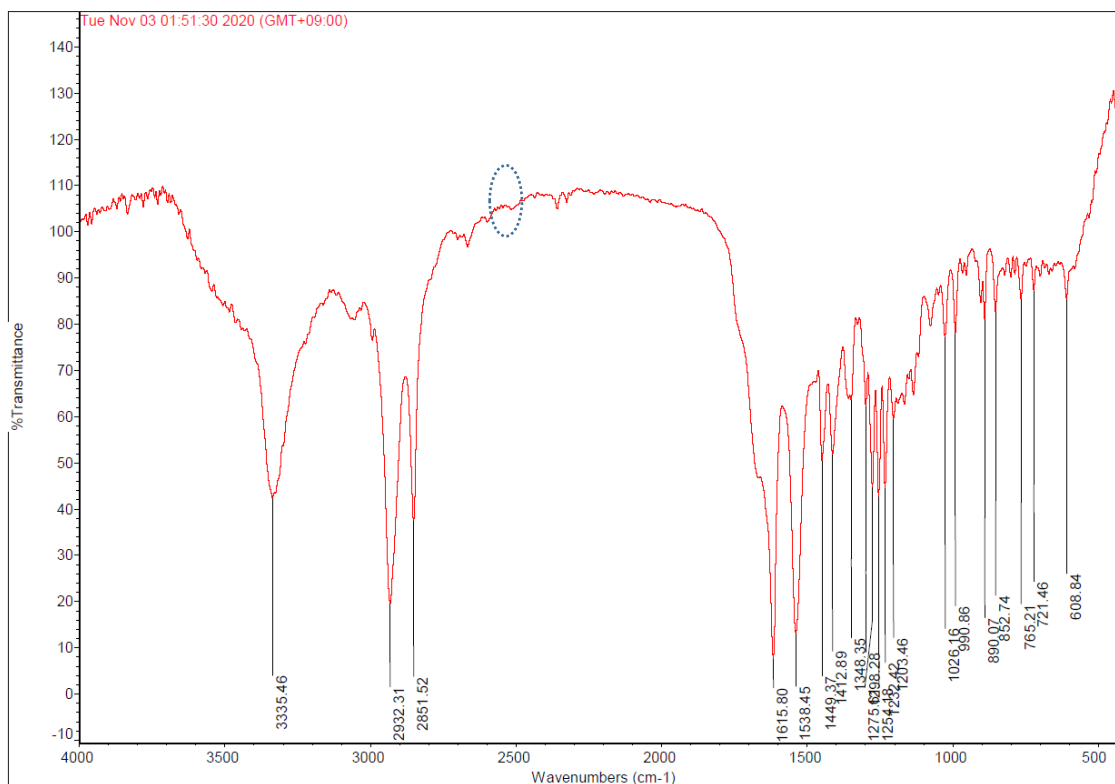
Figure 4.10. FTIR spectrum of AIP-III showing no free thiol group.

S. aureus AIPs are structurally related, for example, they all have a macrocycle and an exocyclic tail. The macrocycle is essential for binding to the specific receptor, while the tail is responsible for the activity. Any mutations in the macrocycle can affect the binding of the AIP to the receptor, and changing or removing the tail can reduce the effect of the AIP by up to 56-fold [168]. Herein, AIP-III was synthesized by a standard Fmoc SPPS method. AIP-III consists of a macrocyclic head and a linear exocyclic tail. To produce the analog HAK, the tail was cyclized into a 12-membered ring because this might affect bacterial virulence, while

the head was kept unchanged to allow binding to the receptor. Study of QS is paramount for researchers who wish to control emergent bacterial drug-resistance. In the new method described here, I_2/EDCI.HCl was used for the first time in the total synthesis of *S. aureus* QS peptide AIP-III. Other *S. aureus* QS peptides have similar structures, and they can be prepared by the same technique. Furthermore, analogs can also be prepared by this method, which will be useful in the study of QQ. This technique has many merits, for example, it is easy, cheap, reproducible, no dimers are formed during cyclization, the final side-products can be removed with water, and the yield of the target peptide is high. The 3D minimized secondary structures was computationally calculated by MOE 18.0 as shown in Figure 4.11.
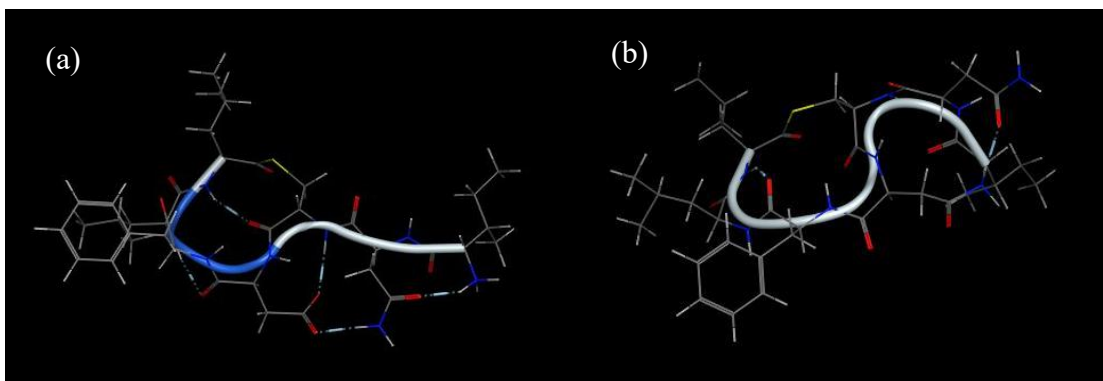
Figure 4.11. 3D minimized structures of (a) AIP-III and (b) HAK computationally drawn by MOE 18.0 software

4.4. Conclusions

QS systems in Gram-positive bacteria are AIP-dependent, although the QS systems' controlling virulence has not yet been identified in all microbes. Most QS systems are not induced only by cell density but can be affected by other metabolic and environmental stimuli.

Here, *S. aureus* AIP-III, an example QS peptide, was chemically synthesized using a simple method. This technique has not been used before for the total synthesis of complex compounds. An I$_2$/DTT system was used for the selective deprotection of Cys-S–Tr*t* without affecting other protecting groups. DTT reduces any resultant disulfide bonds to produce free thiol groups. The *N*-terminus of the peptide was kept protected with the Fmoc group. An EDCI.HCl/DMAP system was used for intramolecular cyclization. Most of the side-products were water-soluble, so could be removed easily by washing with water. This method has the advantage of a higher yield (86%) than other synthetic methods. AIP-III antagonist HAK, having a bicyclic structure, was also produced. The head-macrocycle will allow effective binding with the agr receptor, while the tail cyclization will inhibit bacterial virulence. The technique described in this chapter opens up ample opportunities for more and novel in-depth studies of QS and QQ.

Chapter 5

General Conclusions

Antimicrobial peptides are one of the most vital classes of antimicrobials because they exclusively affect pathogens by targeting their negatively-charged membrane components. This unique ability can minimize the incidence of microbial resistance [3]. The developing global disaster of antibiotic resistance acquired by virulent bacteria highlights the value of finding replacements for existing antimicrobials [4]. The failure of the most effective antimicrobials to inhibit resistant pathogens underlines the vital need for potent alternatives. Infectious diseases were the major reason for mortality and morbidity in the human population before the application of standard antibiotics in the clinical field. Antimicrobial peptides have arisen as an alternative therapy for the treatment of antibiotic-resistant pathogens [28]. Antimicrobial peptides can directly affect bacterial cells, therefore, they can target antibiotic-resistant cells such as persistent cells and cells in biofilms. Although microbes have many mechanisms for resisting the action of antimicrobial peptides, the structure of the lipid bilayer in the bacterial cell membrane renders it difficult to acquire full resistance to them. Furthermore, the resistance acquired by microbes to antimicrobial peptides is not similar to that acquired to other types of antibiotics, and resistance has only been documented for a limited number of antimicrobial peptides.

The first cyclic decapeptide and its linear counterpart were synthesized by an SPPS method with a quantitative yield of the linear decapeptide (97%) and a good yield of the cyclic form (45%) [55]. Antibacterial studies were performed using *E. coli* (a widespread Gram-negative

pathogen) and *B. thuringiensis* as a representative Gram-positive pathogen. MIC values were determined by the broth microdilution method. The cyclic peptide and its linear counterpart exhibited MIC values of 0.16 and 0.3 mg/mL, respectively, against *E. coli*. In the case of *B. thuringiensis*, the peptides had the same MIC value, 0.24 mg/mL. Time–kill studies were performed using *E. coli*, which indicated a fast-killing effect of both peptides (≥99% of the bacterial cells after 1 h of incubation using a concentration of twice the MIC value for each peptide). Moreover, cell viability studies against *E. coli* carried out using a high bacterial concentration showed that both peptides had a maximum killing effect of >80% of the tested bacterial cells.

In Chapter 3, cyclic undecapeptides (QNRNFYFNRNQ and QNRNFHFNRNQ) and their linear counterparts were synthesized by an SPPS method with quantitative yields of the linear peptides (97%) and good yields of the cyclic forms (75%). These peptides were designed to have hydrophobic centers consisting of three amino acids, connected to two symmetrical wings containing a total of eight polar and/or cationic amino acid residues. Changing the structure of the hydrophobic center from tyrosine-containing (amphipathic) to histidine-containing (cationic) affected the antimicrobial activity of the whole peptide. The antibacterial effects of the peptides were studied against the clinically-important pathogens *E. coli* and *P. aeruginosa* (Gram-negative bacteria), and *B. subtilis* and *S. aureus* (Gram-positive). MIC values were evaluated *via* the broth microdilution method. The tyrosine-containing peptides showed promising MIC values, while the peptides containing histidine showed even greater effectiveness against the bacteria. The antibacterial activities of the peptides were comparable to that of gentamycin sulfate. Time–inhibition studies were

performed to investigate the antibacterial behavior of these peptides against the four bacterial species. The tyrosine-containing peptides showed faster antibacterial effects against most of the test bacteria than the histidine-containing peptides when applied at concentrations greater than or equal to the MIC values. Moreover, most of the bacteria did not show any significant resistance to the tyrosine-containing peptides even after 24 h of incubation.

AIPs are not only used for communication between bacteria (QS), but they also have other biological effects. The study of AIPs allows researchers to understand bacterial communications and virulence. To facilitate these studies, it is desirable to develop new, simplified techniques for the synthesis of AIPs and their analogs with high yields. Here, in Chapter 4, *S. aureus* AIP-III and an AIP-III antagonist, HAK, having a bicyclic structure, were synthesized. The *C*-terminal macrocycle of HAK allows effective binding with the agr receptor, while the tail cyclization will inhibit bacterial virulence. This peptide synthesis technique opens up opportunities for more in-depth studies of QS and QQ.

References

1. Loll, P.J.; Upton, E.C.; Nahoum, V.; Economou, N.J.; Cocklin, S. The high resolution structure of tyrocidine A reveals an amphipathic dimer. *Biochim. Biophys. Acta - Biomembr.* **2014**, *1838*, 1199–1207, doi:10.1016/j.bbamem.2014.01.033.

2. Madani, F.; Lindberg, S.; Langel, Ü.; Futaki, S.; Gräslund, A. Mechanisms of Cellular Uptake of Cell-Penetrating Peptides. *J. Biophys.* **2011**, *2011*, 1–10, doi:10.1155/2011/414729.

3. Lohner, K. New strategies for novel antibiotics: peptides targeting bacterial cell membranes. *Gen. Physiol. Biophys.* **2009**, *28*, 105–116, doi:10.4149/gpb_2009_02_105.

4. World Health Organization, W. Global priority list of antibiotic-resistant bacteria to guide research, discovery, and development of new antibiotics. **2017**, 1–7.

5. Centers for Disease Control and Prevention, C. Antibiotic resistance threats in the United States, 2013. **2013**, 1–114.

6. Shankar, P.R.; Piryani, R.M.; Piryani, S. The state of the world's antibiotics 2015. *J. Chitwan Med. Coll.* **2017**, *6*, 68–69, doi:10.3126/jcmc.v6i4.16721.

7. Aungkulanon, S.; McCarron, M.; Lertiendumrong, J.; Olsen, S.J.; Bundhamcharoen, K. Infectious Disease Mortality Rates, Thailand, 1958–2009. *Emerg. Infect. Dis.* **2012**, *18*, 1794–1801, doi:10.3201/eid1811.120637.

8. Aminov, R. History of antimicrobial drug discovery: Major classes and health

impact. *Biochem. Pharmacol.* **2017**, *133*, 4–19, doi:10.1016/j.bcp.2016.10.001.

9.   Bush, K.; Bradford, P.A. β-Lactams and β-Lactamase Inhibitors: An Overview. *Cold Spring Harb. Perspect. Med.* **2016**, *6*, a025247, doi:10.1101/cshperspect.a025247.

10. LaVie, K.W.; Anderson, S.W.; O'Neal, H.R.; Rice, T.W.; Saavedra, T.C.; O'Neal, C.S. Neutropenia Associated with Long-Term Ceftaroline Use. *Antimicrob. Agents Chemother.* **2016**, *60*, 264–269, doi:10.1128/AAC.01471-15.

11. Krause, K.M.; Serio, A.W.; Kane, T.R.; Connolly, L.E. Aminoglycosides: An Overview. *Cold Spring Harb. Perspect. Med.* **2016**, *6*, a027029, doi:10.1101/cshperspect.a027029.

12. Taubert, M.; Zoller, M.; Maier, B.; Frechen, S.; Scharf, C.; Holdt, L.; Frey, L.; Vogeser, M.; Fuhr, U.; Zander, J. Predictors of Inadequate Linezolid Concentrations after Standard Dosing in Critically Ill Patients. *Antimicrob. Agents Chemother.* **2016**, *60*, 5254–5261, doi:10.1128/AAC.00356-16.

13. Kushner, B.; Allen, P.D.; Crane, B.T. Frequency and Demographics of Gentamicin Use. *Otol. Neurotol.* **2016**, *37*, 190–195, doi:10.1097/MAO.0000000000000937.

14. Borisova, S.A.; Zhao, L.; Sherman, D.H.; Liu, H. Biosynthesis of Desosamine: Construction of a New Macrolide Carrying a Genetically Designed Sugar Moiety. *Org. Lett.* **1999**, *1*, 133–136, doi:10.1021/ol9906007.

15. Liu, W.-B.; Yu, W.-B.; Gao, S.; Ye, B.-C. Genome Sequence of Saccharopolyspora erythraea D, a Hyperproducer of Erythromycin. *Genome Announc.* **2013**, *1*, 3–4,

doi:10.1128/genomeA.00718-13.

16. Kanoh, S.; Rubin, B.K. Mechanisms of Action and Clinical Application of Macrolides as Immunomodulatory Medications. *Clin. Microbiol. Rev.* **2010**, *23*, 590–615, doi:10.1128/CMR.00078-09.

17. Sugimoto, T.; Tanikawa, T. Synthesis and Antibacterial Activity of a Novel Class of 15-Membered Macrolide Antibiotics, "11a-Azalides." *ACS Med. Chem. Lett.* **2011**, *2*, 234–237, doi:10.1021/ml100252s.

18. Amsden, G.. Advanced-generation macrolides: tissue-directed antibiotics. *Int. J. Antimicrob. Agents* **2001**, *18*, 11–15, doi:10.1016/S0924-8579(01)00410-1.

19. Weisblum, B. Erythromycin resistance by ribosome modification. *Antimicrob. Agents Chemother.* **1995**, *39*, 577–585, doi:10.1128/AAC.39.3.577.

20. Serisier, D.J.; Martin, M.L.; McGuckin, M.A.; Lourie, R.; Chen, A.C.; Brain, B.; Biga, S.; Schlebusch, S.; Dash, P.; Bowler, S.D. Effect of Long-term, Low-Dose Erythromycin on Pulmonary Exacerbations Among Patients With Non–Cystic Fibrosis Bronchiectasis. *JAMA* **2013**, *309*, 1260, doi:10.1001/jama.2013.2290.

21. Hamilton-Miller, J.M. Chemistry and biology of the polyene macrolide antibiotics. *Bacteriol. Rev.* **1973**, *37*, 166–96.

22. Walsh, T.J.; Lewis, R.E.; Adler-moore, J. Pharmacology of Liposomal Amphotericin B : An Introduction to Preclinical and Clinical Advances for Treatment of Life-threatening Invasive Fungal Infections. **2019**, *68*, 241–243, doi:10.1093/cid/ciz091.

23.   Dubos, R.J. Studies on a bactericidal agent extracted from a soil bacillus. *J. Exp. Med.* **1939**, *70*, 1–10, doi:10.1084/jem.70.1.1.

24.   Dubos, R.J.; Hotchkiss, R.D. The production of bactericidal substances by aerobic sporulating bacilli. *J. Exp. Med.* **1941**, *73*, 629–640, doi:10.1084/jem.73.5.629.

25.   Van Epps, H.L. René Dubos: unearthing antibiotics. *J. Exp. Med.* **2006**, *203*, 259–259, doi:10.1084/jem.2032fta.

26.   Ohtani, K.; Okada, T.; Yoshizumi, H.; Kagamiyama, H. Complete Primary Structures of Two Subunits of Purothionin A, a Lethal Protein for Brewer's Yeast from Wheat Flour. *J. Biochem.* **1977**, *82*, 753–767, doi:10.1093/oxfordjournals.jbchem.a131752.

27.   Hirsch, J.G. Phagocytin: a bactericidal substance from polymorphonuclear leucocytes. *J. Exp. Med.* **1956**, *103*, 589–611, doi:10.1084/jem.103.5.589.

28.   Bahar, A.; Ren, D. Antimicrobial Peptides. *Pharmaceuticals* **2013**, *6*, 1543–1575, doi:10.3390/ph6121543.

29.   Shai, Y. Mode of action of membrane active antimicrobial peptides. *Biopolymers* **2002**, *66*, 236–248, doi:10.1002/bip.10260.

30.   Zhang, L.; Rozek, A.; Hancock, R.E.W. Interaction of Cationic Antimicrobial Peptides with Model Membranes. *J. Biol. Chem.* **2001**, *276*, 35714–35722, doi:10.1074/jbc.M104925200.

31.   Jenssen, H.; Hamill, P.; Hancock, R.E.W. Peptide Antimicrobial Agents. *Clin.*

Microbiol. Rev. **2006**, *19*, 491–511, doi:10.1128/CMR.00056-05.

32.   Park, C.B.; Kim, H.S.; Kim, S.C. Mechanism of Action of the Antimicrobial Peptide Buforin II: Buforin II Kills Microorganisms by Penetrating the Cell Membrane and Inhibiting Cellular Functions. *Biochem. Biophys. Res. Commun.* **1998**, *244*, 253–257, doi:10.1006/bbrc.1998.8159.

33.   Brumfitt, W.; Salton, M.R.J.; Hamilton-Miller, J.M.T. Nisin, alone and combined with peptidoglycan-modulating antibiotics: activity against methicillin-resistant Staphylococcus aureus and vancomycin-resistant enterococci. *J. Antimicrob. Chemother.* **2002**, *50*, 731–734, doi:10.1093/jac/dkf190.

34.   Bastian, A.; Schäfer, H. Human α-defensin 1 (HNP-1) inhibits adenoviral infection in vitro. *Regul. Pept.* **2001**, *101*, 157–161, doi:10.1016/S0167-0115(01)00282-8.

35.   Sitaram, N.; Nagaraj, R. Interaction of antimicrobial peptides with biological and model membranes: structural and charge requirements for activity. *Biochim. Biophys. Acta - Biomembr.* **1999**, *1462*, 29–54, doi:10.1016/S0005-2736(99)00199-6.

36.   Yasin, B.; Wang, W.; Pang, M.; Cheshenko, N.; Hong, T.; Waring, A.J.; Herold, B.C.; Wagar, E.A.; Lehrer, R.I. θ Defensins Protect Cells from Infection by Herpes Simplex Virus by Inhibiting Viral Adhesion and Entry. *J. Virol.* **2004**, *78*, 5147–5156, doi:10.1128/JVI.78.10.5147-5156.2004.

37.   Tamamura, H.; Ishihara, T.; Otaka, A.; Murakami, T.; Ibuka, T.; Waki, M.;

Matsumoto, A.; Yamamoto, N.; Fujii, N. Analysis of the interaction of an anti-HIV peptide, T22 ([Tyr5,12, Lys7]-polyphemusin II), with gp 120 and CD4 by surface plasmon resonance. *Biochim. Biophys. Acta - Protein Struct. Mol. Enzymol.* **1996**, *1298*, 37–44, doi:10.1016/S0167-4838(96)00113-6.

38.   Jenssen, H.; Sandvik, K.; Andersen, J.H.; Hancock, R.E.W.; Gutteberg, T.J. Inhibition of HSV cell-to-cell spread by lactoferrin and lactoferricin. *Antiviral Res.* **2008**, *79*, 192–198, doi:10.1016/j.antiviral.2008.03.004.

39.   Sinha, S.; Cheshenko, N.; Lehrer, R.I.; Herold, B.C. NP-1, a Rabbit α-Defensin, Prevents the Entry and Intercellular Spread of Herpes Simplex Virus Type 2. *Antimicrob. Agents Chemother.* **2003**, *47*, 494–500, doi:10.1128/AAC.47.2.494-500.2003.

40.   De Lucca, A.J.; Walsh, T.J. Antifungal peptides: novel therapeutic compounds against emerging pathogens. *Antimicrob. Agents Chemother.* **1999**, *43*, 1–11, doi:10.1128/AAC.43.1.1.

41.   Lee, Y.-T.; Kim, D.-H.; Suh, J.; Chung, J.H.; Lee, B.L.; Lee, Y.; Choi, B.-S. Structural characteristics of tenecin 3, an insect antifungal protein. *IUBMB Life* **1999**, *47*, 369–376, doi:10.1080/15216549900201393.

42.   Yokoyama, S.; Iida, Y.; Kawasaki, Y.; Minami, Y.; Watanabe, K.; Yagi, F. The chitin-binding capability of Cy -AMP1 from cycad is essential to antifungal activity. *J. Pept. Sci.* **2009**, *15*, 492–497, doi:10.1002/psc.1147.

43.	Lehrer, R.I.; Szklarek, D.; Ganz, T.; Selsted, M.E. Correlation of binding of rabbit granulocyte peptides to Candida albicans with candidacidal activity. *Infect. Immun.* **1985**, *49*, 207–11, doi:10.1128/IAI.49.1.207-211.1985.

44.	Moerman, L.; Bosteels, S.; Noppe, W.; Willems, J.; Clynen, E.; Schoofs, L.; Thevissen, K.; Tytgat, J.; Van Eldere, J.; van der Walt, J.; et al. Antibacterial and antifungal properties of α-helical, cationic peptides in the venom of scorpions from southern Africa. *Eur. J. Biochem.* **2002**, *269*, 4799–4810, doi:10.1046/j.1432-1033.2002.03177.x.

45.	van der Weerden, N.L.; Hancock, R.E.W.; Anderson, M.A. Permeabilization of Fungal Hyphae by the Plant Defensin NaD1 Occurs through a Cell Wall-dependent Process. *J. Biol. Chem.* **2010**, *285*, 37513–37520, doi:10.1074/jbc.M110.134882.

46.	Jenssen, H.; Hamill, P.; Hancock, R.E.W. Peptide Antimicrobial Agents. *Clin. Microbiol. Rev.* **2006**, *19*, 491–511, doi:10.1128/CMR.00056-05.

47.	Barbault, F.; Landon, C.; Guenneugues, M.; Meyer, J.-P.; Schott, V.; Dimarcq, J.-L.; Vovelle, F. Solution Structure of Alo-3: A New Knottin-Type Antifungal Peptide from the Insect Acrocinus longimanus ‡. *Biochemistry* **2003**, *42*, 14434–14442, doi:10.1021/bi035400o.

48.	Srivastava, S.K.; Babu, N.; Pandey, H. Traditional insect bioprospecting - As human food and medicine. *Indian J. Tradit. Knowl.* **2009**, *8*, 485–494, doi:10.1128/CMR.00056-05.

49. Lee, D.G.; Hahm, K.; Shin, S.Y. Structure and fungicidal activity of a synthetic antimicrobial peptide, P18, and its truncated peptides. *Biotechnol. Lett.* **2004**, *26*, 337–341, doi:10.1023/B:BILE.0000015472.09542.6d.

50. Cornelio, K.; Espiritu, R.A.; Hanashima, S.; Todokoro, Y.; Malabed, R.; Kinoshita, M.; Matsumori, N.; Murata, M.; Nishimura, S.; Kakeya, H.; et al. Theonellamide A, a marine-sponge-derived bicyclic peptide, binds to cholesterol in aqueous DMSO: Solution NMR-based analysis of peptide-sterol interactions using hydroxylated sterol. *Biochim. Biophys. Acta - Biomembr.* **2019**, *1861*, 228–235, doi:10.1016/j.bbamem.2018.07.010.

51. Park, Y.; Jang, S.; Lee, D.G.; Hahm, K. Antinematodal effect of antimicrobial peptide, PMAP-23, isolated from porcine myeloid againstCaenorhabditis elegans. *J. Pept. Sci.* **2004**, *10*, 304–311, doi:10.1002/psc.518.

52. Zasloff, M. Magainins, a class of antimicrobial peptides from Xenopus skin: isolation, characterization of two active forms, and partial cDNA sequence of a precursor. *Proc. Natl. Acad. Sci.* **1987**, *84*, 5449–5453, doi:10.1073/pnas.84.15.5449.

53. Alberola, J.; Rodríguez, A.; Francino, O.; Roura, X.; Rivas, L.; Andreu, D. Safety and Efficacy of Antimicrobial Peptides against Naturally Acquired Leishmaniasis. *Antimicrob. Agents Chemother.* **2004**, *48*, 641–643, doi:10.1128/AAC.48.2.641-643.2004.

54. Farrag, H.N.; Maeda, T.; Kato, T. Design, Synthesis and Antibacterial Studies of Novel Cationic Amphipathic Cyclic Undecapeptides and Their Linear Counterparts

against Virulent Bacterial Strains. *Sci. Pharm.* **2021**, *89*, 10, doi:10.3390/scipharm89010010.

55.   Farrag, H.N.; Metwally, K.; Ikeno, S.; Kato, T. Design and Synthesis of a New Amphipathic Cyclic Decapeptide with Rapid , Stable , and Continuous Antibacterial Effects. *Pertanika J. Sci. Technol.* **2020**, *28*, 183–196, doi:https://doi.org/10.47836/pjst.28.S2.15.

56.   Steffen, H.; Rieg, S.; Wiedemann, I.; Kalbacher, H.; Deeg, M.; Sahl, H.-G.; Peschel, A.; Götz, F.; Garbe, C.; Schittek, B. Naturally Processed Dermcidin-Derived Peptides Do Not Permeabilize Bacterial Membranes and Kill Microorganisms Irrespective of Their Charge. *Antimicrob. Agents Chemother.* **2006**, *50*, 2608–2620, doi:10.1128/AAC.00181-06.

57.   Lai, R.; Liu, H.; Hui Lee, W.; Zhang, Y. An anionic antimicrobial peptide from toad Bombina maxima. *Biochem. Biophys. Res. Commun.* **2002**, *295*, 796–799, doi:10.1016/S0006-291X(02)00762-3.

58.   Borah, A.; Deb, B.; Chakraborty, S. A Crosstalk on Antimicrobial Peptides. *Int. J. Pept. Res. Ther.* **2020**, doi:10.1007/s10989-020-10075-x.

59.   Robinson, W.E.; McDougall, B.; Tran, D.; Selsted, M.E. Anti-HIV-1 activity of indolicidin, an antimicrobial peptide from neutrophils. *J. Leukoc. Biol.* **1998**, *63*, 94–100, doi:10.1002/jlb.63.1.94.

60.   Selsted, M.E.; Novotny, M.J.; Morris, W.L.; Tang, Y.Q.; Smith, W.; Cullor, J.S.

Indolicidin, a novel bactericidal tridecapeptide amide from neutrophils. *J. Biol. Chem.* **1992**, *267*, 4292–5.

61.   Krajewski, K.; Marchand, C.; Long, Y.; Pommier, Y.; Roller, P.P. Synthesis and HIV-1 integrase inhibitory activity of dimeric and tetrameric analogs of indolicidin. *Bioorg. Med. Chem. Lett.* **2004**, *14*, 5595–5598, doi:10.1016/j.bmcl.2004.08.061.

62.   Subbalakshmi, C.; Sitaram, N. Mechanism of antimicrobial action of indolicidin. *FEMS Microbiol. Lett.* **1998**, *160*, 91–96, doi:10.1111/j.1574-6968.1998.tb12896.x.

63.   Lee, D.G.; Kim, H.K.; Kim, S.A.; Park, Y.; Park, S.; Jang, S.; Hahm, K. Fungicidal effect of indolicidin and its interaction with phospholipid membranes. *Biochem. Biophys. Res. Commun.* **2003**, *305*, 305–310, doi:10.1016/S0006-291X(03)00755-1.

64.   Lee, D.G.; Kim, P. Il; Park, Y.; Woo, E.; Choi, J.S.; Choi, C.; Hahm, K. Design of novel peptide analogs with potent fungicidal activity, based on PMAP-23 antimicrobial peptide isolated from porcine myeloid. *Biochem. Biophys. Res. Commun.* **2002**, *293*, 231–238, doi:10.1016/S0006-291X(02)00222-X.

65.   Zhang, Y.; Rock, C.O. Transcriptional regulation in bacterial membrane lipid synthesis: TABLE 1. *J. Lipid Res.* **2009**, *50*, S115–S119, doi:10.1194/jlr.R800046-JLR200.

66.   He, K.; Ludtke, S.J.; Worcester, D.L.; Huang, H.W. Neutron scattering in the plane of membranes: structure of alamethicin pores. *Biophys. J.* **1996**, *70*, 2659–2666, doi:10.1016/S0006-3495(96)79835-1.

67. Bolintineanu, D.S.; Kaznessis, Y.N. Computational studies of protegrin antimicrobial peptides: A review. *Peptides* **2011**, *32*, 188–201, doi:10.1016/j.peptides.2010.10.006.

68. Wu, M.; Maier, E.; Benz, R.; Hancock, R.E.W. Mechanism of Interaction of Different Classes of Cationic Antimicrobial Peptides with Planar Bilayers and with the Cytoplasmic Membrane of Escherichia coli †. *Biochemistry* **1999**, *38*, 7235–7242, doi:10.1021/bi9826299.

69. Chen, F.; Lee, M.; Huang, H.W. Evidence for Membrane Thinning Effect as the Mechanism for Peptide-Induced Pore Formation. *Biophys. J.* **2003**, *84*, 3751–3758, doi:10.1016/S0006-3495(03)75103-0.

70. Shimazaki, K.; Tazume, T.; Uji, K.; Tanaka, M.; Kumura, H.; Mikawa, K.; Shimo-oka, T. Properties of a Heparin-binding Peptide Derived from Bovine Lactoferrin. *J. Dairy Sci.* **1998**, *81*, 2841–2849, doi:10.3168/jds.S0022-0302(98)75843-6.

71. Otvos, L. Antibacterial peptides and proteins with multiple cellular targets. *J. Pept. Sci.* **2005**, *11*, 697–706, doi:10.1002/psc.698.

72. Marchand, C.; Krajewski, K.; Lee, H.; Antony, S.; Johnson, A.A.; Amin, R.; Roller, P.; Kvaratskhelia, M.; Pommier, Y. Covalent binding of the natural antimicrobial peptide indolicidin to DNA abasic sites. *Nucleic Acids Res.* **2006**, *34*, 5157–5165, doi:10.1093/nar/gkl667.

73. Nicolas, P. Multifunctional host defense peptides: intracellular-targeting

antimicrobial peptides. *FEBS J.* **2009**, *276*, 6483–6496, doi:10.1111/j.1742-4658.2009.07359.x.

74. Xiong, Y.; Yeaman, M.R.; Bayer, A.S. In Vitro Antibacterial Activities of Platelet Microbicidal Protein and Neutrophil Defensin against Staphylococcus aureus Are Influenced by Antibiotics Differing in Mechanism of Action. *Antimicrob. Agents Chemother.* **1999**, *43*, 1111–1117, doi:10.1128/AAC.43.5.1111.

75. Castle, M.; Nazarian, A.; Yi, S.S.; Tempst, P. Lethal Effects of Apidaecin on Escherichia coli Involve Sequential Molecular Interactions with Diverse Targets. *J. Biol. Chem.* **1999**, *274*, 32555–32564, doi:10.1074/jbc.274.46.32555.

76. Shrestha, P.; Hashimoto, J.; Takagi, H.; Yamada, K.; Mori, M.; Kanehira, T.; Wang, P.; Kuboki, Y. Immunoreactive Histatin 5 in salivary gland tumors. *Acta Histochem. Histochem.* **1994**, *27*, 527–534.

77. Couto, M.A.; Harwig, S.S.; Lehrer, R.I. Selective inhibition of microbial serine proteases by eNAP-2, an antimicrobial peptide from equine neutrophils. *Infect. Immun.* **1993**, *61*, 2991–2994, doi:10.1128/IAI.61.7.2991-2994.1993.

78. Wu, Q.; Patočka, J.; Kuča, K. Insect Antimicrobial Peptides, a Mini Review. *Toxins (Basel).* **2018**, *10*, 461, doi:10.3390/toxins10110461.

79. Reddy, E.S.P.; Das, M.R.; Reddy, E.P.; Bhargava, P.M. Inhibition of reverse transcriptases by seminalplasmin. *Biochem. J.* **1983**, *209*, 183–188, doi:10.1042/bj2090183.

80. Chitnis, S.N.; Prasad, K.S.N.; Bhargava, P.M. Isolation and Characterization of Autolysis-Defective Mutants of Escherichia Coli that are Resistant to the Lytic Activity of Seminalplasmin. *J. Gen. Microbiol.* **1990**, *136*, 463–469, doi:10.1099/00221287-136-3-463.

81. Jones, A.T. Macropinocytosis: searching for an endocytic identity and role in the uptake of cell penetrating peptides. *J. Cell. Mol. Med.* **2007**, *11*, 670–684, doi:10.1111/j.1582-4934.2007.00062.x.

82. Mayor, S.; Pagano, R.E. Pathways of clathrin-independent endocytosis. *Nat. Rev. Mol. Cell Biol.* **2007**, *8*, 603–612, doi:10.1038/nrm2216.

83. Kobayashi, S.; Takeshima, K.; Park, C.B.; Kim, S.C.; Matsuzaki, K. Interactions of the Novel Antimicrobial Peptide Buforin 2 with Lipid Bilayers: Proline as a Translocation Promoting Factor †. *Biochemistry* **2000**, *39*, 8648–8654, doi:10.1021/bi0004549.

84. Park, C.B.; Yi, K.-S.; Matsuzaki, K.; Kim, M.S.; Kim, S.C. Structure-activity analysis of buforin II, a histone H2A-derived antimicrobial peptide: The proline hinge is responsible for the cell-penetrating ability of buforin II. *Proc. Natl. Acad. Sci.* **2000**, *97*, 8245–8250, doi:10.1073/pnas.150518097.

85. Tossi, A.; Sandri, L.; Giangaspero, A. Amphipathic, α-helical antimicrobial peptides. *Biopolymers* **2000**, *55*, 4–30, doi:10.1002/1097-0282(2000)55:1<4::AID-BIP30>3.0.CO;2-M.

86. Jiang, Z.; Vasil, A.I.; Hale, J.D.; Hancock, R.E.W.; Vasil, M.L.; Hodges, R.S. Effects of net charge and the number of positively charged residues on the biological activity of amphipathic α-helical cationic antimicrobial peptides. *Biopolymers* **2008**, *90*, 369–383, doi:10.1002/bip.20911.

87. Westerhoff, H. V; Juretić, D.; Hendler, R.W.; Zasloff, M. Magainins and the disruption of membrane-linked free-energy transduction. *Proc. Natl. Acad. Sci.* **1989**, *86*, 6597–6601, doi:10.1073/pnas.86.17.6597.

88. Subbalakshmi, C.; Nagaraj, R.; Sitaram, N. Biological activities of C-terminal 15-residue synthetic fragment of melittin: design of an analog with improved antibacterial activity. *FEBS Lett.* **1999**, *448*, 62–66, doi:10.1016/S0014-5793(99)00328-2.

89. Huang, Y.; Huang, J.; Chen, Y. Alpha-helical cationic antimicrobial peptides: relationships of structure and function. *Protein Cell* **2010**, *1*, 143–152, doi:10.1007/s13238-010-0004-3.

90. Lee, D.G.; Kim, H.N.; Park, Y.; Kim, H.K.; Choi, B.H.; Choi, C.; Hahm, K. Design of novel analogue peptides with potent antibiotic activity based on the antimicrobial peptide, HP (2–20), derived from N-terminus of Helicobacter pylori ribosomal protein L1. *Biochim. Biophys. Acta - Proteins Proteomics* **2002**, *1598*, 185–194, doi:10.1016/S0167-4838(02)00373-4.

91. Vivès, E.; Schmidt, J.; Pèlegrin, A. Cell-penetrating and cell-targeting peptides in drug delivery. *Biochim. Biophys. Acta - Rev. Cancer* **2008**, *1786*, 126–138,

doi:10.1016/j.bbcan.2008.03.001.

92.   Kustanovich, I.; Shalev, D.E.; Mikhlin, M.; Gaidukov, L.; Mor, A. Structural Requirements for Potent Versus Selective Cytotoxicity for Antimicrobial Dermaseptin S4 Derivatives. *J. Biol. Chem.* **2002**, *277*, 16941–16951, doi:10.1074/jbc.M111071200.

93.   Zelezetsky, I.; Pacor, S.; Pag, U.; Papo, N.; Shai, Y.; Sahl, H.; Tossi, A. Controlled alteration of the shape and conformational stability of α-helical cell-lytic peptides: effect on mode of action and cell specificity. *Biochem. J.* **2005**, *390*, 177–188, doi:10.1042/BJ20042138.

94.   Dathe, M.; Wieprecht, T.; Nikolenko, H.; Handel, L.; Maloy, W.L.; MacDonald, D.L.; Beyermann, M.; Bienert, M. Hydrophobicity, hydrophobic moment and angle subtended by charged residues modulate antibacterial and haemolytic activity of amphipathic helical peptides. *FEBS Lett.* **1997**, *403*, 208–212, doi:10.1016/S0014-5793(97)00055-0.

95.   Fernández-Vidal, M.; Jayasinghe, S.; Ladokhin, A.S.; White, S.H. Folding Amphipathic Helices Into Membranes: Amphiphilicity Trumps Hydrophobicity. *J. Mol. Biol.* **2007**, *370*, 459–470, doi:10.1016/j.jmb.2007.05.016.

96.   Harro, J.M.; Peters, B.M.; O'May, G.A.; Archer, N.; Kerns, P.; Prabhakara, R.; Shirtliff, M.E. Vaccine development in Staphylococcus aureus : taking the biofilm phenotype into consideration. *FEMS Immunol. Med. Microbiol.* **2010**, *59*, 306–323, doi:10.1111/j.1574-695X.2010.00708.x.

97. Lewis, K. Persister cells and the riddle of biofilm survival. *Biochem.* **2005**, *70*, 267–274, doi:10.1007/s10541-005-0111-6.

98. Chen, X.; Zhang, M.; Zhou, C.; Kallenbach, N.R.; Ren, D. Control of Bacterial Persister Cells by Trp/Arg-Containing Antimicrobial Peptides. *Appl. Environ. Microbiol.* **2011**, *77*, 4878–4885, doi:10.1128/AEM.02440-10.

99. Compans, R.W.; Cooper, M.D.; Honjo, T.; Melchers, F.; Olsnes, S.; Wagner, H. *Antimicrobial Peptides and Human Disease*; Shafer, W.M., Ed.; Current Topics in Microbiology and Immunology; Springer Berlin Heidelberg: Berlin, Heidelberg, 2006; Vol. 306; ISBN 978-3-540-29915-8.

100. Singh, P.K.; Parsek, M.R.; Greenberg, E.P.; Welsh, M.J. A component of innate immunity prevents bacterial biofilm development. *Nature* **2002**, *417*, 552–555, doi:10.1038/417552a.

101. Gao, G.; Lange, D.; Hilpert, K.; Kindrachuk, J.; Zou, Y.; Cheng, J.T.J.; Kazemzadeh-Narbat, M.; Yu, K.; Wang, R.; Straus, S.K.; et al. The biocompatibility and biofilm resistance of implant coatings based on hydrophilic polymer brushes conjugated with antimicrobial peptides. *Biomaterials* **2011**, *32*, 3899–3909, doi:10.1016/j.biomaterials.2011.02.013.

102. Andersson, D.I.; Hughes, D.; Kubicek-Sutherland, J.Z. Mechanisms and consequences of bacterial resistance to antimicrobial peptides. *Drug Resist. Updat.* **2016**, *26*, 43–57, doi:10.1016/j.drup.2016.04.002.

103. Vuong, C.; Voyich, J.M.; Fischer, E.R.; Braughton, K.R.; Whitney, A.R.; Deleo, F.R.; Otto, M. Polysaccharide intercellular adhesin (PIA) protects Staphylococcus epidermidis against major components of the human innate immune system. *Cell. Microbiol.* **2004**, *6*, 269–275, doi:10.1111/j.1462-5822.2004.00367.x.

104. Sifri, C.D. Healthcare Epidemiology: Quorum Sensing: Bacteria Talk Sense. *Clin. Infect. Dis.* **2008**, *47*, 1070–1076, doi:10.1086/592072.

105. Rutherford, S.T.; Bassler, B.L. Bacterial Quorum Sensing: Its Role in Virulence and Possibilities for Its Control. *Cold Spring Harb. Perspect. Med.* **2012**, *2*, a012427–a012427, doi:10.1101/cshperspect.a012427.

106. Taga, M.E.; Bassler, B.L. Chemical communication among bacteria. *Proc. Natl. Acad. Sci.* **2003**, *100*, 14549–14554, doi:10.1073/pnas.1934514100.

107. Li, Z.; Nair, S.K. Quorum sensing: How bacteria can coordinate activity and synchronize their response to external signals? *Protein Sci.* **2012**, *21*, 1403–1417, doi:10.1002/pro.2132.

108. Bassler, B.L. How bacteria talk to each other: regulation of gene expression by quorum sensing. *Curr. Opin. Microbiol.* **1999**, *2*, 582–587, doi:10.1016/S1369-5274(99)00025-9.

109. Shin, J.M.; Gwak, J.W.; Kamarajan, P.; Fenno, J.C.; Rickard, A.H.; Kapila, Y.L. Biomedical applications of nisin. *J. Appl. Microbiol.* **2016**, *120*, 1449–1465, doi:10.1111/jam.13033.

110. Capasso, C.; Supuran, C.T. Sulfa and trimethoprim-like drugs – antimetabolites acting as carbonic anhydrase, dihydropteroate synthase and dihydrofolate reductase inhibitors. *J. Enzyme Inhib. Med. Chem.* **2014**, *29*, 379–387, doi:10.3109/14756366.2013.787422.

111. Burkhart, B.M.; Gassman, R.M.; Langs, D.A.; Pangborn, W.A.; Duax, W.L.; Pletnev, V. Gramicidin D conformation, dynamics and membrane ion transport. *Biopolymers* **1999**, *51*, 129–144, doi:10.1002/(SICI)1097-0282(1999)51:2<129::AID-BIP3>3.0.CO;2-Y.

112. Jayachandran, S.; Lleras-Muney, A.; Smith, K. V Modern Medicine and the Twentieth Century Decline in Mortality: Evidence on the Impact of Sulfa Drugs. *Am. Econ. J. Appl. Econ.* **2010**, *2*, 118–146, doi:10.1257/app.2.2.118.

113. Aminov, R. History of antimicrobial drug discovery: Major classes and health impact. *Biochem. Pharmacol.* **2017**, *133*, 4–19, doi:10.1016/j.bcp.2016.10.001.

114. Oh, D.; Sun, J.; Nasrolahi Shirazi, A.; LaPlante, K.L.; Rowley, D.C.; Parang, K. Antibacterial activities of amphiphilic cyclic cell-penetrating peptides against multidrug-resistant pathogens. *Mol. Pharm.* **2014**, *11*, 3528–36, doi:10.1021/mp5003027.

115. Dartois, V.; Sanchez-Quesada, J.; Cabezas, E.; Chi, E.; Dubbelde, C.; Dunn, C.; Granja, J.; Gritzen, C.; Weinberger, D.; Ghadiri, M.R.; et al. Systemic antibacterial activity of novel synthetic cyclic peptides. *Antimicrob. Agents Chemother.* **2005**, *49*, 3302–10, doi:10.1128/AAC.49.8.3302-3310.2005.

116. Nouioui, I.; Klenk, H.; Igual, J.M.; Gulvik, C.A.; Lasker, B.A.; McQuiston, J.R.
Streptacidiphilus bronchialis sp. nov., a ciprofloxacin-resistant bacterium from a
human clinical specimen; reclassification of Streptomyces griseoplanus as
Streptacidiphilus griseoplanus comb. nov. and emended description of the genus
Streptacidiphilus. *Int. J. Syst. Evol. Microbiol.* **2019**, *69*, 1047–1056,
doi:10.1099/ijsem.0.003267.

117. Wright, L.T.; Schreiber, H. The clinical value of aureomycin; a review of current
literature and some unpublished data. *J. Natl. Med. Assoc.* **1949**, *41*, 195–201.

118. Grossman, T.H. Tetracycline Antibiotics and Resistance. *Cold Spring Harb.
Perspect. Med.* **2016**, *6*, a025387, doi:10.1101/cshperspect.a025387.

119. Mariottini, G.; Grice, I. Antimicrobials from Cnidarians. A New Perspective for
Anti-Infective Therapy? *Mar. Drugs* **2016**, *14*, 48, doi:10.3390/md14030048.

120. Speer, B.S.; Bedzyk, L.; Salyers, A.A. Evidence that a novel tetracycline resistance
gene found on two Bacteroides transposons encodes an NADP-requiring
oxidoreductase. *J. Bacteriol.* **1991**, *173*, 176–183, doi:10.1128/JB.173.1.176-
183.1991.

121. Hill, G.B. Therapeutic Evaluation of Minocycline and Tetracycline for Mixed
Anaerobic Infection in Mice. *Antimicrob. Agents Chemother.* **1977**, *11*, 625–630,
doi:10.1128/AAC.11.4.625.

122. Aminov, R.I. Evolution in action: dissemination of tet(X) into pathogenic

microbiota. *Front. Microbiol.* **2013**, *4*, 4–7, doi:10.3389/fmicb.2013.00192.

123. Eliakim-Raz, N.; Lador, A.; Leibovici-Weissman, Y.; Elbaz, M.; Paul, M.; Leibovici, L. Efficacy and safety of chloramphenicol: joining the revival of old antibiotics? Systematic review and meta-analysis of randomized controlled trials. *J. Antimicrob. Chemother.* **2015**, 979–996, doi:10.1093/jac/dku530.

124. Wisseman, C.L.; Smadel, J.E.; Hahn, F.E.; Hopps, H.E. Mode of action of chloramphenicol. I. Action of chloramphenicol on assimilation of ammonia and on synthesis of proteins and nucleic acids in Escherichia coli. *J. Bacteriol.* **1954**, *67*, 662–73, doi:10.1128/JB.67.6.662-673.1954.

125. Cannon, J.G. Goodman and Gilman's The Pharmacological Basis of Therapeutics. 11th Edition Edited by Laurence Brunton, John Lazo, and Keith Parker. McGraw Hill, New York. 2005. xxiii + 2021 pp. 21 × 26 cm. ISBN 0-07-142280-3. $149.95. *J. Med. Chem.* **2006**, *49*, 1222–1222, doi:10.1021/jm058286b.

126. Schwarz, S.; Kehrenberg, C.; Doublet, B.; Cloeckaert, A. Molecular basis of bacterial resistance to chloramphenicol and florfenicol. *FEMS Microbiol. Rev.* **2004**, *28*, 519–542, doi:10.1016/j.femsre.2004.04.001.

127. Vincent, J. Nosocomial infections in adult intensive-care units. *Lancet* **2003**, *361*, 2068–2077, doi:10.1016/S0140-6736(03)13644-6.

128. Curtis, L.T. Prevention of hospital-acquired infections: review of non-pharmacological interventions. *J. Hosp. Infect.* **2008**, *69*, 204–219,

doi:10.1016/j.jhin.2008.03.018.

129. Raab, W.; Kaiser, E. Die Wirkung des Hautsekretes der Gelbbauchunke (Bombina variegata L.) auf das Hautbindegewebe von Meerschweinchen, Ratten und Mousen. *Arch. Klin. und Exp. Dermatologie* **1964**, *220*, 374–382, doi:10.1007/BF00522675.

130. Mohanty, D.; Jena, R.; Choudhury, P.K.; Pattnaik, R.; Mohapatra, S.; Saini, M.R. Milk Derived Antimicrobial Bioactive Peptides: A Review. *Int. J. Food Prop.* **2016**, *19*, 837–846, doi:10.1080/10942912.2015.1048356.

131. Malawista, S.; Oliver, J.; Rudolph, S. Microtubules and cyclic amp in human leukocytes: on the order of things. *J. Cell Biol.* **1978**, *77*, 881–886, doi:10.1083/jcb.77.3.881.

132. Schauber, J.; Gallo, R.L. Antimicrobial peptides and the skin immune defense system. *J. Allergy Clin. Immunol.* **2008**, *122*, 261–266, doi:10.1016/j.jaci.2008.03.027.

133. Park, A.J.; Okhovat, J.P.; Kim, J. Antimicrobial peptides. *Clin. Basic Immunodermatology Second Ed.* **2017**, 81–95, doi:10.1007/978-3-319-29785-9_6.

134. Hancock, R.E.W.; Scott, M.G. The role of antimicrobial peptides in animal defenses. **2000**, *97*.

135. Dutta, S.R.; Gauri, S.S.; Ghosh, T.; Halder, S.K.; DasMohapatra, P.K.; Mondal, K.C.; Ghosh, A.K. Elucidation of structural and functional integration of a novel antimicrobial peptide from Antheraea mylitta. *Bioorganic Med. Chem. Lett.* **2017**,

27, 1686–1692, doi:10.1016/j.bmcl.2017.03.003.

136. Yeung, A.T.Y.; Gellatly, S.L.; Hancock, R.E.W. Multifunctional cationic host defence peptides and their clinical applications. *Cell. Mol. Life Sci.* **2011**, *68*, 2161–2176, doi:10.1007/s00018-011-0710-x.

137. Hsu, C. Structural and DNA-binding studies on the bovine antimicrobial peptide, indolicidin: evidence for multiple conformations involved in binding to membranes and DNA. *Nucleic Acids Res.* **2005**, *33*, 4053–4064, doi:10.1093/nar/gki725.

138. Silhavy, T.J.; Kahne, D.; Walker, S. The Bacterial Cell Envelope. *Cold Spring Harb. Perspect. Biol.* **2010**, *2*, a000414–a000414, doi:10.1101/cshperspect.a000414.

139. Gottenbos, B. Antimicrobial effects of positively charged surfaces on adhering Gram-positive and Gram-negative bacteria. *J. Antimicrob. Chemother.* **2001**, *48*, 7–13, doi:10.1093/jac/48.1.7.

140. Epand, R.M.; Vogel, H.J. Diversity of antimicrobial peptides and their mechanisms of action. *Biochim. Biophys. Acta - Biomembr.* **1999**, *1462*, 11–28, doi:10.1016/S0005-2736(99)00198-4.

141. Kreutzer, A.G.; Salveson, P.J.; Yang, H. *Standard practices for Fmoc-based solid-phase peptide synthesis in the Nowick laboratory*;

142. Amblard, M.; Fehrentz, J.; Martinez, J.; Subra, G. Methods and Protocols of Modern Solid Phase Peptide Synthesis. *Mol. Biotechnol.* **2006**, *33*, 239–254, doi:10.1385/MB:33:3:239.

143. Huber, U.; Majors, R.E. *Principles in Preparative HPLC*; 2007;

144. Tapeinou, A.; Matsoukas, M.-T.; Simal, C.; Tselios, T. Review cyclic peptides on a merry-go-round; towards drug design. *Biopolymers* **2015**, *104*, 453–461, doi:10.1002/bip.22669.

145. Standards, P.; Testing, A.S. *M100 Performance Standards for Antimicrobial*; 2018; ISBN 1562388045.

146. Jo, J.T.H.; Brinkman, F.S.L.; Hancock, R.E.W. Aminoglycoside Efflux in Pseudomonas aeruginosa: Involvement of Novel Outer Membrane Proteins. *Antimicrob. Agents Chemother.* **2003**, *47*, 1101–1111, doi:10.1128/AAC.47.3.1101-1111.2003.

147. Mikkelsen, H.; McMullan, R.; Filloux, A. The Pseudomonas aeruginosa Reference Strain PA14 Displays Increased Virulence Due to a Mutation in ladS. *PLoS One* **2011**, *6*, e29113, doi:10.1371/journal.pone.0029113.

148. Roos, V.; Ulett, G.C.; Schembri, M.A.; Klemm, P. The Asymptomatic Bacteriuria Escherichia coli Strain 83972 Outcompetes Uropathogenic E. coli Strains in Human Urine. *Infect. Immun.* **2006**, *74*, 615–624, doi:10.1128/IAI.74.1.615-624.2006.

149. Hancock, R.E.W.; Chapple, D.S. Peptide Antibiotics. *Antimicrob. Agents Chemother.* **1999**, *43*, 1317–1323, doi:10.1128/AAC.43.6.1317.

150. Boman, H.G. Peptide Antibiotics and their Role in Innate Immunity. *Annu. Rev. Immunol.* **1995**, *13*, 61–92, doi:10.1146/annurev.iy.13.040195.000425.

151. Rozek, A.; Powers, J.S.; Friedrich, C.L.; Hancock, R.E.W. Structure-Based Design of an Indolicidin Peptide Analogue with Increased Protease Stability † , ‡. *Biochemistry* **2003**, *42*, 14130–14138, doi:10.1021/bi035643g.

152. O'Connell, K.M.G.; Hodgkinson, J.T.; Sore, H.F.; Welch, M.; Salmond, G.P.C.; Spring, D.R. Combating Multidrug-Resistant Bacteria: Current Strategies for the Discovery of Novel Antibacterials. *Angew. Chemie Int. Ed.* **2013**, *52*, 10706–10733, doi:10.1002/anie.201209979.

153. Rasko, D.A.; Sperandio, V. Anti-virulence strategies to combat bacteria-mediated disease. *Nat. Rev. Drug Discov.* **2010**, *9*, 117–28, doi:10.1038/nrd3013.

154. Ribet, D.; Cossart, P. How bacterial pathogens colonize their hosts and invade deeper tissues. *Microbes Infect.* **2015**, *17*, 173–183, doi:10.1016/j.micinf.2015.01.004.

155. Atkinson, S.; Williams, P. Quorum sensing and social networking in the microbial world. *J. R. Soc. Interface* **2009**, *6*, 959–78, doi:10.1098/rsif.2009.0203.

156. Hentzer, M.; Wu, H.; Andersen, J.B.; Riedel, K.; Rasmussen, T.B.; Bagge, N.; Kumar, N.; Schembri, M.A.; Song, Z.; Kristoffersen, P.; et al. Attenuation of Pseudomonas aeruginosa virulence by quorum sensing inhibitors. *EMBO J.* **2003**, *22*, 3803–3815, doi:10.1093/emboj/cdg366.

157. Berube, B.J.; Sampedro, G.R.; Otto, M.; Bubeck Wardenburg, J. The psmα locus regulates production of Staphylococcus aureus alpha-toxin during infection. *Infect.*

Immun. **2014**, *82*, 3350–8, doi:10.1128/IAI.00089-14.

158.   Zhu, L.; Lau, G.W. Inhibition of competence development, horizontal gene transfer and virulence in Streptococcus pneumoniae by a modified competence stimulating peptide. *PLoS Pathog.* **2011**, *7*, e1002241, doi:10.1371/journal.ppat.1002241.

159.   Dong, Y.; Wang, L.; Zhang, L. Quorum-quenching microbial infections: mechanisms and implications. *Philos. Trans. R. Soc. B Biol. Sci.* **2007**, *362*, 1201–1211, doi:10.1098/rstb.2007.2045.

160.   Wright, J.S.; Jin, R.; Novick, R.P. Transient interference with staphylococcal quorum sensing blocks abscess formation. *Proc. Natl. Acad. Sci. U. S. A.* **2005**, *102*, 1691–6, doi:10.1073/pnas.0407661102.

161.   Gordon, C.P.; Williams, P.; Chan, W.C. Attenuating Staphylococcus aureus virulence gene regulation: a medicinal chemistry perspective. *J. Med. Chem.* **2013**, *56*, 1389–404, doi:10.1021/jm3014635.

162.   Tal-Gan, Y.; Stacy, D.M.; Foegen, M.K.; Koenig, D.W.; Blackwell, H.E. Highly potent inhibitors of quorum sensing in Staphylococcus aureus revealed through a systematic synthetic study of the group-III autoinducing peptide. *J. Am. Chem. Soc.* **2013**, *135*, 7869–82, doi:10.1021/ja3112115.

163.   Gless, B.H.; Peng, P.; Pedersen, K.D.; Gotfredsen, C.H.; Ingmer, H.; Olsen, C.A. Structure–Activity Relationship Study Based on Autoinducing Peptide (AIP) from Dog Pathogen S. schleiferi. *Org. Lett.* **2017**, *19*, 5276–5279,

doi:10.1021/acs.orglett.7b02550.

164. Wuts, P.G.M.; Greene, T.W. Protection for the Thiol Group. In *Greene's Protective Groups in Organic Synthesis*; John Wiley & Sons, Inc.: Hoboken, NJ, USA, 2006; Vol. 9, pp. 647–695 ISBN 0471160199.

165. Kamber, B.; Hartmann, A.; Eisler, K.; Riniker, B.; Rink, H.; Sieber, P. The Synthesis of Cystine Peptides by Iodine Oxidation of S -Trityl-cysteine and S -. *Helv. Chim. Acta* **2004**, *63*, 899–915.

166. Nandiyanto, A.B.D.; Oktiani, R.; Ragadhita, R. How to Read and Interpret FTIR Spectroscope of Organic Material. *Indones. J. Sci. Technol.* **2019**, *4*, 97, doi:10.17509/ijost.v4i1.15806.

167. Neises, B.; Steglich, W. Simple Method for the Esterification of Carboxylic Acids. *Angew. Chemie Int. Ed. English* **1978**, *17*, 522–524, doi:10.1002/anie.197805221.

168. Gless, B.H.; Peng, P.; Pedersen, K.D.; Gotfredsen, C.H.; Ingmer, H.; Olsen, C.A. Structure-Activity Relationship Study Based on Autoinducing Peptide (AIP) from Dog Pathogen S. schleiferi. *Org. Lett.* **2017**, *19*, 5276–5279, doi:10.1021/acs.orglett.7b02550.

ACKNOWLEDGMENTS

ACHIEVEMENTS

Publications

1. **Farrag, H.N**.; Metwally, K.; Ikeno, S.; Kato, T. Design and Synthesis of a New Amphipathic Cyclic Decapeptide with Rapid, Stable, and Continuous Antibacterial Effects. *Pertanika Journal of. Science and Technology.* **2020**, *28*, 183–196

   doi: https://doi.org/10.47836/pjst.28.S2.15

2. **Farrag, H.N**.; Maeda, T.; Kato, T. Design, Synthesis and Antibacterial Studies of Novel Cationic Amphipathic Cyclic Undecapeptides and Their Linear Counterparts against Virulent Bacterial Strains. *Scientia Pharmaceutica.* **2021**, *89*, 10,

   doi: https://doi:10.3390/scipharm89010010.

Conferences

1. **Hisham N. Farrag**, Toshinari Maeda, Tamaki Kato. Japan Peptide Symposium 57, (2020). "Design, Synthesis and Antibacterial Studies of Novel Cyclic Undecapeptides and their Linear Counterparts against Virulent Bacterial Strains"

2. **Hisham N. Farrag**, Khaled Metwally, Shinya Ikeno, Tamaki Kato. 7th International Symposium on Applied Engineering and Sciences (SAES), (2019). "The Design and Synthesis of a New Amphipathic Cyclic Decapeptide with Rapid, Stable and Continuous Antibacterial Effect "

3. **Hisham N. Farrag**, Khaled Metwally, Shinya Ikeno, Tamaki Kato. The Twelfth Japan – Korea Joint Symposium on Bio-microsensing Technology (12th JKBT),

(2019). "The Antibacterial Studies of a Newly Designed Cyclic Decapeptide & Its Linear Counterpart with Rapid, Stable and Continuous Antibacterial Effects"

4. **Hisham N. Farrag**, Khaled Metwally, Shinya Ikeno, Tamaki Kato. The Eleventh Japan – Korea Joint Symposium on Bio-microsensing Technology (11th JKBT), (2018). "New Design of a Cyclic Decapeptide To Be Used as Antimicrobial Agent"

5. **Hisham N. Farrag**, Tamaki Kato. The Tenth Japan – Korea Joint Symposium on Bio-microsensing Technology (10th JKBT), (2017). "Cyclic Hexa-peptide Nanotube formation by Assisted-assembly using Sidechain" Reaction"

6. **Hisham N. Farrag**, Tamaki Kato. 97th Chemical Society of Japan Annual Meeting (2017) "Cyclic peptide Nanotube formation by Assisted-assembly using Sidechain Reaction"